

Diss. ETH No. 17159

Tight junctions as a target for permeation enhancement

A dissertation submitted to the
SWISS FEDERAL INSTITUTE OF TECHNOLOGY ZURICH

for the degree of
Doctor of Natural Sciences

presented by

JIŘÍ HOFMANN

Pharmacist, Charles University in Prague

born September 22, 1978

citizen of Czech Republic

accepted on the recommendation of
Prof. Dr. Heidi Wunderli-Allenspach, examiner
Prof. Dr. Dario Neri, co-examiner
PD Dr. Stefanie D. Krämer, co-examiner

2007

'Donde una puerta se cierra, otra se abre.'

El ingenioso hidalgo Don Quixote de la Mancha
Miguel de Cervantes y Saavedra

Contents

List of Tables	V
List of Figures	VIII
Abbreviations	X
Summary	XII
Zusammenfassung	XIV
1 Introduction	1
1.1 The junctional complex	1
1.2 Tight junctions	1
1.2.1 Functions	1
1.2.2 Morphology	2
1.2.3 Molecular structure	3
1.2.4 Transmembrane proteins	5
1.2.4.1 Occludin	5
1.2.4.2 Claudins	7
1.2.5 Plaque proteins	9
1.2.5.1 Zonulae occludens proteins	9
1.2.5.2 Cingulin	10
1.3 Permeation across <i>in-vivo</i> barriers	10
1.3.1 Routes of permeation	10
1.3.2 Strategies to enhance paracellular permeation	10
1.4 Models to study tight junctions	14
1.4.1 Cell cultures	14
1.4.2 Proteoliposomes	15
1.5 Aim of the study	16
2 Materials and methods	19
2.1 Chemicals	19
2.2 Peptides	19
2.3 High performance liquid chromatography (HPLC)	21
2.4 Circular dichroism	21
2.5 Cell cultures	22

2.5.1	Madin Darby canine kidney (MDCK) cell line	22
2.5.2	Human colon carcinoma (Caco-2) cell line	22
2.5.3	<i>Spodoptera frugiperda</i> (Sf9) cell line	22
2.6	Transfection of mammalian cells	23
2.7	Functional assays of tight junctions	23
2.7.1	Treatment of cells with synthetic peptides	23
2.7.2	Transepithelial electrical resistance measurement (TEER)	23
2.7.3	Paracellular permeation assay	24
2.7.4	Calcium chelation method	24
2.8	Confocal laser scanning microscopy (CLSM)	25
2.9	DNA manipulations	27
2.9.1	Generation of constructs	27
2.9.2	DNA isolation	29
2.9.3	DNA quantification	29
2.9.4	Digestion by restriction endonucleases	30
2.9.5	Dephosphorylation of plasmid DNA	30
2.9.6	DNA ligation	30
2.9.7	Polymerase chain reaction (PCR)	31
2.9.8	DNA sequencing	31
2.9.9	Agarose gel electrophoresis	31
2.10	Bacteria manipulations	32
2.10.1	Media and agar plates for bacteria	32
2.10.2	Bacteria suspension cultures	32
2.10.3	Transformation of DH10Bac competent bacteria	32
2.10.4	Transformation of DH5 α competent bacteria	33
2.11	Baculovirus expression system	33
2.11.1	Generation and analysis of bacmids	33
2.11.2	Transfection of insect cells	35
2.11.3	Amplification of recombinant baculoviruses	35
2.11.4	Titration of baculoviral stocks	35
2.11.5	Protein expression in insect cells	36
2.11.5.1	Expression of β -glucuronidase	36
2.11.5.2	Expression of his-tagged claudin-1	36
2.12	Protein purification and analysis	37
2.12.1	Quantification of proteins	37
2.12.2	Preparation of crude membranes	37
2.12.3	Affinity chromatography	37
2.12.4	SDS polyacrylamide gel electrophoresis	38
2.12.5	Silver staining	38
2.12.6	Western blotting	38
2.13	Preparation and analysis of proteoliposomes	39
2.13.1	Detergent dialysis	39
2.13.2	Dynamic light scattering	40

2.13.3	Sucrose density gradient	40
3	Results	41
3.1	Morphological studies on the modulation of tight junctions	41
3.1.1	Calcium chelation method	41
3.1.2	Dynamic behavior of cingulin	41
3.1.3	Dynamic behavior of GFP-tagged claudin-1	46
3.2	Synthetic peptide homologues to claudin and occludin sequences as a strategy to modulate tight junctions	50
3.2.1	Influence of peptide homologues to claudin on tight junctions	50
3.2.2	Influence of peptide homologues to occludin on tight junctions	60
3.3	Development of claudin-containing proteoliposomes as an <i>in-vitro</i> model for the screening of tight junction modulators	63
3.3.1	Production of His-tagged claudin-1	63
3.3.1.1	Characterization of the insect cell line	63
3.3.1.2	Generation of recombinant baculoviruses	63
3.3.1.3	Expression and purification of His-CLD1	65
3.3.2	Preparation and characterization of His-CLD1-proteoliposomes	69
4	Discussion	73
4.1	Morphological studies on the modulation of tight junctions	73
4.2	Synthetic peptide homologues to claudin and occludin sequences as a strategy to modulate tight junctions	77
4.3	Development of claudin-containing proteoliposomes as an <i>in-vitro</i> model for the screening of the tight junction modulators	83
5	Outlook	89
	References	91
	Acknowledgements	118
	Curriculum vitæ	119

List of Tables

1.1	Paracellular permeation enhancers	12
2.1	Synthetic peptide homologues based on sequences of occludin and claudins . .	20
2.2	Antibodies and dyes used for immunocytochemistry	26
2.3	Antibiotics and reagents for agar plates and liquid media	32

List of Figures

1.1	Freeze-fracture replica micrograph of mouse intestine	3
1.2	Complex interactions between tight junction proteins	4
1.3	Predicted folding topology of human occludin	6
1.4	Predicted folding topology of human claudin-1	7
1.5	Transport pathways through a cell monolayer	11
1.6	Liposomes with reconstituted claudins	16
2.1	Schematic representation of optical sections	25
2.2	Map of construct pEGFP-CLDN1	27
2.3	Map of constructs pFastBacHTB-CLDN1 and pFastBac1-GUS	28
2.4	The baculovirus expression system	34
3.1	Effect of calcium depletion on TEER and localization of ZO-1	42
3.2	Optical sectioning and regions of interest defined for statistical analysis of co-localization	43
3.3	Co-localization of cingulin with ZO-1, OCLN and F-actin	44
3.4	Statistical analysis of cingulin co-localization with different TJ proteins	45
3.5	Localization of GFP-CLD1 in transfected MDCK cells	47
3.6	Localization of GFP-CLD1 and ZO-1 upon disruption and re-assembly of tight junctions	49
3.7	Design of peptide homologues corresponding to the first extracellular loop of claudin	50
3.8	Amino acid alignment of the first extracellular loop of claudins	51
3.9	Permeation of mannitol through the MDCK monolayer	52
3.10	Effect of CLD2 peptide homologues on TEER and mannitol permeability of MDCK cells	53
3.11	Effect of CLD4 peptide homologues on TEER and mannitol permeability of MDCK cells	54
3.12	Effect of CLD1, CLD2 and CLD4 peptide homologues on TEER and mannitol permeability of MDCK cells under reducing conditions	55
3.13	Effect of a high concentration of CLD1 and CLD2 peptide homologues on TEER and mannitol permeability of MDCK cells	56
3.14	Morphology of MDCK cells after treatment with CLD1 homologue 49-60	57
3.15	Effect of solubilized CLD1 peptide homologue 49-60 on TEER and mannitol permeability of MDCK cells	58
3.16	Circular dichroism pattern of CLD1 peptide homologue 49-60	59

3.17	Effect of charged CLD1 peptide homologues on TEER and mannitol permeability of MDCK cells	60
3.18	Effect of OCLN peptide homologues on TEER and mannitol permeability of MDCK cells	61
3.19	Effect of OCLN peptide homologues on TEER and mannitol permeability of Caco-2 cells	61
3.20	Localization of 5(6)-FAM-labelled OCLN peptide homologue 90-103 in MDCK and Caco-2 cells	62
3.21	Growth curve of Sf9 cells	63
3.22	Analysis of recombinant bacmids CLDN1 and GUS by PCR	64
3.23	Sf9 cells transfected with bacmids CLDN1 and GUS	65
3.24	Characteristics of CLDN1-baculovirus-infected Sf9 cells	66
3.25	Expression of His-CLD1 in Sf9 cells	67
3.26	Isolation of crude membranes containing His-CLD1	67
3.27	Purification of His-CLD1 by affinity chromatography	68
3.28	Purification of His-CLD1 by affinity chromatography	68
3.29	Size distribution profiles of liposomes and His-CLD1-proteoliposomes	69
3.30	Correlograms of His-CLD1-proteoliposomes and control liposomes	70
3.31	Kinetics of detergent removal during dialysis	70
3.32	Sucrose density gradient of His-CLD1-proteoliposomes	71
3.33	Confirmation of His-CLD1 reconstitution into proteoliposomes	72

List of Abbreviations

BOC	Butyloxycarbonyl
BSA	Bovine serum albumin
Caco-2	Human colon adenocarcinoma cells
CD	Circular dichroism
CLD	Claudin
CLSM	Confocal laser scanning microscopy
DMSO	Dimethylsulfoxide
DTT	(R,R)-1,4-dimercapto-2,3-butanediol
EDTA	Ethylenediaminetetraacetic acid
EGTA	O,O'-bis-(2-aminoethyl)-ethyleneglycol-N,N,N',N'-tetraacetic acid
FCS	Foetal calf serum
GFP	Green fluorescent protein
GFP-CLD1	N-terminal GFP-tagged human claudin-1
GUS	β -glucuronidase
His-CLD1	N-terminal His-tagged human claudin-1
HPLC	High pressure liquid chromatography
kDa	Kilo-Dalton
MDCK	Madin-Darby canine kidney cells
MDCK-GFP-CLD1	MDCK expressing GFP-CLD1
MOI	Multiplicity of infection
OCLN	Occludin
PAGE	Polyacrylamide gel electrophoresis
PBS	Phosphate buffered saline
PC	Polycarbonate
PCR	Polymerase chain reaction
PET	Polyethylene terephthalate
SDS	Sodium dodecylsulfate
Sf9	<i>Spodoptera frugiperda</i> cells
TEER	Transepithelial electrical resistance
TJs	Tight junctions
ROI	Regions of interest
RT	Room temperature, 25°C
v/v	Volume over volume
w/v	Weight over volume
ZO-1	Zonula occludens-1

Summary

Tight junctions (TJs) form a seal between adjacent cells, regulating the free diffusion of solutes and ions. A controlled and reversible opening of TJs would improve the permeation of hydrophilic drugs across tight epithelial and endothelial cell sheets. A number of paracellular permeation enhancers have been published, however, their effect is generally mediated by an activation of signalling pathways, which leads to an uncontrolled opening of TJs and in consequence to cellular toxicity.

In order to learn more about the behavior of single TJ proteins upon the TJ modulation, we applied the calcium chelation method in a cell culture of epithelial phenotype (MDCK, Madin Darby canine kidney). We have chosen cingulin and claudin-1 as the representatives for the plaque and transmembrane proteins of TJs, respectively, and investigated their co-localization and dynamic behavior in combination with other proteins of TJs. According to the morphology of the cells after the TJ opening, we defined two regions of interest for the co-localization analysis, the membrane areas and the filaments remaining between the cells. Statistical analysis of the CLSM data revealed one major peak of co-localization for cingulin with zonula occludens-1 protein (ZO-1), occludin (OCLN) and F-actin, respectively, under normal calcium conditions. After calcium depletion, this pattern was not significantly changed in the membrane regions. The maximum of co-localization shifted to a more basal position for the protein pair cingulin with ZO-1 and F-actin, respectively, due to the changed geometry of cells (rounding up). In the filaments remaining between the cells, the co-localization was slightly reduced for the protein pairs of cingulin with OCLN and F-actin. In contrast, the co-localization of cingulin with ZO-1 was significantly reduced. To explore the kinetics of the TJ re-assembly, MDCK cells were transfected with green fluorescent protein-tagged claudin-1 (GFP-CLD1). Unfortunately, the live-imaging of the GFP-CLD1 dynamics failed due to a photoinstability of the fusion protein, and thus fixed samples were used to describe the kinetics of re-sealing of GFP-CLD1 in combination with ZO-1, claudin-4 (CLD4) and F-actin, respectively. We observed no significant differences between the kinetics of the respective proteins upon the TJ re-formation. The studies on the localization and co-localization of TJ proteins provide us with important information about the behavior of different proteins in the state of disassembly and re-assembly of TJs and contribute to evaluate the safety of new paracellular permeation enhancers.

The current model of TJs suggests that the extracellular domains of CLDs interact homotypically or heterotypically to bridge the paracellular space. Therefore, we used a recently developed strategy to modulate TJs that is based on the use of peptides containing sequences of the extracellular loops of transmembrane TJ proteins. These homologous peptides should compete for the seal between adjacent cells and induce a transient loosening of TJs, without complete disruption of the complexes and without inducing unwanted cell reactions. The modulation of TJs was monitored with transepithelial electrical resistance measurements (TEER) and

the mannitol permeability assay. We tested a set of peptide homologues to the loop sequences of human CLD1, CLD2 and CLD4 for their ability to modulate TJs in MDCK cells. To find optimal conditions for a TJ-modulating activity, we varied several critical factors in the assays, such as the concentration of foetal calf serum (FCS) in cell cultures, the oxidation-reduction state of peptides, the seeding density of the cultured cells and the peptide concentration for incubation. From the 14 tested CLD peptide homologues, two sequences (CLD1 49-60 and CLD2 31-49) decreased the TEER and increased the paracellular flux of mannitol. However, a closer inspection of the effect by CLSM revealed alterations in the immunostaining for ZO-1 and OCLN as well as massive changes in the cell morphology. These morphology changes were due to an unspecific influence of the peptide aggregates on the cell layer, as we confirmed in re-designed assays with fully solubilized peptides. We also included two peptide homologues to OCLN that had been described to modulate TJs in epithelial cells as a positive control for our assays. Contrary to what has previously been reported, none of the peptides increased the paracellular mannitol flux in MDCK and Caco-2 cells, respectively. A fluorescent analogue of an OCLN peptide was endocytosed by the MDCK cells and no binding to TJ structures was observed. In Caco-2 cells, only a non-specific binding to the cell layer occurred. We demonstrated that the approach to modulate TJs with peptides emulating the sequences of the extracellular loops of CLDs and OCLN is inefficient and associated with non-specific effects of peptides.

A simple *in-vitro* assay based on interactions between the extracellular loop of claudins allows to screen for novel permeation enhancers. In this assay, purified transmembrane claudins are reconstituted into the liposomes. The reconstituted proteins display their hydrophobic extracellular domains and should interact together to mediate an aggregation of the liposomes. Because the claudin-1 is expressed in most mammalian epithelia and studies with knock-out mice confirmed the crucial role of this protein for the formation of TJs, we have chosen this protein as a suitable candidate to establish the proteoliposomal assay. His-tagged claudin-1 (His-CLD1) was expressed in the baculovirus system, purified and reconstituted by detergent dialysis into phosphatidyl choline liposomes. In this pilot study, we showed a successful reconstitution of the His-CLD1 into the phosphatidyl liposomes. Characterization of the proteoliposomes by dynamic laser scattering revealed no differences between the size of the proteoliposomes and control liposomes (prepared without the protein), and we did not observe an interaction between the reconstituted proteins, i.e. no significant aggregation of liposomes. The low yield of His-CLD1 in the purification represented a major problem, and can be attributed to the low expression level of His-CLD1 in the baculovirus system. An increase in the protein concentration should be the next step to investigate the His-CLD1 proteoliposomal system. Thus, the protocols regarding the expression and purification must be further optimized to obtain a high yield of purified protein to achieve this goal.

Zusammenfassung

Die 'Tight Junctions' (TJs) bilden eine Barriere zwischen benachbarten Zellen. Diese Barriere reguliert die Diffusion von Molekülen und Ionen. Eine kontrollierte und reversible Öffnung von TJs könnte die Permeation von vielen hydrophilen Arzneistoffen durch Epithelien und Endothelien verbessern. Eine Reihe von sogenannten 'parazellulären Permeationsverstärkern' ist bereits veröffentlicht worden. Ihr Effekt wird jedoch im Allgemeinen durch eine Aktivierung von Signalkaskaden vermittelt, die oft zu einer irreversiblen TJ-Öffnung und somit zu Zelltoxizität führt.

Um mehr über das Verhalten der einzelnen TJ-Proteine bei einer TJ-Modulation zu erfahren, wurde eine epitheliale Zelllinie (MDCK-Zellen) kurzfristig mit einem Calcium-Chelator (EGTA) behandelt. Dies bewirkte eine reversible Öffnung der TJs. Als Repräsentanten für die Plaques- und Transmembranproteine der TJs wählten wir Claudin-1 und Cingulin, deren Colokalisierung und dynamisches Verhalten im Bezug auf andere TJ-Proteine wir mittels 'Konfokaler Laser Scanning Mikroskopie' (CLSM) untersuchten. Aufgrund unterschiedlicher Zellmorphologie nach einer Öffnung der TJs haben wir zwei Interessensregionen für die Colokalisierungsanalyse definiert: einerseits die Membranbereiche und andererseits die Filamente, die nach der Öffnung der TJs zwischen benachbarten Zellen sichtbar waren. Unter normalen Calcium-Bedingungen zeigten statistische Analysen eine hauptsächlich Colokalisierung von Cingulin mit Zonula occludens-1 Protein (ZO-1), Occludin (OCLN), als auch mit F-Actin. Dieses Muster veränderte sich nach dem Entzug von Calcium in den Membranregionen nur unwesentlich. Jedoch verschoben sich die Colokalisierungen von Cingulin mit ZO-1 und F-Actin in basaler Richtung. Dieser Effekt liess sich mit dem Abrunden der Zellen, also einer Veränderung der Zellgeometrie erklären. In der Filamentenregion nahm die Colokalisierung der Proteinpaares Cingulin/OCLN und Cingulin/F-Actin etwas ab. Für Cingulin und ZO-1 wurde hingegen eine markante Reduktion der Colokalisierung festgestellt. Um die Kinetik des TJ-Wiederaufbaus zu studieren, wurde ein Fusionsprotein mit Claudin-1 und dem grün fluoreszierenden Protein (GFP-CLD1) hergestellt. Dieses wurde in MDCK Zellen exprimiert. Unglücklicherweise verhinderte eine Photoinstabilität des Fusionsproteins eine Lebendaufnahme der GFP-CLD1 Dynamik. Stattdessen wurden fixierte Proben verwendet, um die Kinetik von GFP-CLD1 mit ZO-1, Claudin-4 (CLD4) und F-Actin zu studieren. Wir konnten jedoch keine wesentlichen Unterschiede im Verhalten der entsprechenden Proteine bei der Neubildung der TJs feststellen. Die Studien der Verteilung und Colokalisierung der TJ-Proteine liefern uns viele Informationen über das Verhalten der Proteine in verschiedenen TJ-Zuständen. Ausserdem helfen solche Studien, die Sicherheit neuer parazellulären Permeationsverstärker besser zu evaluieren.

Das aktuelle TJ-Modell nimmt an, dass die extrazellulären Domänen der verschiedenen CLDs homo- und heterotypisch miteinander interagieren und so den parazellulären Raum schliessen. Wir benutzten eine vor kurzem entwickelte Strategie, die auf diesem Modell auf-

baut: freie Peptide bestehend aus Sequenzen aus den extrazellulären Domänen von TJ-Proteinen könnten kompetitiv die Interaktionen zwischen benachbarten Zellen konkurrenzieren. Dies sollte zu einer vorübergehenden Öffnung der TJ führen, ohne die involvierten Komplexe zu zerstören und ohne unerwünschte Nebenwirkungen auszulösen. Wir testeten einen Satz Peptide mit homologen Sequenzen zu den extrazellulären Domänen von humanen CLD1, CLD2 und CLD4 auf die Fähigkeit, TJs in MDCK Zellen zu beeinflussen. Der Einfluss auf TJs wurde mittels Messung des transepithelialen elektrischen Widerstands (TEER) und Permeationsuntersuchungen mit Mannitol überprüft. Wir veränderten verschiedene Faktoren, um die optimalen Bedingungen für eine modulierende Aktivität zu finden. Dazu gehörten unter anderem die Konzentration von foetalem Kalbserum (FCS) in der Zellkultur, der Redox-Zustand der Peptide, die Zelldichte und die Peptidkonzentration. Von 14 getesteten Sequenzen führten zwei (CLD1 49-60 und CLD2 31-49) zu einer Abnahme des TEERs bei gleichzeitiger Zunahme der Mannitol Permeabilität. Leider zeigten genauere Untersuchungen mit CLSM eine starke Veränderung der Zellmorphologie und veränderte Immunfärbungen von ZO-1 und OCLN, die auf den Einfluss von Peptidaggregaten zurückzuführen sind. Als Positivkontrolle testeten wir auch zwei Peptide mit homologen Sequenzen zu der ersten extrazellulären Domäne von Occludin, von welchen vorher gezeigt wurde, dass sie TJs in Zellen beeinflussen können. Im Gegensatz dazu fanden wir aber bei keinem der beiden Peptide einen Anstieg der Mannitol Permeation, weder in MDCK noch in Caco-2 Zellen. Ein fluoreszierendes Peptid mit homologer Sequenz zu Occludin wurde im Versuch mit MDCK Zellen endozytiert, ohne dass eine Bindung an TJ-Strukturen beobachtet werden konnte. In Versuchen mit Caco-2 Zellen fanden wir nur eine unspezifische Bindung an die Zellschicht. Wir konnten also zeigen, dass die Methode, TJs mit homologen Sequenzen zu den extrazellulären Domänen von CLDs and OCLN zu beeinflussen, uneffizient ist und die teilweise Modulation der TJs durch unspezifische Effekte der Peptide hervorgerufen wird.

Ein einfacher *in-vitro* Assay, welcher auf die Wechselwirkungen zwischen den extrazellulären Domänen von Claudinen aufbaut, wäre nützlich, neue Permeationsverstärker zu finden. In diesem Assay werden aufgereinigte Claudin-Proteine in Liposomen eingebaut. Die eingebauten Proteine könnten über die exponierten extrazellulären Domänen interagieren und so ein Aggregieren der Liposomen verursachen. Für einen Pilotversuch entschieden wir uns, mit CLD1 zu arbeiten, weil CLD1 in den meisten Epithelien von Säugetieren exprimiert wird und weil knock-out Studien in Mäusen die äusserst wichtige Rolle von CLD1 für den TJ-Aufbau gezeigt haben. Wir exprimierten His-tagged Claudin-1 (His-CLD1) in einem Baculovirus System, reicherten es an und bauten es mit Hilfe von Detergendsialyse in Phosphatidylcholin-Liposomen ein. In einer Pilotstudie konnten wir einen erfolgreichen Einbau von His-CLD1 in die Liposomen zeigen. Die Charakterisierung der Proteoliposomen durch 'dynamische Lichtstreuung' zeigte keinen Grössenunterschied zwischen Proteoliposomen und Kontrollliposomen (ohne Protein). Wir konnten auch keine Interaktion zwischen den Proteinen feststellen, d.h. keine signifikante Aggregation von Liposomen. Das Hauptproblem war die geringe Ausbeute an His-CLD1 nach der Aufreinigung, welche wohl auf den schlechten Expressionsgrad im Baculovirus zurückzuführen ist. Um diesen Assay weiter zu entwickeln, werden sowohl Expression als auch Reinigung verbessert werden müssen, um genügend CLD1 für den Einbau in Proteoliposomen zu produzieren.

1 Introduction

1.1 The junctional complex

The key role of epithelia and endothelia is the formation of barriers that allow the generation and maintenance of compartments with different compositions, a fundamental requirement for the physiological functioning of organs (Balda and Matter, 1998). In the cell sheets a set of specialised structures form the junctional complex, which is responsible for the intercellular contacts and sealing. The junctional complex of epithelial cells is located at the apical part of the lateral membrane and consists of tight junctions (TJs), adherens junctions (AJs), desmosomes (Farquhar and Palade, 1963) and gap junctions (Goodenough et al., 1996). Desmosomes are buttonlike points of intercellular contact that hold cells together and provide anchoring sites for intermediate filaments (Garrod et al., 1996). Adherens junctions form a continuous adhesion belt and hold neighboring cells together through a family of calcium-dependent cell-cell adhesion molecules (cadherins) that are linked to actin and myosin filaments (Gumbiner, 1996; Yap et al., 1997). Gap junctions mediate communication between cells by allowing small molecules to pass from cytoplasm to cytoplasm of neighboring cells, thereby metabolically and electrically coupling them together (Kumar and Gilula, 1996; Simon and Goodenough, 1998). In the following the focus will be on TJs.

1.2 Tight junctions

1.2.1 Functions

The TJs possess multiple functions. The fundamental role of TJs is a barrier function, i.e. to form a barrier for the diffusion of solutes through the intercellular space (Anderson et al., 2004). The diffusion barrier is not an absolute one but semipermeable. It allows a selective passage of solutes, depending on their charge and size (Aijaz et al., 2006; Tsukita et al., 2001). Charge selectivity varies little among different epithelia and in most cases shows a cation selectivity (Fanning et al., 1999). An anion-selective transport was also found in a few cases, such as the rabbit colon or the frog skin (Powell, 1981). The paracellular barrier is also size selective. Only small hydrophilic molecules (up to 400 Da, in case of rat small intestine) can pass through the paracellular space (Artursson et al., 1993). The apparent permeability of hydrophilic non-electrolyte markers decreases with the increasing hydrodynamic radius of the marker up to a certain point, which is interpreted as the pore size (Watson et al., 2001). The reported pore sizes vary widely (4-40 Å), although most are in the range of 8-9 Å in diameter (Van Itallie and Anderson, 2006).

In addition to the barrier function, TJs act as a fence within the plasma membrane to create and maintain the apical and basolateral membrane domains. This has been demonstrated first by Dragsten et al. (1981), who showed that fluorescent probes capable of flip-flop transition can redistribute from the apical to the basolateral membrane, whereas the probes that are not able to flip-flop from the outer to the inner membrane leaflet remain in the apical membrane. This result was later confirmed with fluorescent lipids (van Meer and Simons, 1986).

TJs are also involved in basic cell processes like cell growth and differentiation (Balda and Matter, 1998; Matter et al., 2005). For example, a fraction of ZO-1 accumulates in the nucleus of growing cells suggesting that it might be directly involved in nuclear processes (Gottardi et al., 1996). Moreover, ZO-1 and the transcription factor ZONAB (ZO-1-associated nucleic acid binding) function in the regulation of the expression of ErbB-2, a tyrosine kinase co-receptor important for epithelial differentiation and morphogenesis, indicating that there is a direct linkage between the TJs and regulation of gene expression (Balda and Matter, 2000).

Disturbance of the fence or barrier function is relevant to a number of human diseases, such as the Crohn's disease, multiple sclerosis, primary biliary cirrhosis, cystic fibrosis and many others, including several types of cancer (Sawada et al., 2003). Particularly, the expression of transmembrane proteins of TJs (see Sec. 1.2.4) has been found to be altered in several cancers (Morin, 2005). For example, claudin-1 has been found reduced in breast carcinoma, where it has been suggested to act as a potential tumor suppressor (Tokes et al., 2005; Kramer et al., 2000). Claudin-7 was reported downregulated in the invasive breast carcinoma, correlating with histological grade and metastasis (Kominsky et al., 2003; Sauer et al., 2005). On the other hand, many studies have shown that certain claudins are upregulated in cancer. Claudin-1 has been found upregulated in the colorectal (de Oliveira et al., 2005; Miwa et al., 2000) and pancreatic cancer (Iacobuzio-Donahue et al., 2002). Claudin-4 upregulation in the pancreatic cancer cells caused reduced invasiveness, tumorigenicity and metastatic potential (Michl et al., 2003). Although the exact roles of claudins in tumorigenesis are still being uncovered, it is clear that they represent promising targets for cancer detection, diagnosis and therapy (Morin, 2005; Offner et al., 2005; de Oliveira and Morgado-Diaz, 2007).

1.2.2 Morphology

The TJ as a distinct morphological entity was described first in 1963 as a series of discrete contacts between the plasma membranes of adjacent cells (Farquhar and Palade, 1963). The morphology of TJs was intensively analysed by freeze-fracture replica electron microscopy (Staehelin et al., 1969; Staehelin, 1973). On the replica micrograph (Fig. 1.1), TJs appear as a set of continuous, anastomosing intramembranous particle strands on the protoplasmatic fracture face (P-face) with complementary grooves on the exoplasmatic fracture face (E-face) (Tsukita et al., 2001).

Two models have been proposed to explain the nature of TJs. The lipid model postulates that the TJ fibrils are derived from an unusual lipid arrangement, probably inverted cylindrical micelles (Kachar and Reese, 1982; Pinto da Silva and Kachar, 1982), whereas in the protein model, TJ strands are represented by units of integral membrane proteins within the lipid bilayers (van Meer and Simons, 1986). In the lipid model, the exoplasmatic leaflets of the two apical

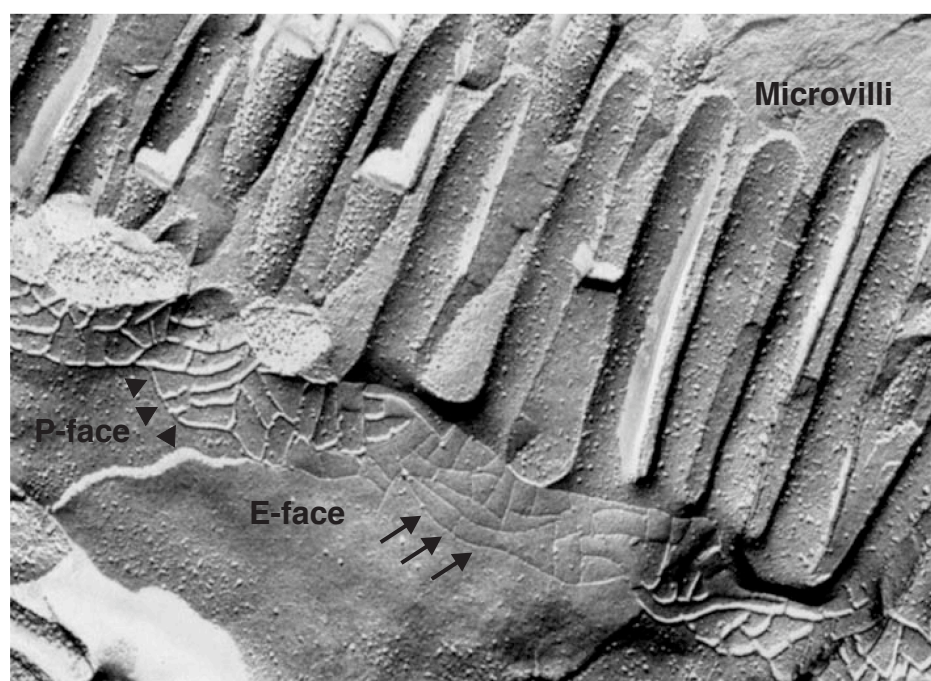


Figure 1.1: **Freeze-fracture replica micrograph of mouse intestine.** Freeze-fracture replica electron microscopic image revealing TJs as intramembranous strands or fibrils (arrowheads) on the protoplasmic fracture face (P-face) with complementary vacant grooves (arrows) on the exoplasmic fracture face (E-face). Modified from Van Itallie and Anderson (2006).

plasma membranes of neighboring cells would be continuous, allowing lipids to diffuse from one cell to the other. However, it has been found that an endogenous glycolipid (the Forssman antigen) present in the exoplasmic leaflet of the apical membrane of MDCK strain II cells is unable to pass to MDCK strain I cells, which lack this glycolipid (van Meer et al., 1986). Similarly, fluorescent lipids loaded into the apical membrane of MDCK do not diffuse to the adjacent cells. In addition, a change of the total composition of phospholipids, sphingolipids and cholesterol in epithelial cells does not alter the appearance of TJ strands nor the gate or fence function (Calderon et al., 1998). These findings and the discovery of integral membrane proteins within the TJs (Furuse et al., 1993, 1998a) strongly favor the protein model.

1.2.3 Molecular structure

Studies on the protein components of the vertebrate TJs revealed a complex network of proteins (Fig. 1.2), which may be divided into three groups. The group of integral TJ proteins, such as occludin (Furuse et al., 1993), claudins (Furuse et al., 1998a), junctional adhesion molecule (JAM) (Martin-Padura et al., 1998), interact homo- or heterotypically to bridge the apical intercellular space. Claudins are believed to be responsible for the actual sealing mechanism of TJs (Koval, 2006). The JAM protein is involved in the regulation of transmigration of monocytes through the vessel wall (Lechner et al., 2000; Martin-Padura et al., 1998). The group of

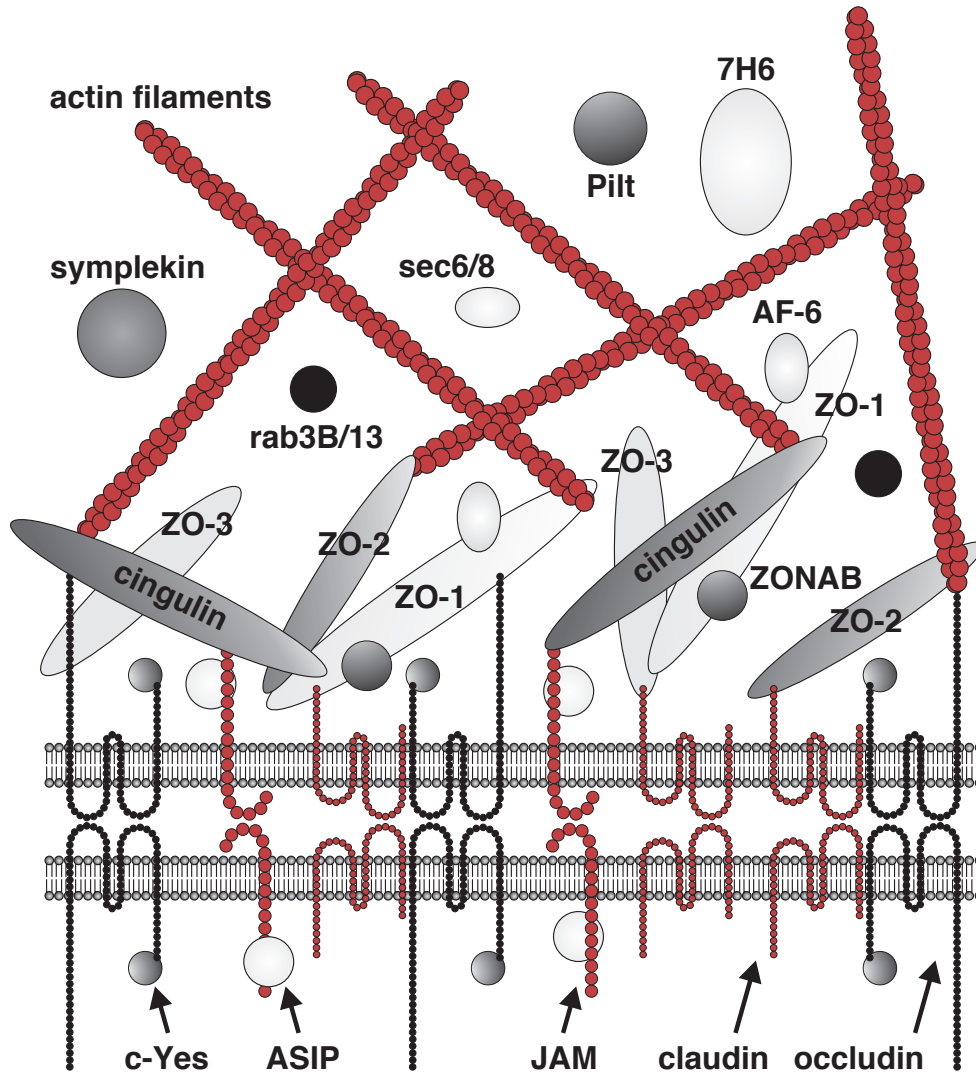


Figure 1.2: **Complex interactions between tight junction proteins.** Current model of interaction between TJ proteins. The transmembrane proteins claudins and occludin form linear co-polymers within the membrane of two adjacent cells. The plaque proteins are interacting directly with the transmembrane proteins and serve as a link to the cytoskeleton. Abbreviations: AF6, afadin; 7H6, barmotin; ASIP, atypical PKC isotype-specific interacting protein; c-Jun, non-receptor tyrosine kinase; JAM, junctional adhesion molecule; Pilt, protein incorporated later into TJs; rab3B/13, proteins rab3B and rab13 responsible for vesicular transport or fusion; sec6/8, mammalian homologues of sec6 and sec8 yeast gene products; ZONAB, ZO-1-associated nucleic acid-binding protein; ZO-1, -2, -3, zonula occludens-1, -2, -3. Adapted from Tsukita et al. (2001) and assembled according to Aijaz et al. (2006).

TJ plaque proteins, such as zonula occludens proteins (ZO-1, -2, -3) (Stevenson et al., 1986; Gumbiner et al., 1991; Haskins et al., 1998) or cingulin (Citi et al., 1988), serve as a link between the integral TJ proteins and the actin cytoskeleton. The group of cytosolic and nuclear proteins, tumor suppressors, transcriptional and posttranscriptional factors, such as symplekin (Keon et al., 1996), AF-6 (Yamamoto et al., 1997), ZO-1-associated nucleic acid binding protein (ZONAB) (Balda and Matter, 2000), rab3B and rab13 (Sunshine et al., 2000; Zahraoui et al., 1994; Novick and Zerial, 1997), 7H6 (Zhong et al., 1993), Pilt (Kawabe et al., 2001) and many others, regulate the assembly and polarization of the junctional complex.

1.2.4 Transmembrane proteins

1.2.4.1 Occludin

Occludin (Fig. 1.3), a 60 kDa protein, was identified as the first integral membrane protein localized at TJs of chicken (Furuse et al., 1993) and later on also in TJs of mammals (Ando-Akatsuka et al., 1996; Saitou et al., 1997). Occludin in vertebrates is encoded by a single occludin gene, nevertheless, five different isoforms have been described, which arise by alternative splicing (Ghassemifar et al., 2002; Mankertz et al., 2002; Muresan et al., 2000). The Kyte and Doolittle hydrophobicity analysis (Kyte and Doolittle, 1982) of occludin predicts four transmembrane domains, a long carboxy-terminal cytoplasmic domain, a short amino-terminal cytoplasmic domain and two extracellular loops of approximately the same size (Tsukita et al., 1999, 2001). Both extracellular loops of occludin are rich in tyrosines. More than half of the first loop residues are tyrosines and glycines (Gonzalez-Mariscal et al., 2003) and this feature is well conserved phylogenetically (Ando-Akatsuka et al., 1996). The sequence leucine-tyrosine-histidine-tyrosine (LYHY) found within the second extracellular loop of occludin was suggested to be an occludin cell adhesion recognition sequence (CAR) (Blaschuk et al., 2002). The last 150 amino acids of the carboxy tail of occludin are important for the interaction with F-actin (Wittchen et al., 1999), proteins ZO-1, -2 and -3 (Furuse et al., 1994; Haskins et al., 1998; Itoh et al., 1999b), protein kinase C- ζ , non-receptor tyrosine kinase (c-Yes) and phosphatidylinositol 3-kinase as well as with gap junction component connexin-26 (Nusrat et al., 2000a). Additionally, this region could interact with the same region on another occludin (Nusrat et al., 2000a). Occludin is phosphorylated on serine, threonine and tyrosine residues, and phosphorylation appears to be an important mechanism for the regulation of occludin (Farshori and Kachar, 1999; Hirase et al., 2001; Andreeva et al., 2001; Sakakibara et al., 1997; Wong, 1997; Chen et al., 2002; Tsukamoto and Nigam, 1999).

When overexpressed in mouse L-fibroblasts, occludin concentrates in a punctate manner at the cell-cell borders, where short TJ strand-like structures occur (Furuse et al., 1998b). In transfected fibroblasts, occludin shows some adhesion activity (Van Itallie and Anderson, 1997). Furthermore, overexpression of chicken occludin in cultured Madin Darby canine kidney (MDCK) cells increases the number of TJ strands, with a concomitant elevation of their transepithelial electrical resistance (TEER) (McCarthy et al., 1996). Overexpression of mutant forms of occludin in epithelial cells leads to changes in the gate and fence function of TJs (Balda et al., 1996; Bamforth et al., 1999). Thus, there is considerable evidence that occludin is involved in

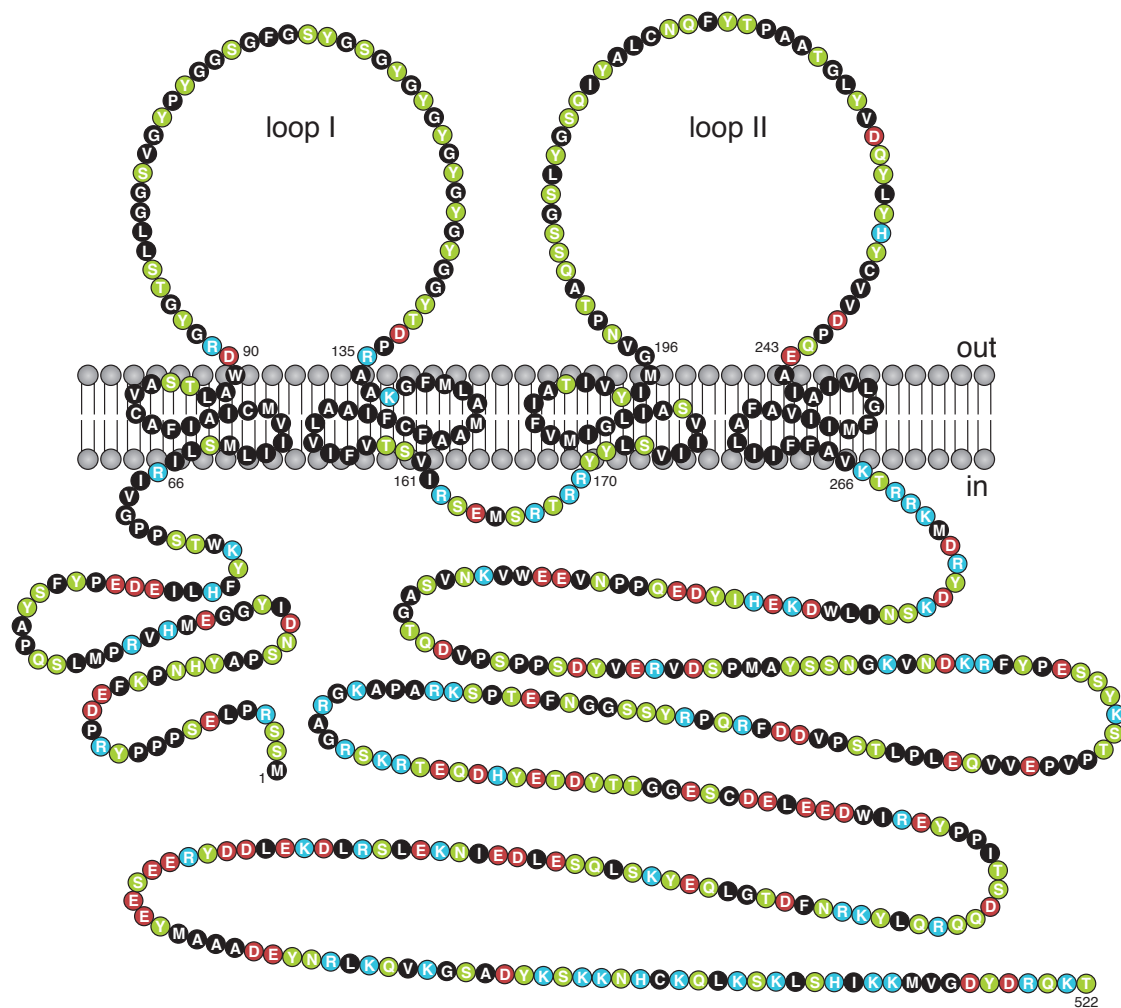


Figure 1.3: **Predicted folding topology of human occludin.** Amino acids are written in one-letter code according to the IUPAC convention (IUPAC-IUB, 1984). Acidic (red color), basic (blue color), nonpolar (black color) and polar uncharged (green color) residues are indicated. Occludin sequence and domain topology retrieved from UniProtKB/Swiss-Prot database (Boeckmann et al., 2003; Wu et al., 2006) under accession number Q16625. Abbreviations: out, extracellular space; in, intracellular space.

the formation of the TJs. However, occludin is absent in the TJs of Sertoli cells in guinea pig and human (Moroi et al., 1998). Moreover, occludin deficient-embryonic stem cells differentiate into polarized epithelial cells with well-developed TJ structures (Saitou et al., 1998). These different findings led to searching for other integral components of TJs and resulted in the discovery of the claudins (see below).

Tricellulin, a protein concentrated at the vertically oriented TJ strands of tricellular contacts, is structurally similar to occludin, bearing four transmembrane domains and two extracellular loops (Ikenouchi et al., 2005). When tricellulin expression was suppressed with RNA interference, the epithelial barrier was compromised, and tricellular contacts and TJs were disorganized. Mutations that remove all or most of the cytosolic domain of tricellulin that binds to ZO-1

were associated with a hearing loss in humans (Riazuddin et al., 2006).

1.2.4.2 Claudins

The paradoxical results obtained with occludin-deficient embryonic stem cells led to a renewed effort by Tsukita and co-workers to identify other integral membrane proteins of the TJs, using the same chick liver fraction used to identify occludin. By a guanidine extraction as well as sonication, followed by sucrose density gradient centrifugation, a 22 kDa-band was detected on the silver stain (Furuse et al., 1998a). Peptide sequencing revealed that this band consists of two proteins (named claudin-1 and -2) with 211 (Fig. 1.4) and 230 amino acids, respectively. Both proteins did not show any sequence similarity to occludin. To date, 23 human claudins have been identified, including two splice variants (Koval, 2006). All encode 20-27 kDa proteins with four transmembrane domains, two extracellular loops and a short carboxyl intracellular tail (Gonzalez-Mariscal et al., 2003). The first extracellular loop is significantly larger and more hy-

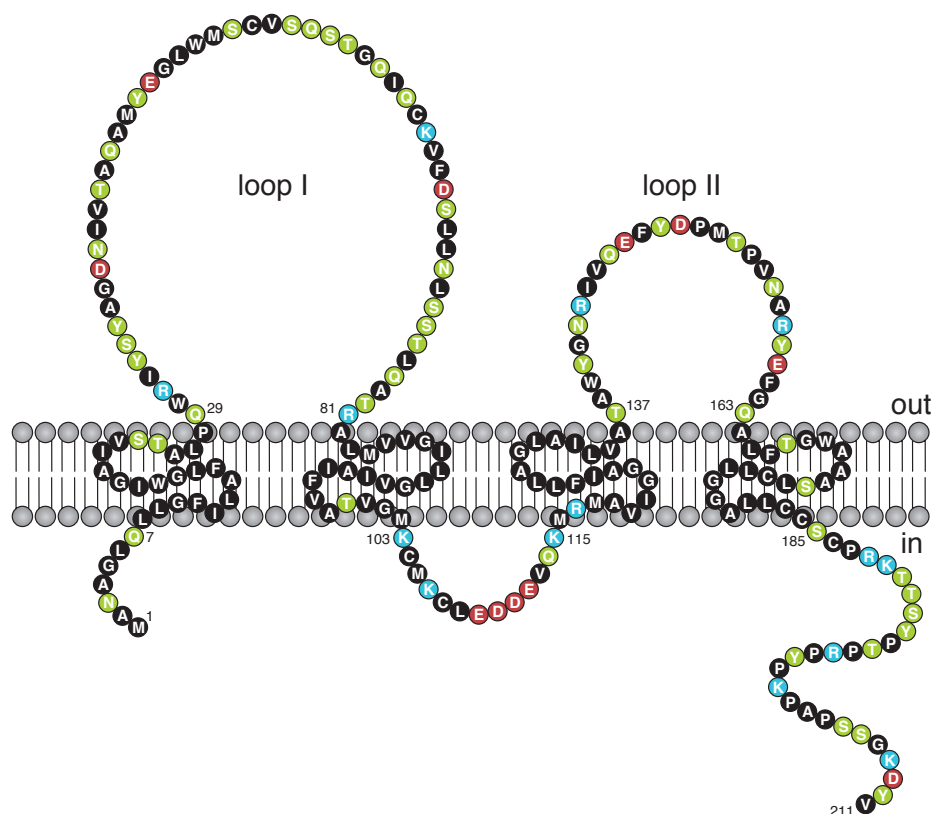


Figure 1.4: **Predicted folding topology of human claudin-1.** Amino acids are written in one-letter code according to the IUPAC convention (IUPAC-IUB, 1984). Acidic (red color), basic (blue color), nonpolar (black color) and polar uncharged (green color) residues are indicated. Claudin-1 sequence and domain topology retrieved from UniProtKB/Swiss-Prot database (Boeckmann et al., 2003; Wu et al., 2006) under accession number O95832. Abbreviations: out, extracellular space; in, intracellular space.

drophobic than the second extracellular loop; both claudin loops display a number of charged residues. The first extracellular loop contains a highly conserved sequence of amino acids GLW-XX-C-X(8-10)-C (Morita et al., 1999; Turksen and Troy, 2004). Although it has not been directly demonstrated, the conserved cysteine residues may stabilize intra- or inter-loop interactions via disulfide bridges (Van Itallie and Anderson, 2006). The second extracellular loop acts as a receptor for a bacterial enterotoxin (Fujita et al., 2000). All claudins (except claudin-12) end in PDZ¹-binding motifs, which can interact with cytoplasmic TJ proteins such as ZO-1, -2, -3, MUPP1 and PATJ (Itoh et al., 1999a; Hamazaki et al., 2002; Jeansonne et al., 2003; Roh et al., 2002). Furthermore, the C-terminal end of some claudins is palmitoylated (Van Itallie et al., 2005) and/or phosphorylated (Fujibe et al., 2004; Tanaka et al., 2005).

Claudins are expressed in a tissue-specific manner (Morita et al., 1999) and variations of the tightness in different tissues were proposed to be determined by the combinations and mixing ratios of different types of claudins (Tsukita and Furuse, 2000; Balkovetz, 2006). The evidence for the latter comes from the observation, that when claudin-2 was introduced into MDCK I (primarily expressing claudin-1 and -4; $\sim 10'000 \Omega \cdot \text{cm}^2$) the TEER value of these transfectants fell to the level of MDCK II (expressing large amounts of claudin-2 in addition to claudin -1 and -4; $150-500 \Omega \cdot \text{cm}^2$) without any changes in the number of TJ strands (Furuse et al., 2001). By contrast, the exogenously expressed claudin-3 did not affect the TEER value of MDCK I cells. In addition, epidermal growth factor inhibits the expression of claudin-2 while simultaneously inducing the expression of claudin-1, -3 and -4 in MDCK cells, which results in a 3-fold increase of the TEER (Singh and Harris, 2004). Claudins can adhere to each other homotypically or heterotypically (Furuse et al., 1999), and the respective extracellular domains directly contribute to the formation of ion-selective channels or pores, which influence the passage of ions through the paracellular space (Tsukita and Furuse, 2000; Colegio et al., 2002, 2003; Furuse et al., 1999; Van Itallie et al., 2001, 2003; Amasheh et al., 2002).

The paired strands consisted of claudins are not rigid structures but highly dynamic. When a fusion protein of green fluorescent protein (GFP) with claudin-1 was expressed in L-fibroblasts, considerable re-organization of paired strands was observed. The strands were occasionally broken and re-annealed, and dynamically associated with each other. In addition, during movements of mouse Eph4 epithelial cells within the cellular sheets, endocytosis of GFP-claudin-3 (together with endogenous claudins) was observed (Matsuda et al., 2004), suggesting that endocytosis is important mechanism for a TJ re-organisation.

The importance of claudins in the function of TJs was further demonstrated by claudin knock-out mice, revealing their highly specialized roles in particular cell types. In claudin-1-deficient mice, the epidermal barrier is severely affected, leading to dehydration, wrinkled skin and death of the animals within one day of birth (Furuse, 2002). In the brains of claudin-5-deficient mice, the permeability of the blood brain barrier was selectively affected only for small molecules (< 800 D) (Nitta et al., 2003). Claudin-11-null mice exhibit neurological and reproductive deficits due to the absence of TJs in the central nervous system and between Sertoli cells (Gow et al., 1999; Kitajiri et al., 2004). Claudin-14-null mice were deaf due to rapid degeneration of cochlear

¹PDZ is an acronym combining the first letters of three proteins, the post synaptic density protein (PSD95), the *Drosophila* disc large tumor suppressor (DlgA), and ZO-1 protein, which were first discovered to share a common domain (Cereijido and Anderson, 2001).

outer hair cells (Ben-Yosef et al., 2003) and claudin-19-null mice exhibited behavioral abnormalities due to an affected conductivity of the peripheral myelinated nerve fibers (Miyamoto et al., 2005).

In summary, claudins constitute the backbone of TJs and play a crucial role in the formation of the TJ barrier. However, little is known about the mechanism of the interaction between claudins. Detailed claudin structural information would be extremely useful to help provide a mechanistic framework for claudin function and assembly, and for therapeutic strategies.

1.2.5 Plaque proteins

1.2.5.1 Zonulae occludens proteins

Zonula occludens-1 (ZO-1) was the first peripheral membrane protein identified within the TJs of epithelia and endothelia (Stevenson et al., 1986). Non-epithelial cells, such as fibroblasts, show ZO-1 dispersed in the cytoplasm and concentrated at the cell-cell adhesion sites that contain also cadherin (Itoh et al., 1993). The cDNA sequencing showed that ZO-1 exists in two isoforms (ZO-1 α^+ and ZO-1 α^-) differing by an internal 80-residue domain (Willott et al., 1992). Expression in different tissues showed that the α^- isoform is associated with structurally dynamic junctions, whereas the α^+ isoform with junctions, which are less dynamic (Balda and Anderson, 1993). Other alternative splicing domains were also identified, however, their functional significance still remains unclear (Gonzalez-Mariscal et al., 1999).

When ZO-1 was immunoprecipitated from cell lysates of MDCK cells, two proteins with a molecular weight 160 kDa and 130 kDa, respectively, were co-immunoprecipitated (Gumbiner et al., 1991; Balda et al., 1993; Haskins et al., 1998). These proteins, ZO-2 and ZO-3, show sequence similarity with ZO-1 (Jesaitis and Goodenough, 1994; Haskins et al., 1998). All three proteins belong to the same protein family named MAGUK (membrane associated guanylate kinase homologues) (Gonzalez-Mariscal et al., 2003). The MAGUK family is composed of a diverse group of proteins, each containing a PDZ domain (one to three copies), a src-homology 3 (SH3) domain and a guanylate kinase homologous region (GUK) (Gonzalez-Mariscal et al., 2000; Funke et al., 2005). ZO-1 can interact with JAM, claudins and occludin, form stable complexes with either ZO-2 or ZO-3 via a PDZ-PDZ domain mediated interaction, bind to other proteins such as cingulin, and contains a discrete actin-binding domain in its C-terminal half (Bazzoni et al., 2000; Cordenonsi et al., 1999a; Ebnet et al., 2000; Fanning et al., 1998; Furuse et al., 1994; Itoh et al., 1999a). In addition, ZO-1 was found to interact with multiple connexins, the major components of gap junctions (Aijaz et al., 2006).

Experimental evidence suggests that ZO-1 is required for the control of TJ assembly. When ZO-1 is deleted from cultured epithelial cells by either homologous recombination or short interfering RNA (siRNA), the TJ assembly is markedly slowed down (Umeda et al., 2004; McNeil et al., 2006). In addition, Umeda et al. (2006) demonstrated that cultured cells with reduced levels of both ZO-1 and ZO-2 fail to form TJs, and that re-expression of ZO-1 alone in these cells is sufficient to restore TJ structure and the paracellular barrier. Finally, the expression of mutant ZO-1 lacking an unique motif (U6) in cultured cells induces the formation of ectopic TJ strands containing occludin and claudins (Fanning et al., 2007).

1.2.5.2 Cingulin

Cingulin (140-160 kDa) is an acidic, heat stable phosphoprotein, identified by monoclonal antibodies that recognized a protein copurifying with myosin from the chicken intestinal epithelial cells (Citi et al., 1988, 1989; Citi and Denisenko, 1995). Cingulin is a parallel dimer of two subunits, each with a globular head, a coiled-coil rod, and a globular tail (Cordenonsi et al., 1999a). The coiled-coil region mediates a self-interaction, whereas the globular region interacts directly with ZO-1, -2, -3 and JAM (Cordenonsi et al., 1999a; D'Atri et al., 2002; Bazzoni et al., 2000). Glutathione S-transferase pull-down experiments revealed that cingulin interacts directly with the C-terminal region of occludin (Cordenonsi et al., 1999b). In addition, purified recombinant cingulin co-pellets with F-actin after a high speed centrifugation and promotes the sedimentation of F-actin under a low speed centrifugation (D'Atri and Citi, 2001). Finally, the C-terminal fragment of cingulin interacts with myosin (Cordenonsi et al., 1999a). These findings suggest that cingulin act as an F-actin cross-linking protein, which may recruit actin filaments and transmit the mechanical force generated by the actin-myosin contraction to the membrane domain of TJs, resulting in a modulation of the TJ barrier (D'Atri and Citi, 2001). In addition, cingulin may play an important role in the biology of vertebrate epithelia, because it is one of the first proteins that assembles into the TJs in early vertebrate embryos (Cardellini et al., 1996; Fesenko et al., 2000; Fleming et al., 1993). The expression of a mutant cingulin, lacking the head domain, in embryonic bodies derived from the embryonic stem cells did not prevent TJ formation, but increased the transcription levels of occludin, claudin-2, claudin-6 and claudin-7 due to an increase in the expression of transcription factors involved in the endodermal differentiation (Guillemot et al., 2004). Furthermore, the cingulin-depleted MDCK cells show a higher protein and mRNA level of claudin-2 and ZO-3, but not altered barrier functions (Guillemot and Citi, 2006). These data support the role of cingulin in the biogenesis and organization of TJs.

1.3 Permeation across *in-vivo* barriers

1.3.1 Routes of permeation

Molecules cross the epithelial and endothelial cell sheets by the transcellular or the paracellular pathway (Fig. 1.5). The transcellular transport is an active or passive process. Active processes, such as a carrier-mediated transport and transcytosis are energy-dependent. Passive transcellular processes are energy-independent and typical for lipophilic molecules, which easily cross the membrane by diffusion. The paracellular component of the transport is a completely passive process along the concentration gradient and is relevant only for hydrophilic compounds with low molecular weights, e.g. < 400 Da for the small intestine (Tsukita et al., 2001; Anderson, 2001; Ward et al., 2000; Fanning et al., 1999; Artursson et al., 1993).

1.3.2 Strategies to enhance paracellular permeation

Mucosal surfaces are the most common and convenient routes for delivering drugs to the body (Sharma et al., 2006). However, many useful therapeutic molecules, such as insulin, octreotide,

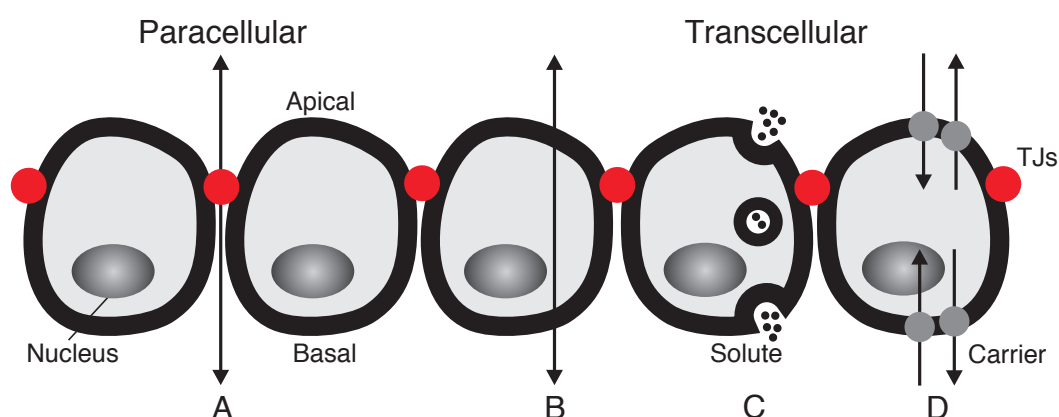


Figure 1.5: **Transport pathways through a cell monolayer (schematically).** (A) Paracellular flux through tight junctions (TJs) occurs strictly by passive diffusion in contrast to transcellular flux, which can occur either by (B) passive (diffusion) or active processes, such as carrier-mediated transport (D) and transcytosis (C). Adapted from Ho et al. (2000).

nesiritide, buserelin, vasopressin and many others, are large and hydrophilic, thus displaying a poor oral bioavailability. Low oral bioavailability leads to a poor control of the plasma concentrations and to a variability in the effects of the drugs. Thus, these therapeutics must be applied parenterally, which reduces the patient's compliance. Considerable attention has been given to strategies for improving the absorption of hydrophilic drugs (LeCluyse and Sutton, 1997). Various approaches, including the chemical modification to form prodrugs and improved or new drug formulations (e.g. microemulsions), have been described. One of them is the use of permeation enhancers. An enormous number of permeation enhancers has been published. The 'paracellular permeation enhancers' (Tab. 1.1) represent a way to increase the absorption by a TJ opening. However, most of the TJ modulators mediate their effect by an activation of intracellular signaling pathways, such as the protein kinase C pathway. The triggered cellular response leads to a change in the phosphorylation pattern of the cytoskeletal proteins associated with TJs and results in an increased permeability to solutes. Due to a complex activation of signaling cascades, often an irreversible opening of the TJs occurs. Additionally, many TJ modulators are more or less surface-active, which leads to a solubilisation of membrane components (Aungst, 2000; Fasano, 1998; Madara, 1998; Mullin et al., 2000; Ward et al., 2000; Salama et al., 2006). All these effects result in mucosal irritation and toxic effects on the epithelia. Up to now, only a few countries (e.g. Japan and Sweden) have approved molecules belonging to the group of permeation enhancers for therapeutic use (LeCluyse and Sutton, 1997).

Recently, a new approach to induce a transient loosening of TJs, without complete disruption of the complexes and unwanted cell reactions was suggested. The strategy is based on the use of peptide homologues containing the sequences of the extracellular loops of the TJ transmembrane proteins to compete for the potential sealing sequences between the adjacent cells. Synthetic peptides were previously used as specific probes for the mapping of protein

Table 1.1: Paracellular permeation enhancers

Class	Molecule	Reference
Alkylglycerols	Pentylglycerol	Erdlenbruch et al. (2000)
Analogues of bradykinin	Lobradimil	Warren et al. (2001)
Anionic surfactants	SDS	Anderberg and Artursson (1993)
Bile salts	Sodium glycocholate	Lindhardt and Bechgaard (2003)
Calcium chelators	EDTA, EGTA	Tomita et al. (1996)
Cationic surfactants	Chitosans	van der Merwe et al. (2004)
Fatty acid esters	Palmitoyl carnitine	Duizer et al. (1998)
Medium fatty acids	Sodium caprate	Chao et al. (1999)
Osmotic agents	Mannitol, arabinose	Rapoport (2001)
Phosphate esters	DPC	Liu et al. (1999)

Abbreviations: DPC; dodecylphosphocholine; EDTA, ethylenediaminetetraacetic acid; EGTA, O,O'-bis-(2-aminoethyl)-ethyleneglycol-N,N,N',N'-tetraacetic acid; SDS, sodium dodecylsulfate

binding of cell adhesion molecules (Kamboj et al., 1989). For example, two synthetic peptides representing most of the two presumed extracellular loops of connexin 32 and shorter peptides representing subsets of these larger peptides were found to inhibit cell-cell channel formation (Dahl et al., 1994).

A homologue to the second extracellular domain of chicken occludin (sequence 184-227) disrupted the transepithelial barrier of the *Xenopus* kidney epithelial cell line A6. The disruption of TJs was concentration-dependent (up to 10 μ M), with a slow onset of the effect over 24 hrs. In contrast, the first extracellular domain peptide and a peptide composed of the scrambled sequence of the same residues as peptide 184-227 were found to be ineffective (Wong and Gumbiner, 1997). Similar results were obtained by Vietor et al. (2001). By treatment of mouse mammary epithelial cells EpH4 with peptide homologue to the second extracellular domain of chick occludin (sequence 184-227), the TEER and the amount of occludin at the TJs decreased with a subsequent formation of multilayered unpolarized cell clusters. Peptides corresponding to the first extracellular domain had no effect. In addition, a synthetic peptide bearing the sequence (209-230) from the second external loop of rat occludin perturbed the assembly of TJs of rat Sertoli cells. The disruption of the TJs was dose-dependent (0.2-4 μ M) and reversible. When this peptide was intratesticularly administered to adult Sprague-Dawley rats, the germ cells were completely depleted from the epithelium within 27 days post-application. This antispermatogenic effect was a completely reversible process (Chung et al., 2001). It was also demonstrated that a cyclic peptide containing the amino acid sequence leucine-tyrosine-histidine-tyrosine (LYHY), which is found in the second extracellular domain of all mammalian occludins, is sufficient to disrupt the human umbilical vein endothelial (HUVEC) cells and to block the aggregation of fibroblasts stably transfected to express occludin (Blaschuk et al., 2002). Finally, a peptide homologue to the second extracellular loop of human occludin (se-

quence 210-228) was shown to influence the TJ assembly of the human epithelial intestinal cell line T84 and to interact with occludin, claudin-1 and JAM (Nusrat et al., 2005). Peptide homologues to the first extracellular domain failed to influence the TJs. All these findings are supported by studies demonstrating a critical role of the second extracellular loop of occludin (Medina et al., 2000; Wang et al., 2005).

Other groups reported opposite findings, namely that not the second but the first domain homologues of occludin possess the ability to modulate TJs. Peptides of the first extracellular domain of human occludin (sequence 90-112 and 113-135, respectively) inhibited adhesion in occludin-transfected rat fibroblasts; complete inhibition was achieved at 100 μ M for both peptides. A peptide with an equal isoelectric point as the peptide 90-112 did not inhibit the cell adhesion (Van Itallie and Anderson, 1997). Lacaz-Vieira and colleagues showed that small peptide homologues to segments of the first external loop (sequence 100-108/109 and 102-109) of chick occludin impair the calcium-induced TJ resealing after the TJ opening by a calcium depletion. Peptide bearing the sequence corresponding to a segment of the second extracellular loop had no effect (Lacaz-Vieira et al., 1999). Furthermore, Tavelin et al. (2003) assayed a number of synthetic peptides (6 to 48 amino acids in length) covering both the first and second extracellular loop of human occludin. A peptide corresponding to the sequence (196-243) of the second external loop of occludin showed no effect on TEER and mannitol permeability in the human colon adenocarcinoma (Caco-2) cell line. In contrast, a peptide corresponding to the N-terminal half of the first extracellular loop (sequence 90-103; 100 μ M) increased the mannitol permeability in a time-dependent manner (5- and 22-times after 240 and 360 min, respectively), when applied from both apical and basolateral side of the cell culture. However, when applied apically only, no significant increase in the permeability of mannitol was observed. In contrast, the peptide 90-103 conjugated to 2-aminotetradodecanoic acid (lipoamino acid) was also active if only added from the apical side. For the TJ-modulating effect, cleavage of the lipoamino acyl residue was required to release the free peptide homologue 90-103. The D-stereoisomer of the peptide conjugate displayed a rapid and transient effect within 20 min post-application, as compared to the L-stereoisomer that showed a sustained increase in the permeability over 180 min. The lipoamino acid-peptide 90-103 conjugate reduced the TEER, altered the TJ permeability and the distribution of occludin in human airway epithelial cells (Everett et al., 2006).

It is unclear why such variability is observed between the above mentioned studies using peptides corresponding to the first and second extracellular loop of occludin. It is possible that these differences arise from different cell culture models and occludin peptide sequences derived from a variety of animal species (Nusrat et al., 2005; Mrsny, 2005).

A similar strategy to modulate TJs by peptide homologues to claudins has not been reported up to now. However, preliminary data from our group showed that claudin peptide homologues had an influence on cultured MDCK cells (Riesen, 2002).

A peptide modulator specifically interacting with claudin was previously described. This modulator is derived from *Clostridium perfringens* enterotoxin (CPE), a single polypeptide with molecular mass of 35 kDa, which is responsible for the diarrheal symptoms associated with food poisoning in humans (McClane et al., 1988). The enterotoxin has two functional domains, an N-terminal cytotoxic region and a C-terminal binding region (C-CPE). The C-CPE was shown to modulate TJs by binding to the second extracellular loops of claudin-3 and -4 (Sonoda et al.,

1999; Katahira et al., 1997; Fujita et al., 2000). Treatment with C-CPE caused an absorption of 4 kDa-dextran in rats. This enhanced activity was 400-fold above the one observed for sodium caprate and these effects were not accompanied by injury of the intestinal mucosa (Kondoh et al., 2005). Deletion analysis revealed that the C-terminal 16 amino acids of C-CPE, particularly the tyrosine residues, are responsible for the interaction with claudin-4 and the disruption of the TJ barrier (Takahashi et al., 2005; Ebihara et al., 2006; Harada et al., 2007).

1.4 Models to study tight junctions

1.4.1 Cell cultures

Currently, many cell cultures are available as a tool to study TJs. Among them, two well-characterized cell culture models, MDCK and Caco-2 cell line, are often used.

The MDCK cell line is one of the best-characterized epithelial cell lines (Cho et al., 1989; Irvine et al., 1999). It was established in 1958 by Madin and Darby from the kidney of a normal female cocker spaniel. The cells represent morphologically and functionally polarized epithelium, where during the formation of monolayers, TJs are formed as a gasket-like seal in the apical domains of the cells (Cereijido et al., 1978; Gaush et al., 1966; Rothen-Rutishauser et al., 1998a; Braun et al., 2000). The major advantage of the MDCK cells is that the monolayers reach their full differentiation already after 3-7 days in culture (Barker and Simmons, 1981; van de Waterbeemd et al., 2003).

The Caco-2 cells represent a human cell line mostly used as a model for drug absorption studies (Artursson et al., 1996). The cells were derived from a primary colonic tumor by the explant technique (Quaroni and Hochman, 1996) and form highly differentiated epithelia with numerous characteristics of small intestine such as the microvilli formation, a network of TJs, the expression of brush border enzymes and P-glycoprotein (P-gp) (Hidalgo and Li, 1996; Hunter et al., 1993). Labeling of P-gp with specific antibodies shows a 'patchy' localization of P-gp at the apical surface of the cell layer (Braun et al., 2000). The non-homogenous expression of P-gp may explain the fact, that in directed transport studies the differences between the transport rate in the two directions (apical to basal and basal to apical, respectively) are smaller than expected for a cell layer with a homogenous distribution of the efflux protein (Braun et al., 2000). When grown on polycarbonate cell culture membranes, Caco-2 cells form monolayers. In contrast, on polyethylene terephthalate membranes multilayers occur, where the polarization of cells is partially lost (Braun et al., 2000; Rothen-Rutishauser et al., 2000). A major disadvantage of the Caco-2 cell line is the large interclonal variability, i.e. the cells have tendency to alter their phenotype upon subculture (Audus et al., 1990; van de Waterbeemd et al., 2003), and the long cultivation time (21 days) that is required to obtain a full differentiation (Briske-Anderson et al., 1997; Irvine et al., 1999).

Mouse L-fibroblasts lack the expression of endogenous TJ proteins. They are thus used as a model to study the structure and function of selectively expressed transmembrane proteins of TJs. For example, FLAG-tagged claudin-1 and -2 expressed in fibroblasts were found to be highly concentrated at the cell-cell contacts and freeze-fracture replica of these sites

showed a well-developed network of strands, similar to those found in epithelia (Furuse et al., 1998b). Interestingly, when two L-fibroblasts singly expressing claudin-1, -2 or -3 were co-cultured, claudin-3 strands laterally associated with claudin-1 and claudin-2 strands to form paired strands, whereas claudin-1 strands did not interact with claudin-2 strands (Furuse et al., 1999). These findings suggested that claudins can adhere homo- and heterotypically to form the paracellular barrier. Finally, Sasaki et al. (2003) visualized the individual strands of claudins by expressing a GFP-tagged claudin-1, showing an unexpectedly high dynamic behavior of the strands within fibroblasts.

1.4.2 Proteoliposomes

The complexity of biological membranes makes it difficult to study membrane proteins *in-situ*. Therefore, purification and re-incorporation into artificial membranes is a powerful tool to analyze functional as well as structural aspects of membrane proteins (Eytan, 1982; Banerjee and Datta, 1983; Rigaud, 2002). This system is widely used for the characterization of membrane protein transporters and channels, such as P-glycoprotein (Ambudkar, 1995; Sharom, 1995; Rothnie et al., 2001), calcium channels (Nakao et al., 1988; Lee et al., 1994) and water channels (Zeidel et al., 1992). A reconstitution of purified connexins contributed to a better understanding of the structure, assembly, permeability and gating function of gap junctions (Kam et al., 1998; Ramundo-Orlando et al., 2005; Herve et al., 2004). Proteoliposomes have also been used to study specific interactions between solutes and membrane proteins (Gottschalk et al., 2002; Yang and Lundahl, 1995). In addition, reconstitution of membrane proteins into artificial membranes in order to form crystals has opened a new way to solve structures of transmembrane proteins inside a 'native-like' environment (Rigaud, 2002).

A similar approach to study an interaction of TJ proteins has not been described so far. The current model of TJs is based on the hypothesis that the extracellular domains of claudin molecules interact homotypically or heterotypically to bridge the paracellular space (Koval, 2006). Proteoliposomes with reconstituted claudins (Fig. 1.6) would represent a simple *in-vitro* model of TJs based on these interaction. If the interaction of the extracellular loops is sufficient to mediate association of proteoliposomes, we would be able to screen for molecules capable of breaking this interaction. These molecules would specifically target the extracellular domains of claudins, and thus, possibly, represent non-toxic and effective permeation enhancers. Apart from the screening of molecules binding to the CLD extracellular loops, proteoliposomes would be suitable to explore the interaction between different CLDs in order to refine the current model of TJs. The absence of a significant association of the proteoliposomes would suggest that also other interactions than those between the extracellular domains of claudins are responsible for the TJ sealing mechanism.

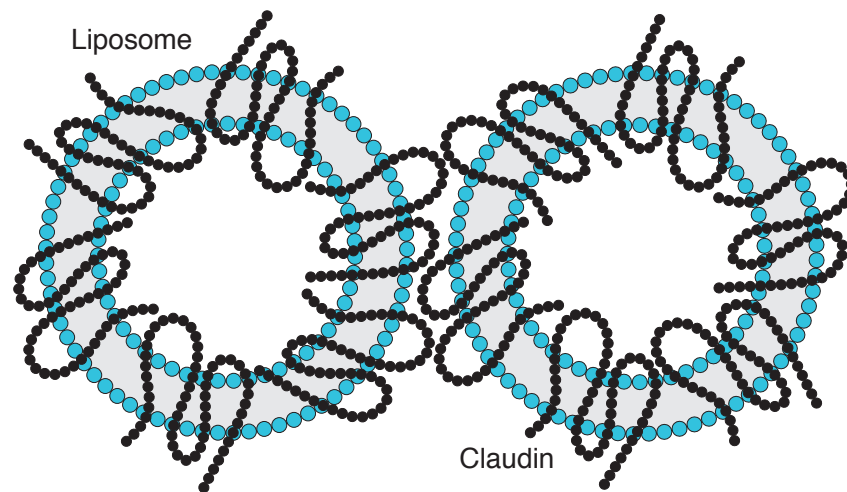


Figure 1.6: Liposomes with reconstituted claudins.

1.5 Aim of the study

The central aim of the present thesis is to investigate modulation of TJs, in order to gain insight into the mechanism of the specific interaction of the transmembrane and plaque proteins of TJs that will allow the development of new therapeutic strategies to enhance drug delivery of poorly absorbed drugs. For this purpose, well-characterized epithelial cell cultures and proteoliposomes are used as models for TJs.

In the first part of the study (Section 3.1), the morphological and functional aspects of TJs under the influence of EGTA, a known TJ modulator, are investigated. We have chosen cingulin and claudin-1 as the representatives for the plaque and transmembrane proteins of TJs, respectively. In order to visualize the claudin-1 in living cells, the sequence was tagged with green fluorescent protein (GFP). Under an experimentally induced TJ opening, the co-localization and dynamic behavior of cingulin and GFP-tagged claudin-1 in combination with other plaque and transmembrane proteins of TJs are described.

In the second part (Section 3.2), a novel strategy to modulate TJs is tested. This strategy is based on the use of peptide homologues to sequences of the extracellular domain of TJ proteins to compete for the potential sealing sequences between the adjacent cells. For this purpose, 14 peptide homologues of the first extracellular loop of claudin-1, -2, -4 and 2 peptide homologues of the first extracellular loop of occludin are assayed for the ability to modulate TJs in cell culture models (MDCK and Caco-2 cells). The effects of peptides on TJs are monitored by means of the transepithelial electrical resistance measurements (TEER), mannitol permeation and confocal laser scanning microscopy.

In the third part (Section 3.3), a simple *in-vitro* model of TJs is explored, based on current model of TJs, where claudins' extracellular domains interact with each other homo- or heterotypically to bridge the paracellular space. We aim to develop an assay that will allow to

screen for novel permeation enhancers that specifically interact with the extracellular domains of claudins. In this assay, purified transmembrane proteins claudins are reconstituted into the liposomes. The reconstituted proteins display their extracellular domains and interact together to mediate an aggregation of the liposomes. Claudin-1 is expressed in most mammalian epithelia and studies with knock-out mice confirmed the crucial role of this protein for the formation of TJs. Thus, we have chosen this protein as a suitable candidate to establish the proteoliposomal assay. To express His-tagged claudin-1, a baculovirus expression system is used. The protein is solubilized from crude membranes, purified by affinity chromatography and reconstituted into the phosphatidyl choline liposomes by a detergent dialysis method. Proteoliposomes will be characterized regarding their size and the ability to form associates, as well as the amount of residual detergent.

2 Materials and methods

2.1 Chemicals

Ammonium persulfate, 1-bromododecan, calcium chloride, citric acid, diethylacetamidomalonate, di-tert.-butyl dicarbonate, EDTA, EGTA, formaldehyde, glutaraldehyde, glycine, magnesium chloride, magnesium sulfate, paraformaldehyde, potassium acetate, potassium dihydrogen phosphate, potassium ferricyanate, potassium ferrocyanate, sodium, sodium bicarbonate, sodium dodecylsulfate, sodium hydroxide, sodium chloride, sodium phosphate dibasic, sucrose, tert.-butanol and Tris were purchased from Fluka (Switzerland).

Radiolabeled compounds ^3H -mannitol (629 GBq/mmol) and ^3H -cholic acid (555 GBq/mmol) were both purchased from Perkin Elmer (Switzerland) and octyl ^{14}C - β -D-glucopyranoside (11.1 GBq/mmol) from American Radiolabeled Chemicals (St. Louis, Missouri, USA). All other chemicals are specified in the appropriate sections. If not stated otherwise, chemicals and reagents were of analytical grade. Water was purified by reverse osmosis with a NANOpure Diamond UF system (Barnstead International, USA).

2.2 Peptides

Synthetic peptide homologues corresponding to sequence of the first extracellular loop of occludin and claudins are summarized in Tab. 2.1.

Peptide **4** and peptides **12** to **17** were provided by the group of Prof. Beck-Sickinger (Institute of Biochemistry, University of Leipzig, Germany). Peptides were synthesized by automated, multiple solid phase peptide synthesis with a robot system (Syro, MultiSynTech, Bochum, Germany) on a copoly(styrene-1 % DVB)-matrix using rink amide resin (4-(2',4'-Dimethoxyphenyl-Fmoc-aminomethyl)-phenoxy resin; Novabiochem, Switzerland) or Wang resin (p-Benzyloxybenzyl Alcohol resin; Novabiochem, Switzerland).

Peptide **5** was synthesized by an automated peptide synthesis system (Model 433A, Applied Biosystems) using a standard protocol for 0.1 mmol Fmoc-synthesis (Chan and Chan, 2000). Briefly, Fmoc-protected amino acids (Novabiochem, Switzerland) were coupled on a rink amide MBHA resin (4-(2',4'-Dimethoxyphenyl-Fmoc-aminomethyl)-phenoxyacetamidonorleucyl-MBHA resin; Novabiochem, Switzerland). After the synthesis step, a solution made of 9.45 ml trifluoroacetic acid 99 % (Across Organics), 250 μl water, 250 μl 1,2-ethanedithiol (Aldrich) and 100 μl triisopropylsilan 99 % (Across Organics) was used to cleave the peptide from the resin. The peptide was precipitated by addition of cold diethylether, re-solubilised in a mixture of acetonitril and water (1:1) and lyophilized overnight (Lyophilisator Christ, Alpha 1-4).

Table 2.1: Synthetic peptide homologues based on sequences of occludin and claudins

Identifier	Protein	Residues	Sequence	MW
1	OCLN	90-103	NH ₂ -DRGYGTSLLGGSVG-COOH	1338
2	OCLN	90-103	NH ₂ -CH-(C ₁₂ H ₂₅)-CO ^a NH-DRGYGTSLLGGSVG-COOH	1564
3	OCLN	90-103	5(6)-FAM-NH-DRGYGTSLLGGSVG-COOH	1696
4	CLD1	47-65	NH ₂ -YEGLWMSCVVSQSTGQVQCK-COOH	2131
5	CLD1	47-65	NH ₂ -YEGLWMSCVVSQSTGQVQCK-CONH ₂	2148
6	CLD1	47-65	NH ₂ -YEGLWMSSVSQSTGQIQSK-COOH	2116
7	CLD1	49-60	NH ₂ -GLWMSCVVSQSTG-CONH ₂	1255
8	CLD1	49-60 ^b	NH ₂ -LGSGQCTWVSSM-CONH ₂	1255
9	CLD1	49-60	NH ₂ -KKGLWMSCVVSQSTGKK-COOH	1768
10	CLD1	49-60	NH ₂ -DDGLWMSCVVSQSTGDD-COOH	1715
11	CLD1	54-65	NH ₂ -CVSQSTGQIQCK-CONH ₂	1280
12	CLD2	31-49	NH ₂ -KTSSYVGASIVAVGFSKG-COOH	1858
13	CLD2	47-64	NH ₂ -SKGLWMECATHSTGITCCQ-COOH	2078
14	CLD2	63-81	NH ₂ -QCIDIYSTLLGLPADIQAAQ-COOH	2018
15	CLD4	31-49	NH ₂ -RVTAFIGSNIVTSQTIWEG-COOH	2078
16	CLD4	47-65	NH ₂ -WEGLMNCVVSQSTGQMCK-COOH	2225
17	CLD4	63-81	NH ₂ -QCKVYDSSLALPQDLQAAR-COOH	2130

Notes: ^a2-aminotetradecanoyl moiety (lipoamino acyl), ^bscrambled peptide sequence. Aminoacids are written in one-letter code according to the IUPAC convention (IUPAC-IUB, 1984). Particular modifications of peptide sequences are underlined. Peptide sequences of CLDs and OCLN were retrieved from GenBank and UniProtKB/Swiss-Prot database (Boeckmann et al., 2003; Wu et al., 2006) under following accession numbers: CLD1, AAD22962/O95832; CLD2, P57739; CLD4, O14493; OCLN, Q16625. Abbreviations: CLD, claudin; OCLN, occludin; 5(6)-FAM, 5(6)-carboxyfluorescein; MW, molecular weight.

The lipoamino acyl residue present in peptide **2** was synthesized as previously published by Gibbons et al. (1990). Diethylacetamidomalonate (0.11 mol, 23.9 g) and 1-bromododecan (0.15 mol, 37.4 g) were heated under reflux in a solution of sodium (0.15 mol, 2.5 g) in ethanol (85 ml) for 24 hrs. Upon cooling, the mixture was poured onto ice/water (160 ml) and the precipitate filtered and washed with water. The precipitate was placed into a 500 ml round bottom flask, conc. HCl (180 ml) and dimethylformamide (20 ml) added, and then heated at reflux for 24 hrs. The mixture was allowed to cool, poured into a solution of ethanol/water (3:1) and neutralized with conc. aqueous ammoniak. The precipitate (amino acid) was filtered and washed with ethanol/water. The amino acid (46 mmol, 11.2 g) was resuspended in a 2:3 mixture of tert.-butanol/water (180 ml) and 8 M aqueous NaOH added dropwise to adjust the pH 13. Di-tert.-butyl dicarbonate (69 mmol, 15 g) in tert.-butanol (30 ml) was added at room temperature, the pH value adjusted to 11-12 and the reaction mixture stirred for 2 hrs. Following the dilution of the reaction mixture with water (50 ml), solid citric acid was added to adjust the pH 3 and the oil extracted with ethylacetate. After drying with magnesium sulfate, the organic layer was evaporated, the residue resuspended in acetonitrile and the product filtered. The purification was carried out on Silicagel 60 (Merck) and the identity confirmed by NMR, MS and elementary analysis. The conjugation of lipoamino acid to the appropriate peptide sequence was custom-made by Primm (Milano, Italy).

Peptides **1** to **3** and **7** to **11** were purchased from Primm (Milano, Italy) and supplied with purity $\geq 70\%$.

2.3 High performance liquid chromatography (HPLC)

Analytical HPLC was done with a Merck Hitachi HPLC setup with a Vydac 218TP54 column (Protein & Peptide C18 reversed phase), with a flow rate of 1 ml/min and a 45 min linear gradient from 0.1% trifluoroacetic acid in water-acetonitrile (8:2) to 0.1% trifluoroacetic acid in water-acetonitrile (1.5:8.5). Detection was by UV (220 nm) and fluorescence (excitation wavelength 250 nm; emission wavelength 350 nm).

2.4 Circular dichroism

Circular dichroism measurements were acquired with a spectropolarimeter J-720 (Jasco, USA) attached to a NESLAB 111 bath circulator set to 37°C. CD spectra were obtained between 260 and 185 nm, with a 0.5 mm path-length cell, using 20 nm/min scanning speed, a response time of 4 sec, and a band width of 1 nm. The spectra reported represent the average of 4 scans and are corrected by subtracting the spectrum of the respective solvent system. To estimate the secondary structure content of peptide, an analysis of the spectra was carried out with the CD-Pro software. Spectra of 56 proteins which included 13 membrane proteins along with 43 soluble proteins were used as a reference set. The analysis was performed with three deconvolution algorithms, CONTIN/LL, SELCON3 and CDSSTR (Sreerama et al., 2000; Sreerama and Woody, 2000).

2.5 Cell cultures

2.5.1 Madin Darby canine kidney (MDCK) cell line

MDCK cells, strain II (kind gift from Michel Paccaud, Institut d'Hygiène, Geneva, Switzerland) were cultured as previously described (Rothen-Rutishauser et al., 1998a). Cells were used between passage number 216 and 250 and propagated in 25 cm² plastic flasks (Techno Plastic Products, TPP; Switzerland) in Eagle's Minimal Essential Medium (MEM) with Glutamax-I, Earle's salts and 25 mM HEPES (Invitrogen), supplemented with 10 % (v/v) of heat inactivated (water bath, 30 min, 56°C) foetal calf serum (FCS; PAA Laboratories, Austria), 0.2 % (w/v) sodium bicarbonate, 100 units penicillin and 100 µg streptomycin per ml (Gibco) at 37°C in an atmosphere of 5 % CO₂ (Gassed Incubator BBD 6220, Kendro laboratory products, Germany). Cells were sub-cultured twice per week and seeded on polyethyleneterephthalate (PET) inserts (Falcon, 35-3180; Becton Dickinson Labware) at a density of 0.5×10^5 cells/cm², if not stated otherwise.

2.5.2 Human colon carcinoma (Caco-2) cell line

Caco-2 cells were purchased from the American Type Culture Collection (ATCC, Rockville, MD, HTB-37) and used between passage number 28 and 60. The cells were cultured as described by Braun et al. (2000). Briefly, the cells were grown in 25 cm² plastic flasks (TPP) in Eagle's Minimal Essential Medium with Earle's Salts (EMEM, Gibco) supplemented with 20 % (v/v) of heat inactivated (water bath, 30 min, 56°C) FCS (PAA Laboratories, Austria), 0.2 % (w/v) sodium bicarbonate, 1 mM sodium pyruvate (Invitrogen), 100 units penicillin and 100 µg streptomycin per ml (Gibco) at 37°C in an atmosphere of 5 % CO₂ (Gassed Incubator BBD 6220, Kendro laboratory products, Germany). Cells were sub-cultured twice per week (at 80-90 % confluency) and seeded on PET inserts (see Sec. 2.5.1) or on polycarbonate (PC) cell culture inserts (Costar, 3401) at a density of 1×10^5 cells/cm², if not stated otherwise.

2.5.3 *Spodoptera frugiperda* (Sf9) cell line

Sf9 cells were purchased from Invitrogen (Gibco, 11496-015) and used up to 30 passages. Suspension cultures were maintained in serum-free medium Sf900 II SFM (Invitrogen) at 28°C in an incubator with orbital shaking platform set to 135 rpm (Innova 4230, New Brunswick Scientific, USA). Cell numbers were determined in a Neubauer chamber (Brand, Germany) in the presence of 0.04 % trypan blue (Sigma) to check for viability. The cells were routinely sub-cultured twice a week by seeding 125 ml Erlenmeyer flasks (Corning) at a density of 5×10^5 cells/ml in a total volume of 30 ml. To scale up suspension cultures for baculovirus amplification (see Sec. 2.11.3) or/and protein expression (see Sec. 2.11.5), the cells were seeded at a density of 5×10^5 cells/ml in 500 ml or 2000 ml Erlenmeyer flasks (Corning) in total volumes of 100-200 ml and 500-1000 ml, respectively.

2.6 Transfection of mammalian cells

MDCK cells were transfected with Lipofectamine 2000 (Invitrogen). MDCK cells were seeded at a density of 5×10^4 cells/cm² in a 6-well plate (TPP) and incubated overnight at 37°C in an atmosphere of 5% CO₂ (Gassed Incubator BBD 6220). Approximately 2 µg of pEGFP-CLDN1 (see Sec. 2.9.1) and 15 µl of Lipofectamine 2000 were each separately diluted in 250 µl of OptiMEM I (Invitrogen). After 5 min, both solutions were combined and the mixture incubated for 20 min at room temperature (RT). After media removal and two washing steps with OptiMEM I, the transfection mixture was applied to each well containing 2 ml of OptiMEM I. Control cells received a transfection mixture without DNA. Plates were incubated at 37°C for 6 hrs. After the incubation, the transfection mixture was replaced by 2 ml of cell culture medium (see Sec. 2.5.1) and plates were incubated at 37°C. After 24 hrs, the cells were examined under a fluorescence microscope (Axiovert 40 CFL, Zeiss, Germany) for the presence of a GFP signal and sub-cultured into new 6-well plates by diluting the cells in a split ratio 1:20. The cells were allowed to grow at 37°C for 24 hrs in the normal cell culture medium. Thereafter, the cells were cultured for 14 days in a medium containing 1 mg/ml of G418 (Promega). Resistant colonies were trypsinized, picked with cloning cylinders (Sigma) and expanded in 24-well plates (TPP). Several clones were analysed for the presence of the GFP fluorescence by confocal laser scanning microscopy (CLSM; see Sec. 2.8) and the best clone was expanded to a cell line (GFP-CLD1-MDCK cell line). Transfected cells were maintained in culture medium containing 1 mg/ml G418 and sub-cultured twice a week.

2.7 Functional assays of tight junctions

2.7.1 Treatment of cells with synthetic peptides

Peptides were prepared as 10 mM stock solutions in DMSO (Fluka) or in a mixture of acetonitril/water (50:50 v/v), or in water only. The final concentration of solvent in cell based assays did not exceed 2% (v/v). MDCK and Caco-2 cells, respectively, were seeded on cell culture inserts as described in Sec. 2.5.1 and 2.5.2. Peptides were added from the apical and basolateral side of the cell layer. If not mentioned otherwise, the transport medium consisted of MEM (MDCK) or EMEM (Caco-2), supplemented with 0.2% (w/v) sodium bicarbonate, 100 units penicillin and 100 µg streptomycin per ml (Gibco) and a serine protease inhibitor (Pefabloc SC, Fluka; final concentration 50 µM). The serum protein concentration (FCS) in the transport medium varied between 0-10% v/v (as indicated). After the incubation with peptides (48 hrs, if not mentioned otherwise), transepithelial electrical resistance measurements (see Sec. 2.7.2) and the paracellular permeation assay (see Sec. 2.7.3) were performed.

2.7.2 Transepithelial electrical resistance measurement (TEER)

The TEER was measured with an EvomX (World Precision Instruments, USA) connected to a resistance measurement chamber EndOhm-12 (World Precision Instruments). Prior to the

TEER measurements, the electrode was sterilized with 70 % (v/v) ethanol for 30 min and equilibrated in culture medium with or without FCS for 5 min. Inserts without cells were measured and the value was subtracted from each TEER measurement. The corrected resistance values of the cell layers were normalized to the control.

2.7.3 Paracellular permeation assay

Permeation studies with ^3H -mannitol as a paracellular marker (Krämer et al., 2001) were performed to test the influence of synthetic peptides on tight junctions (TJs). All experiments were carried out in a two chamber system (Falcon Cell Culture Insert System). The permeation assay was performed in an incubator (Memmert GmbH, Germany) at 37°C on a rocking plate (Gasser Apparatenbau & Laborzubehör, Switzerland) at a maximal angle of 10° with a frequency of 20 min⁻¹. The apical compartment contained 0.5 ml and the basolateral compartment 1.5 ml of the transport medium. The ^3H -mannitol (0.3 MBq/ml) was added to the apical compartment and samples of 50 µl were collected from the basolateral side for up to 100 min. The sample volume was not replaced. Collected samples were mixed with 3 ml scintillation cocktail (Ultima Gold, Packard BioScience) and analyzed by liquid scintillation counting (Multipurpose Scintillation Counter, Beckman LS 65000). To determine the background value, 100 µl sample without radioactivity were taken and measured after mixing with the scintillation cocktail. Retention of mannitol by the cells was found to be < 1 %.

The apparent permeability coefficient P_{app} (cm/s) across a cell layer was calculated according to Eqn. 2.1 (Boulenc et al., 1993), which is based on the Fick's first law assuming that the concentration in the receiver chamber is negligible as compared to the concentration in the donor chamber. The transport rate dQ_r/dt corresponds to the slope of the regression line determined from the linear range of the $Q_r(t)$ curve (Eqn. 2.2).

$$P_{\text{app}} = \left(\frac{dQ_r}{dt} \right) \frac{1}{A \cdot c_0} \quad (2.1)$$

$$Q_r(t_n) = c_r(t_n) \cdot V_r(t_n) + \sum_{i=1}^{n-1} [c_r(t_i) \cdot V_s(t_i)] \quad (2.2)$$

where dQ_r/dt is the transport rate (mol/s), A (cm²) the area of the permeable membrane, i.e. the cell layer area, and c_0 (mol/ml) the initial concentration of mannitol in the donor chamber. $V_s(t_i)$ equals the sample volume (0.05 ml) removed at time point t_i .

2.7.4 Calcium chelation method

To study the morphology of TJ proteins upon a disruption and re-sealing of TJs, a calcium chelation method was used. The calcium chelation protocol was followed as previously published by Rothen-Rutishauer et al. (2002). Briefly, MDCK cells (or MDCK-GFP-CLD1 cells, see

Sec. 2.6) were seeded on PET cell culture inserts at a density of $0.5-1 \times 10^5$ cells/cm² and cultured for 11 days (or for 3 days in case of MDCK-GFP-CLD1 cells). The chelation medium was prepared by mixing of 20 mM EGTA in PBS (pH 7.4) and FCS-free culture medium to reach a final concentration of 2 mM EGTA. It was added from both, the apical and basolateral side of the cell culture insert. Twenty minutes after addition of EGTA (incubation at 37°C), cells were washed with culture medium and allowed to recover in culture medium (containing 1.8 mM calcium chloride) at 37°C in an atmosphere of 5% CO₂. At time points indicated, cells were fixed and prepared for CLSM (for details see Sec. 2.8).

2.8 Confocal laser scanning microscopy (CLSM)

A Zeiss LSM 510 Meta inverted microscope was used (lasers: HeNe 543 nm, HeNe 633 nm, Ar 458/477/488/514 nm and He-diode 405 nm; Zeiss, Germany). Optical sections (Fig. 2.1) at intervals of 0.15 or 0.3 μm were taken with a C-Apochromat water objective (63x/1.2W). Image processing was done on a PC workstation using IMARIS, a 3D multi-channel image processing software (Bitplane, Zürich, Switzerland). Deconvolution and co-localization analyses were done according to Rothen-Rutishauser et al. (1998b). CLSM data were recorded simultaneously for pairs of fluorescence signals at the Nyquist frequency of the microscope, which corresponds

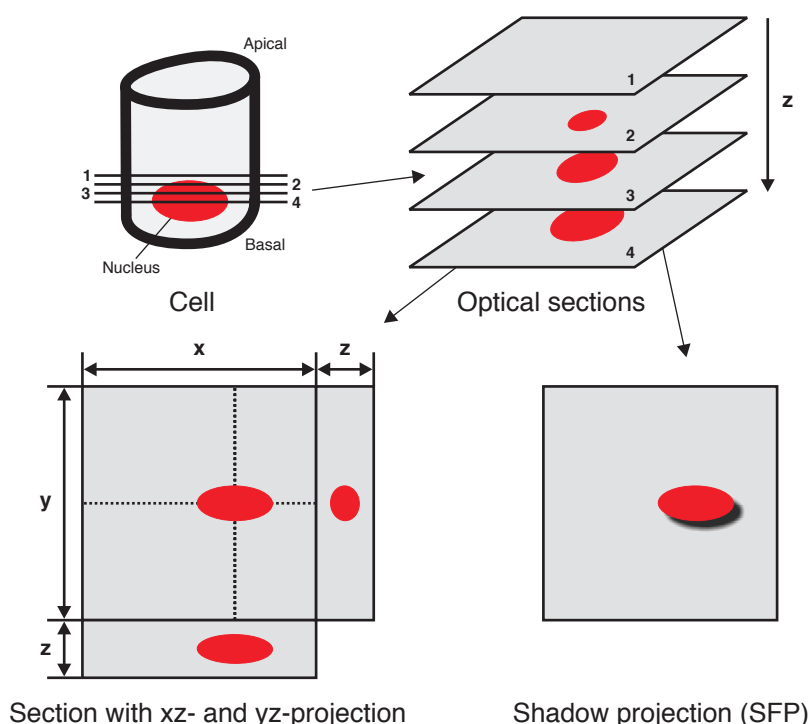


Figure 2.1: **Schematic representation of optical sections.** Optical sections through a sample and the representation of 3D-data stacks. Adapted from Wunderli-Allenspach (2001).

in our microscope to a lateral sampling distance of 50 nm and an axial sampling distance of 150 nm. In order to remove blur, improve resolution and reduce noise, the Huygens software (Scientific Volume Imaging, Netherlands) was applied using a theoretical point spread function. Colocalization analysis was carried out with the Colocalization software (Bitplane, Switzerland). For the statistical analysis, confocal images were recorded as described above. For each pair of proteins, the percentage of co-localized pixels for each layer was calculated for 10 different regions of interest (ROIs).

For studies, cells were seeded at a density of 0.5×10^5 cells/cm² on PET inserts, if not mentioned otherwise. Membranes were excised from cell culture inserts and prepared for CLSM as described previously (Rothen-Rutishauser et al., 1998a). Briefly, cells were washed in phosphate-buffered saline, pH 7.4 (PBS; 130 mM NaCl, 10 mM Na₂HPO₄/KH₂PO₄) and fixed with 3% (w/v) paraformaldehyde in PBS for 15 min at RT. Fixed cells were treated with 0.1 M glycine in PBS for 5 min, permeabilised in 0.2% (v/v) Triton X-100 (Fluka) in PBS for 15 min. Samples were incubated at 37°C with the first antibody for 60 min and with the second antibody for 90 min. Antibodies were diluted in PBS containing 3% (w/v) bovine serum albumin (Fluka). Preparations were mounted in 0.1 M Tris, pH 9 and glycerol (v/v ratio 7:3) containing 50 mg/ml n-propyl-gallate (Sigma). Antibodies and dyes used for immunofluorescent studies are summarized in Tab. 2.2.

A slightly modified protocol was used for the immunostaining of infected insect cells. Fixed cells were washed with PBS containing 5% (w/v) skimmed milk and permeabilised in 0.2% (v/v) Triton X-100 in PBS for 2 min. Samples were incubated with the first antibody at 37°C for

Table 2.2: **Antibodies and dyes used for immunocytochemistry**

Antibody/Dye	Supplier	Dilution
Rat anti ZO-1	Chemicon	1:100
Mouse anti claudin-1	Zymed	1:100
Mouse anti occludin	Zymed	1:100
Rabbit anti cingulin C532	University of Geneva ^a	1:500
Mouse anti Golgi	Sigma	1:50
Goat anti rat IgG Cy5	Chemicon	1:50
Goat anti rabbit IgG Cy3	Amersham	1:50
Hoechst 33342 ^b	Molecular Probes	1:10'000 ^d
DAPI ^c	Hoechst	1:100 ^d
FluoroAlexa Phalloidin 660	Molecular Probes	1:50
LysoTracker Red DND-99	Molecular Probes	1:10'000 ^e

Notes: ^aprovided by Dr. Sandra Citi, Department of Molecular Biology, University of Geneva; ^bused for living cells; ^cused for fixed cells; ^dfinal concentration 1 µg/ml; ^efinal concentration 50 nM. Abbreviations: DAPI, 4,6-Diamidino-2-Phenylindole; ZO-1, zonula occludens 1.

60 min and with the second antibody for 30 min. Antibodies were diluted in PBS containing 5% (w/v) skimmed milk. Preparations were mounted as described above.

To study living cells, they were seeded on PET cell culture inserts (Falcon) or on chambered coverglasses (Nunc). PET membranes were cut out and mounted in culture medium. To study calcium depletion (see Sec. 2.7.4) in living cells, the coverglass was mounted in the CLSM unit connected to a water bath that kept the unit at 37°C. To label acidic organelles, a LysoTracker Red DND-99 was diluted in cell culture medium and cells were incubated for 30 min at 37°C. After a washing step, cells were immediately analyzed by CLSM.

2.9 DNA manipulations

2.9.1 Generation of constructs

The complete human cDNA of claudin-1 (GenBank accession No. BC012471; RZPD clone ID:IRAKp961E1928Q) was obtained from the German Resource Center for Genome Research (Heidelberg, Germany).

To generate N-terminal GFP-tagged human claudin-1 for expression in MDCK cells, the pEGFP-C1 vector (Clontech) was used. The GFP tag was located at the N-terminus of CLDN1 since a free C-terminus is required for direct binding to PDZ domains of TJ associated proteins (Itoh et al., 1999a). The open reading frame (ORF) of human claudin-1 was PCR-amplified (see Sec. 2.9.7) using primers 5'-TTATAGATCTATGGCCAACGCGGGGCTGCA-3' and 5'-TGTAGTCGACCACGTAGTCTTTCCCGCTGGA-3', which were designed to incorporate *Bg*/II

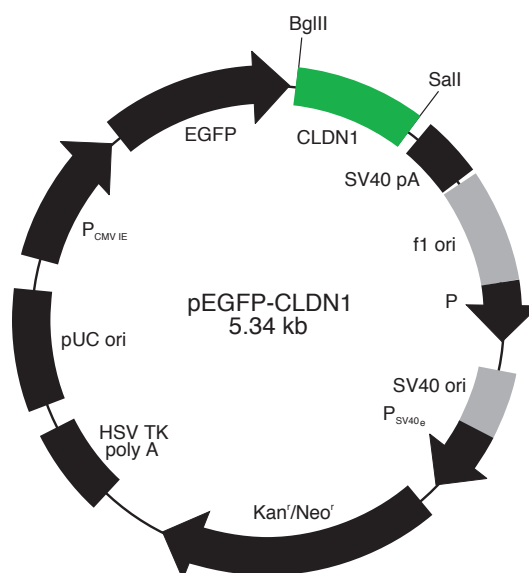


Figure 2.2: **Map of construct pEGFP-CLDN1.** Construct pEGFP-CLDN1 was obtained by subcloning of amplified cDNA of human claudin-1 as described in Sec. 2.9.1.

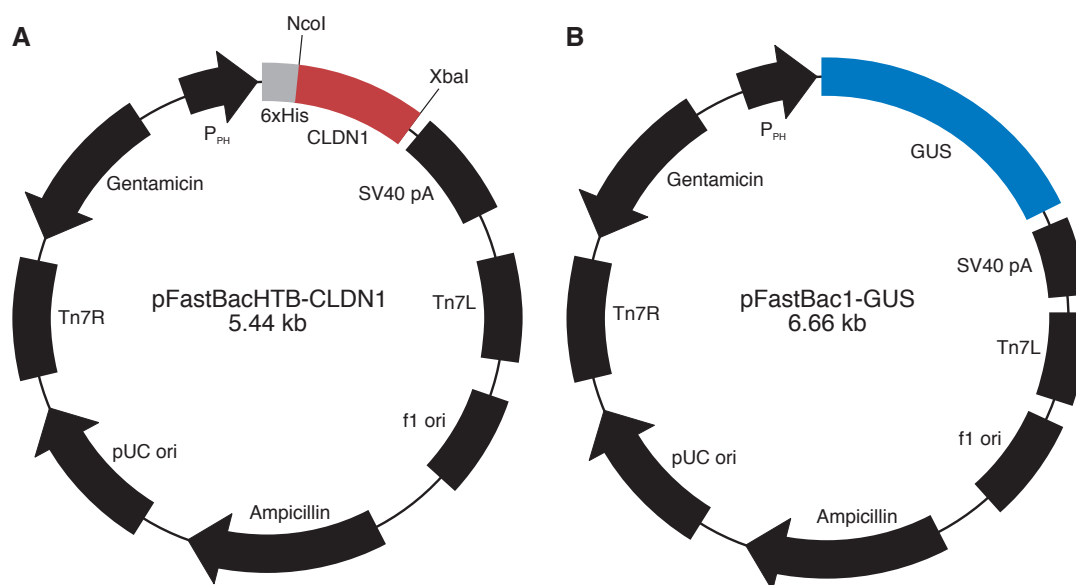


Figure 2.3: **Map of constructs pFastBacHTB-CLDN1 and pFastBac1-GUS.** (A) Construct pFastBacHTB-CLDN1 was obtained by subcloning of amplified cDNA of human claudin-1 as described in 2.9.1. (B) Vector pFastBac1-GUS coding for β -glucuronidase.

and *Sall* restriction sites at the 5' and 3' end, respectively, of the coding sequence. The amplified insert (653 bp) was purified with the High Pure PCR product purification kit (Roche) and subsequently digested with *Bgl*II (Fermentas) and *Sall* (Fermentas) (see Sec. 2.9.4). Digested and purified insert was ligated (see Sec. 2.9.6) to pEGFP-C1 vector. The ligation mixture was used to transform the DH5 α competent cells (see Sec. 2.10.4) and these streaked on LB agar plates containing kanamycin (see Sec. 2.10.1). Several colonies were amplified (see Sec. 2.10.2) and the isolated DNA (see Sec. 2.9.2) was analysed by PCR (see Sec. 2.9.7) for the presence of the insert. Two clones were sequenced (see Sec. 2.9.8) to confirm the identity of the construct. A correct construct pEGFP-CLDN1 (Fig. 2.2) was transfected to MDCK cells (see Sec. 2.6) to generate the MDCK-GFP-CLD1 cell line.

To produce N-terminal His-tagged human claudin-1 for expression in insect cells, the ORF was cloned into a donor plasmid pFastBacHTB (Invitrogen) where the expression is controlled by a baculovirus-specific promoter. Plasmid pFastBacHTB contains hexa-histidine sequence flanking the multiple cloning site and allows addition of N-terminal hexa-his-tag to claudin-1 to facilitate purification. The ORF of claudin-1 gene was PCR-amplified (see Sec. 2.9.7) by using primers 5'-TATCCATGGGAATGGCCAACGCGGGGCTGCA-3' and 5'-GTTGTGTTCTAGAGTGTCACACGTAGTCTTTCCCGCT-3', which were designed to incorporate *Nco*I and *Xba*I restriction sites at the 5' and 3' end, respectively, of the coding sequence. The resulting amplified product (insert) was purified with the High Pure PCR product purification kit (Roche) and subsequently digested with *Nco*I (Fermentas) and *Xba*I (Fermentas) (see Sec. 2.9.4). The digested product was purified with the High Pure PCR product purification kit and ligated (see Sec. 2.9.6) to the pFastBacHTB vector. The ligation mixture was used to transform DH5 α com-

petent cells (see Sec. 2.10.4) and these were streaked on LB agar plates containing ampicillin (see Sec. 2.10.1). After overnight incubation at 37°C (Incubator Binder, Germany), several colonies were amplified (see Sec. 2.10.2) and the isolated DNA (see Sec. 2.9.2) was analysed by PCR (see Sec. 2.9.7) for the presence of the insert. Two positive clones were sequenced (see Sec. 2.9.8) to confirm the identity of the construct. A correct construct named pFastBacHTB-CLDN1 (Fig. 2.3A) was used for the generation of recombinant bacmid DNA (see Sec. 2.11.1).

Expression of β -glucuronidase was chosen as a control for the efficiency of the bacmid transfection to Sf9 cells. Construct pFastBac1-GUS (Fig. 2.3B) containing the gene coding for β -glucuronidase (GUS) was used to generate recombinant bacmid DNA (see Sec. 2.11.1). Construct pFastBac1-GUS was purchased from Invitrogen.

2.9.2 DNA isolation

Small scale isolation of plasmid DNA was done by using a FastPlasmid Mini Kit (minipreps; Eppendorf). Large scale plasmid DNA isolation was achieved by using a HighSpeed Plasmid Midi Kit (midipreps; Qiagen). Usually, 5-8 ml of an overnight bacteria suspension culture (see Sec. 2.10.1) were processed by the minipreps and 100 ml by the midipreps, respectively, according to the manufacturer's protocol. An Eppendorf or a Beckman centrifuge was used for the centrifugation steps.

For bacmid minipreparations, 1.5 ml of an overnight bacteria suspension culture with confirmed white phenotype on re-streaked Bac plates (see Sec. 2.10.3) were processed in a Eppendorf tube. All centrifugation steps were done at 14'000 *g* for the indicated time (at RT). Bacteria were centrifuged for 1 min. The pellet was re-suspended in 0.3 ml of solution I (10 mM Tris-HCl, pH 8.0, 10 mM EDTA) containing 100 μ g/ml of ribonuclease A (Fermentas), and subsequently 0.3 ml of solution II (1 % w/v SDS, 0.2 M NaOH) were added. After 5 min of incubation (RT), 0.3 ml of 3 M potassium acetate pH 5.5 (chilled to 4°C) were added and the sample was left on ice for 10 min. Precipitated proteins and genomic DNA were centrifuged for 10 min. The supernatant was mixed with 0.8 ml of isopropanol and placed on ice for 5-10 min to precipitate bacmid DNA. After a centrifugation step for 10 min, the pellet was washed with 0.5 ml of 70 % (v/v) ethanol. After an additional centrifugation step for 5 min, pellets were air-dried for 10 min and dissolved in 40 μ l of sterile 10 mM TE buffer, pH 8.0 (10 mM Tris, 1 mM EDTA). Bacmid DNA was stored at 4 °C protected from light.

2.9.3 DNA quantification

The DNA concentration c_{DNA} (μ g/ μ l) was estimated spectrophotometrically (Cary 1E UV/VIS spectrophotometer, Varian, USA). DNA (5 μ l) was diluted in a ratio of 1:80 (v/v) with deionized water and the absorption was measured at 260 nm in a quartz cuvette (Hellma, Germany). The concentration of the sample was calculated according to Eqn. 2.3.

$$c_{\text{DNA}} = \frac{OD_{260} \cdot F \cdot Q_s}{1000} \quad (2.3)$$

where OD_{260} equals the absorption at 260 nm, F the dilution factor and Q_s the spectrophotometric equivalent for a double-stranded DNA, which corresponds to 50 $\mu\text{g/ml}$ (Sambrook and Russell, 2001).

2.9.4 Digestion by restriction endonucleases

All incubations were done on an Eppendorf shaker at 600-750 rpm and the optimal temperature recommended by the supplier for each restriction enzyme. For preparative digestions and to confirm the integrity of plasmids, 1-5 μg of DNA were digested with 10-40 U of the appropriate restriction endonuclease in the corresponding restriction buffer for 30 min up to overnight. For cloning, the digested DNA was purified with the High Pure PCR product purification kit (Roche).

2.9.5 Dephosphorylation of plasmid DNA

To inhibit self-ligation, the 5' ends of the linearized plasmid were dephosphorylated by calf intestine alkaline phosphatase (CIAP; Fermentas). Dephosphorylation was done directly after the restriction digestion (see Sec. 2.9.4) by adding 0.5 U of CIAP to 5 μg of DNA and the incubation was performed for 30 min at 37°C with shaking (600-750 rpm). Subsequently, CIAP was inactivated at 85°C for 30 min and the DNA was purified with the High Pure PCR product purification kit (Roche).

2.9.6 DNA ligation

Generally, 50 ng of a digested (and dephosphorylated) vector (see Sec. 2.9.4 and 2.9.5) and the corresponding amount of a digested insert (Eqn. 2.4) were mixed and ligation buffer as well as 2.5 U of T4 DNA ligase (Fermentas) were added to a total volume of 20 μl per reaction mixture. The molar ratios $R_{i/v}$ of insert to vector were 1:1, 1:3 and 3:1, respectively. As a control, vector without insert was ligated. Ligations were incubated on an Eppendorf shaker (600-750 rpm) at 22°C for 3 hrs. Subsequently, the ligase was inactivated by incubation at 65°C for 10 min and the reaction was stopped by incubation on ice. The ligation mixture was used immediately to transform competent DH5 α cells (see Sec. 2.10.4).

$$m_i = \left(\frac{s_i}{s_v} \right) \cdot m_v \cdot R_{i/v} \quad (2.4)$$

where m_i is the amount of insert (ng), m_v the amount of vector (ng), s_i and s_v the size of insert and vector (kb), respectively.

2.9.7 Polymerase chain reaction (PCR)

Reaction mixtures (25-50 μ l) containing template DNA, deoxynucleotides, primers and an appropriate DNA polymerase were prepared in PCR tubes (Biolabo Scientific Instruments). The amount of template DNA was generally 50-100 ng. Primers were obtained as a 100 nmol/ml solution (Microsynth, Switzerland) and used in a standard concentration of 0.5 μ M in the final PCR reaction. Deoxynucleoside triphosphates dATP, dCTP, dGTP and dTTP (Roche) were used in a standard concentration of 0.2 mM in the final PCR reaction. Proof-reading Pfu DNA polymerase (Fermentas) was used to amplify the ORF of claudin-1 for the generation of the pEGFP-CLDN1 and the pFastBacHTB-CLDN1 construct (see Sec. 2.9.1). For a confirmation of the successful ligation (see Sec. 2.9.6) or the transposition in bacmid DNA (see Sec. 2.11.1), the Taq DNA polymerase (Fermentas) was used. Reactions were run in a thermocycler and products were analyzed by agarose gel electrophoresis (see Sec. 2.9.9).

2.9.8 DNA sequencing

The Big Dye Reaction Terminator v3.1 cycle sequencing kit (Applied Biosystems) was used to confirm the identity of the generated constructs (see Sec. 2.9.1). PCR reactions containing the ready reaction premix of the sequencing kit (deoxynucleotides, fluorescently labelled dideoxynucleotides, DNA polymerase) and template DNA (pEGFP-CLDN1 or pFastBacHTB-CLDN1 construct), together with the sequencing primers (5'-AACCACTACCTGAGCACCCAGTC-3' or 5'-TTCAGGTTTCAGGGGAGGTGT-3' for pEGFP-CLDN1; 5'-GATTATTCATACCGTCCCACCAT-3' or 5'-GTTTCAGGTTTCAGGGGAGGTG-3' for pFastBacHTB-CLDN1) were assembled. PCR was performed in a thermocycler according to the manufacturer's recommendation. Extension fragments were purified by means of ethanol-EDTA-precipitation (suggested protocol from Applied Biosystems), re-suspended in Hi-Di Formamide (Applied Biosystems) and denatured for 2 min at 95°C in a heating block. Samples were transferred to a 96-well plate and analyzed by the ABI PRISM 3100-Avant Genetic Analyser (Applied Biosystems).

2.9.9 Agarose gel electrophoresis

Agarose electrophoresis was performed in a horizontal electrophoresis separation system (Owl Separation Systems, Model B1A, USA). Agarose gels (1 % w/v) were prepared by heating the agarose (Invitrogen) suspension in TAE buffer (40 mM Tris-acetate, 1 mM EDTA; pH 8) in a microwave oven until the solution became clear. Ethidium bromide (Fluka) was added to obtain a final concentration of 0.5 μ g/ml and the gel was poured into the casting mold resulting in a gel with thickness of approximately 0.5 cm. Samples were mixed with six-fold concentrated loading buffer (40 % v/v glycerol, 0.03 % w/v bromphenol blue) and loaded into the slots. DNA size standards (Invitrogen) were loaded on the left and right side of the gel. Electrophoresis was performed for 35-45 min at 90-100 V. After separation, the gel was examined by a UV gel documentation system (BioDoc-H Imaging System, UVP, USA).

2.10 Bacteria manipulations

2.10.1 Media and agar plates for bacteria

Bacteria were cultured in Luria-Bertani (LB) medium or on LB agar plates (Bio101 Systems), which were supplemented with antibiotics. Medium and agar were prepared according to the manufacturer's recommendations and sterilized by autoclaving at 121°C for 20 min. Antibiotics and reagents used to prepare agar plates and liquid medium are summarized in Tab. 2.3.

Table 2.3: **Antibiotics and reagents for agar plates and liquid media**

Substance ^a	Supplier	Final conc. ^c
Ampicillin	Sigma	100 µg/ml
Kanamycin	Invitrogen	50 µg/ml
Tetracycline	Sigma	10 µg/ml
Gentamicin	Sigma	7 µg/ml
IPTG	Fermentas	40 µg/ml
Bluo-gal ^b	Fluka	100 µg/ml

Notes: ^aantibiotics and IPTG prepared as stock solutions in water; ^bprepared as stock solution in dimethylformamide; ^cin plates and media. All stock solutions were stored at –20°C. Abbreviations: IPTG, isopropylthiogalactoside; Bluo-gal, 5-Bromo-3-indolyl-β-D-galactopyranoside.

2.10.2 Bacteria suspension cultures

5-8 ml of LB medium supplemented with antibiotics (see Sec. 2.10.1) were inoculated in round-bottom tubes (Falcon) and incubation was performed in a shaking incubator (Innova 4000, New Brunswick Scientific, USA) at 37°C overnight at 200 rpm. For the purpose of midipreps (see Sec. 2.9.2), round-bottom tubes were prepared as described above and incubated for 8 hrs in the shaking incubator at 37°C. In sterile Erlenmeyer flasks (250 ml), 2 ml of the culture were diluted with 100 ml of LB medium supplemented with antibiotics (see Tab. 2.3) and incubation was done in a shaking incubator (Innova 4430, New Brunswick Scientific, USA) at 37°C with an orbital shaking platform set to 200 rpm.

2.10.3 Transformation of DH10Bac competent bacteria

Maximum efficiency DH10Bac competent *E. coli* (Invitrogen) were transformed with the construct pFastBacHTB-CLDN1 or pFastBac1-GUS (see Fig. 2.3) according to the manufacturer's

recommendations. Briefly, 1 ng of each construct was added to 100 μ l of DH10Bac competent cells and the sample was incubated for 30 min on ice. Subsequently, the cells were heat-shocked for 45 sec at 42°C and after addition of S.O.C. medium (Invitrogen), tubes were shaken at 37°C for 4 hrs at 200-225 rpm (Innova 4000, New Brunswick Scientific, USA). After the incubation, three serial 10-fold dilutions of bacteria in S.O.C. medium were prepared and 100 μ l of each dilution were streaked onto selective LB agar plates (Bac plates) containing kanamycin, gentamicin, tetracycline, isopropylthiogalactoside and Bluo-gal (see Tab. 2.3). Plates were inverted and incubated for 48 hrs at 37°C (Incubator Binder, Germany). Several white colonies were selected and restreaked onto the Bac plates. The white phenotype was confirmed after incubation for 48 hrs at 37°C. Three white colonies from the re-streaked plates were selected and amplified in a suspension culture (see Sec. 2.10.2) and bacmid DNA was isolated by minipreps (see Sec. 2.9.2).

2.10.4 Transformation of DH5 α competent bacteria

To introduce plasmid DNA into the bacteria, a heat-shock based protocol was used. Chemically competent DH5 α cells (Invitrogen) were transformed according to the supplier's recommendations. Briefly, 50 μ l of the competent bacteria were transformed with 1-10 ng of DNA (or 5 μ l of ligation mixture). The reaction was incubated for 30 min on ice and subsequently heat-shocked for 20 sec at 37°C. After the addition of LB medium (Sec. 2.10.1), reactions were incubated on an Eppendorf shaker for 1 hr at 37°C at 1000 rpm. After the incubation, bacteria were centrifuged at 800 *g* for 5 min and re-suspended in 100 μ l of LB medium and immediately spread onto selective plates containing the respective antibiotics (Sec. 2.10.1). Plates were inverted and incubated overnight at 37°C.

2.11 Baculovirus expression system

A schematic representation of the Bac-to-Bac baculovirus expression system (Invitrogen) is shown in Fig. 2.4. Protocols are published in the supplier's information and by Ciccarone et al. (1997).

2.11.1 Generation and analysis of bacmids

Recombinant baculovirus shuttle vectors (bacmids) were generated by the transformation of competent DH10Bac cells with the constructs pFastBacHTB-CLDN1 and pFastBac1-GUS (see Fig. 2.3 on page 28), respectively, as described in Sec. 2.10.3. Bacmid CLDN1 (coding for expression of His-CLD1) and bacmid GUS (coding for expression of GUS) were purified by minipreparation (see Sec. 2.9.2) and analysed for the presence of the transposed sequence by PCR. The M13 forward primer (5'-CCCAGTCACGACGTTGTAAAACG-3') and/or M13 reverse primer (5'-AGCGGATAACAATTTCACACAGG-3') and/or the gene specific primer for claudin-1

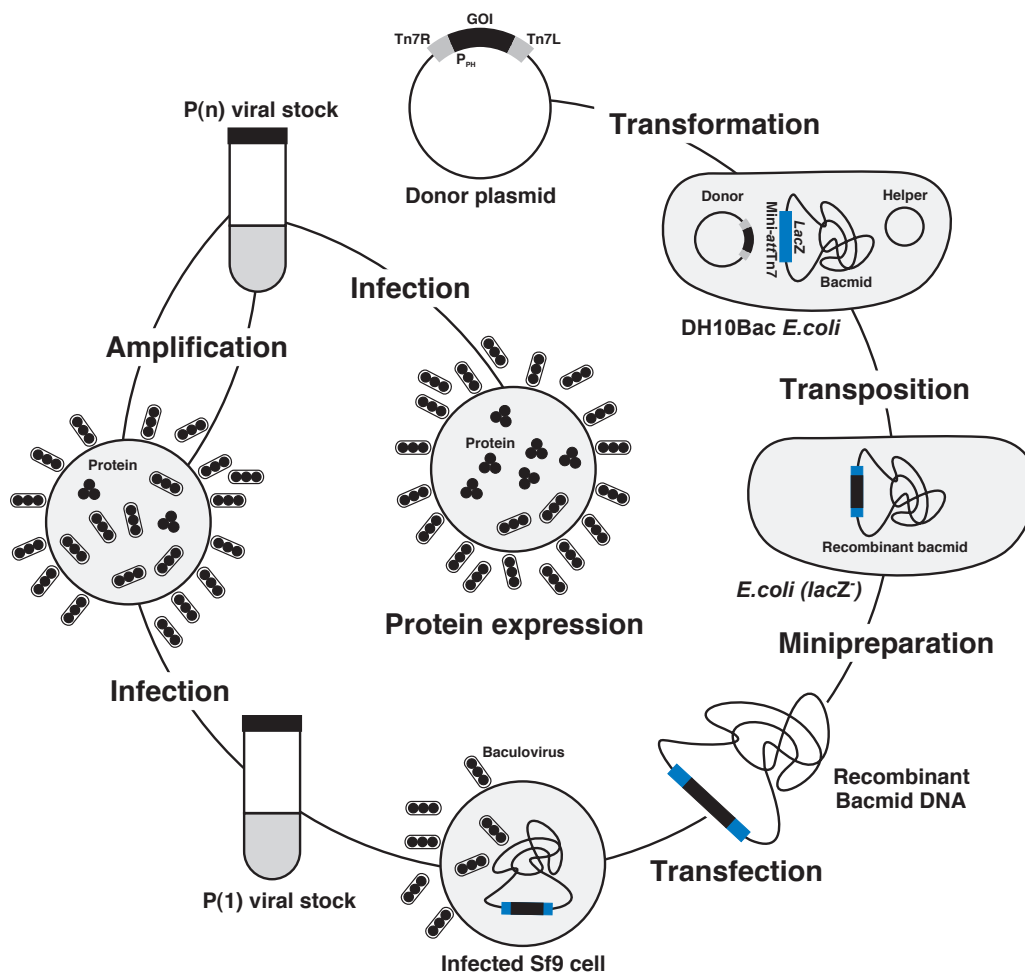


Figure 2.4: **The baculovirus expression system.** Expression of the gene of interest (GOI) is controlled by the *Autographa californica* multiple nuclear polyhedrosis virus polyhedrin (P_{PH}) promoter in the donor vector pFast-Bac. Once the donor plasmid is transformed into DH10Bac *E. coli* cells (see Sec. 2.10.3), a transposition occurs between the mini-Tn7 element in the donor plasmid and the mini-attTn7 target site on the baculovirus shuttle vector (bacmid). The transposition occurs in the presence of proteins supplied by the helper plasmid, and disrupt the expression of *LacZ* peptide. Recombinant bacmid DNA is isolated by minipreparations (see Sec. 2.9.2) and introduced into the Sf9 cells via a lipid-mediated transfection (see Sec. 2.11.2). Transfected cells produce recombinant baculoviruses released to the culture medium. The baculoviruses are collected as a first viral stock P(1), amplified by repeated infections (see Sec. 2.11.3) and collected as high titer P(n) stocks suitable for a large scale protein expression (see Sec. 2.11.5.2). Abbreviations: P_{PH} , polyhedrin promoter; GOI, gene of interest; Tn7L and Tn7R, left and right end of Tn7 transposon; mini-attTn7, target site of the transposition.

(5'-TATCCATGGGAATGGCCAACGCGGGGCTGCA-3') were used under the standard conditions for PCR-amplification (see Sec. 2.9.7). Successfully transposed bacmids were transfected to Sf9 (Sec. 2.11.2), and the released baculoviruses were harvested and amplified as described in Sec. 2.11.3.

2.11.2 Transfection of insect cells

Transfections with purified bacmid DNA (see Sec. 2.11.1) were performed in 6-well plates (TPP). Sf9 cells were seeded at a density of 1×10^6 cells per well and allowed to attach at 28°C at least for one hour. Approximately 6 µg of bacmid DNA were diluted in Sf900 II SFM (Invitrogen) and subsequently 15 µl of Escort transfection reagent (Sigma) was added to reach a final volume of 0.25 ml. The mixture was incubated for 15 min at RT and thereafter diluted with 2.15 ml of Sf900 II SFM. Attachment of Sf9 cells was verified by light microscopy (Axiovert 40 CFL, Zeiss, Germany) and, after media removal, 0.8 ml of the transfection mixture was applied to each well. Control cells received Sf900 II SFM only or transfection mixture without bacmid DNA. Plates were incubated at 28°C for 5-6 hrs. After the incubation, the transfection mixture was replaced by 2 ml of Sf900 II SFM per well, the plates were placed into a humid chamber and moved to 28°C. After 72 hrs of incubation, cells were examined for signs of viral infection under the light microscope. Medium from transfected cells was collected and clarified by a centrifugation at 500 *g* for 5 min at RT. The P(1) baculoviral stock was amplified as described in 2.11.3. Cells transfected with bacmid GUS (see Sec. 2.11.1) were assayed for the expression of β-glucuronidase (see Sec. 2.11.5.1).

2.11.3 Amplification of recombinant baculoviruses

In general, at least 5 rounds of amplification were performed in monolayer cultures and 3 rounds in suspension cultures. Amplification in monolayer culture was performed by seeding the Sf9 cells at a density of 2×10^6 cells per well. The cells were allowed to attach at 28°C for one hour and were subsequently infected with 0.4 ml of baculoviral stock. The plates were incubated for 1 hr at RT and gently shaken every 15 min to achieve an optimal infection. After the incubation, the viral stock was removed and 2 ml of Sf9-900 II SFM medium was added to each well. Plates were placed into a humid chamber and moved to 28°C. After 72 hrs of incubation, medium was collected and clarified by centrifugation at 500 *g* for 5 min at RT. Amplification in suspension was performed by seeding cells in suspension at a density of 2×10^6 cells per ml and infecting the cells with the corresponding baculoviral stock (the ratio of viral stock to culture volume was 1:5 to 1:10; v/v). Amplified stocks were clarified (as described above) and stored at 4°C protected from light.

2.11.4 Titration of baculoviral stocks

Titers of baculoviral stocks were determined by plaque assay. Briefly, the stock was serially diluted (10^{-1} - 10^{-10} dilution) in Sf900 II SFM medium. Sf9 cells were seeded in 6-well plates (TPP) at a density of 1×10^6 cells per well and allowed to attach at 28°C for at least one

hour. Attachment of Sf9 cells was verified by light microscopy. After media removal, 1 ml of the diluted baculoviral stock per well was applied in duplicates. Plates were incubated at 28°C for 1 hr. After the incubation, the baculoviral suspensions were removed and 2 ml of plaquing medium was added per wells. The plaquing medium was prepared by mixing of 4% agarose (Invitrogen), melted in a 70°C water bath, with Sf-900 (1.3x) medium (Invitrogen), previously pre-warmed to 40°C. To decrease the temperature, the plaquing medium was equilibrated at least 10 min in a 40°C water bath before being applied to the cells. The agarose overlay was allowed to harden at RT for 30 min without disturbing. Subsequently, plates were placed in a humid box and moved to 28°C. After 8 days of incubation, plates were examined for the presence of plaques. Visualisation of plaques was enhanced by staining of the agarose overlay with neutral red (0.2 mg/ml in distilled water) for 1 hr at RT. Excess of the dye was removed and plates were stored overnight in the dark at RT. Plaques were counted and the titer was calculated as plaque forming units (pfu) per ml of the baculoviral stock solution.

2.11.5 Protein expression in insect cells

2.11.5.1 Expression of β -glucuronidase

Sf9 cells transfected with bacmid GUS (see Sec. 2.11.1) were assayed for the expression of β -glucuronidase. Briefly, cells were washed once with phosphate-buffered saline containing calcium and magnesium (Invitrogen) and fixed with 2% formaldehyde and 0.05% glutaraldehyde in phosphate buffered-saline (PBS). Developer solution was prepared by mixing of 19 parts of staining solution containing 5 mM potassium ferricyanate, 5 mM potassium ferrocyanate, 2 mM magnesium chloride in PBS with 1 part of X-glucuronide (Fermentas) solution (20 mg/ml) in dimethylformamide. After two washing steps with PBS, the developer solution was added to each well and cells were incubated for 2 hrs at 37°C. After the incubation, wells were washed with PBS and screened in the light microscope for the presence of blue color (cleavage product resulting from the enzymatic processing of X-glucuronide with expressed β -glucuronidase).

2.11.5.2 Expression of his-tagged claudin-1

For small scale expression of His-CLD1, cells were seeded at a density of 2×10^6 cells per ml and infected with amplified baculoviral stock at a multiplicity of infection (MOI) of 3 to 10 as indicated. Cells were incubated at 28 °C for 2-4 days and samples of infected cells were taken as indicated. The samples were subjected to analysis by SDS-PAGE (see Sec. 2.12.4) and Western blot (see Sec. 2.12.6). For large scale expression, cells were seeded at a density of 2×10^6 cells per ml in a total volume of 1000 ml and infected at an MOI of 3. After 2 days of incubation, successful infection was confirmed by light microscopy, and crude membranes were prepared (for details see Sec. 2.12.2).

2.12 Protein purification and analysis

2.12.1 Quantification of proteins

Protein quantification was done by a DC Protein assay kit (Bio-Rad), which is based on the method of Lowry et al. (1951), using bovine serum albumin (Bio-Rad) as a standard. The assay was performed according to the manufacturer's recommendations. Absorbance of standards and samples was measured at 700 nm using a Cary 1E UV/VIS spectrophotometer (Varian, USA). Alternatively, a rough estimation of the protein concentration was done by measuring the absorbance at 280 nm and calculating according to Bollag et al. (1996).

2.12.2 Preparation of crude membranes

The protocol for the preparation of crude membranes is based on Hrycyna et al. (1998). Infected Sf9 cells were harvested at 1178 *g* for 10 min at 4°C and re-suspended in ice-cold PBS (130 mM NaCl, 8.03 mM Na₂HPO₄, 1.97 mM KH₂PO₄) supplemented with a protease inhibitor cocktail (1 tbl per 50 ml; Complete EDTA-free, Roche) to wash them. The cells were centrifuged again at 3838 *g* for 15 min at 4°C and the washing step with ice-cold PBS was repeated once more. Subsequently, the cells were re-suspended in a hypotonic lysis buffer (10 mM Tris, 10 mM NaCl, 5 mM CaCl₂) and incubated on ice for 30 min. Cells were disrupted on ice with 2 times 50 stokes at 1000 rpm with a Potter homogenizator (B. Braun Biotech International, Germany). Cell nuclei and undrupted cells were removed by centrifugation at 500 *g* for 10 min at 4°C (pellet Pt1). The low-speed supernatant (St1) was incubated with 0.1 mg DNase I (Roche) per ml for 20 min on ice. Membranes were pelleted by a centrifugation for 60 min at 28'500 rpm (100'000 *g*) at 4°C in a Beckman ultracentrifuge with the SW41 Ti rotor. The high-speed supernatant (St2) was discarded and the pellets re-suspended in buffer A0 (50 mM NaH₂PO₄, 1 M NaCl, 10 mM imidazole, pH 8). Crude membranes were snap-frozen in liquid nitrogen and stored at -80°C until use.

2.12.3 Affinity chromatography

Crude membranes from infected Sf9 cells were mixed 1:5 (v/v) with buffer A1 (50 mM NaH₂PO₄, 1 M NaCl, 10 mM imidazole, 4 % w/v octyl β-D-glucopyranoside (octylglucoside), pH 8) and proteins solubilized for 1 hr at RT on a rocking plate. Insoluble material was pelleted by centrifugation for 60 min at 28'500 rpm (100'000 *g*) at 4°C in a Beckman ultracentrifuge with the SW41 Ti rotor. The supernatant (cleared lysate) was mixed with Ni-NTA beads (2 ml of 50 % suspension in ethanol; Qiagen) previously equilibrated with buffer A1. The binding of His-CLD1 was done for 1 hr at RT on a rocking plate and subsequently the resin was transferred to a polypropylene column (Qiagen). Four to six washing steps with 4 column volumes of washing buffer (50 mM NaH₂PO₄, 1 M NaCl, 20 mM imidazole, 1 % w/v octylglucoside, pH 8) were performed and protein was eluted with 8 column volumes of elution buffer (50 mM NaH₂PO₄, 1 M NaCl, 400 mM imidazole, 1 % w/v octylglucoside, pH 8). Seven to eight elution fractions were collected. The

protein concentration in the elution fractions was estimated by measuring absorption at 280 nm (see Sec. 2.12.1). Fractions were snap frozen in liquid nitrogen and stored at -80°C until use.

2.12.4 SDS polyacrylamide gel electrophoresis

Sodium dodecylsulfate polyacrylamide gel electrophoresis (SDS-PAGE) was performed with the Mini-Protean 3 Cell electrophoresis system (Bio-Rad) with the method based on Laemmli (1970). A solution of 30% (w/v) acrylamide and N, N'-methylene-bis-acrylamide (monomer to crosslinker ratio 37.5:1; Bio-Rad) was used to prepare a 12% separating gel (12% w/v acrylamide/bis, 0.375 M Tris, pH 8.8, 0.1% SDS) and a 4% stacking gel (4% w/v acrylamide/bis, 0.125 M Tris, pH 6.8, 0.1% SDS). Gels were polymerized chemically by addition of 0.05% (w/v) ammonium persulfate and 0.05% (v/v, in separating gel) or 0.1% (v/v, in stacking gel) N, N, N', N'-tetramethylethylenediamine (Fluka). To decrease the amount of non-polymerized acrylamide, gels were stored overnight at 4°C before use. Protein samples prepared in lysis buffer (0.0649 M Tris, 2.2% w/v SDS, 7% v/v glycerol) were mixed with 1/10 of a solution containing 7% (v/v) glycerol, 34% (v/v) β -mercaptoethanol and 0.1% (w/v) bromphenol blue. Samples prepared in different buffers than lysis buffer were mixed with 1/5 of a solution containing 0.3125 M Tris, 10% (w/v) SDS, 35% (v/v) glycerol, 17% (v/v) β -mercaptoethanol and 0.05% (w/v) bromphenol blue. All samples were heated for 15 min at 60°C . Samples (1-50 μg per slot) were loaded with a Hamilton syringe and electrophoresis was run at 120 V for 1.5 hrs in electrophoresis buffer (25 mM Tris, 0.1% w/v SDS, 192 mM glycine). A protein standard (Dual Color Precision Plus, BioRad) was used for the gel calibration. After the separation, Western blotting (Sec. 2.12.6) or silver staining (Sec. 2.12.5) were performed.

2.12.5 Silver staining

After the electrophoresis, gels were stained with the Silver staining Plus kit (Bio-Rad). Briefly, gels were fixed with 40 ml fixative enhancer solution containing (50% v/v methanol, 10% v/v acetic acid, 10% v/v fixative enhancer concentrate, 30% v/v deionized distilled water) for 20 min at RT. Fixative solution was removed by rinsing the gels twice with 40 ml deionized distilled water for 10 min. Gels were then incubated with staining solution (2.5 ml silver complex solution, 2.5 ml reduction modulator solution, 2.5 ml image development reagent, 1.25 g development acceleration reagent, ad 50 ml deionized distilled water). The staining was stopped with 5% (v/v) acetic acid for 15 min and gels were washed with distilled water for 5 min.

2.12.6 Western blotting

A Mini Trans-Blot Electrophoretic Transfer Cell (Bio-Rad) was used to transfer proteins onto nitrocellulose membranes (Hybond-C extra, Amersham Life Science). The transfer was achieved by applying 350 mA for 1.5 hrs in blotting buffer (25 mM Tris, 0.1% w/v SDS, 192 mM glycine, 20% v/v methanol). For immunostaining, membranes were first blocked in TBBS buffer pH 7.4 (20 mM Tris, 0.5 M NaCl, 0.1% v/v Tween 20) containing 5% (w/v) skimmed milk for 1 hour at RT. After the blocking step, membranes were incubated with primary antibodies in TBBS

buffer containing 1 % (w/v) skimmed milk overnight at 4°C. Primary antibodies were mouse anti claudin-1 antibody (dilution 1:5000; Zymed) or mouse anti His-tag antibody (dilution 1:1000; Zymed), respectively. Following the incubation, three subsequent washing steps with TBBS buffer containing 1 % (w/v) skimmed milk were performed. Secondary antibodies, goat anti mouse alkaline phosphatase-coupled (dilution 1:50'000; Pierce), were diluted in TBBS buffer containing 1 % (w/v) skimmed milk and membranes incubated for 4 hrs at 4°C. Membranes were subjected to three washing steps with TBBS buffer and proteins were detected with the enhanced chemiluminescence immunoblotting detection system (Bio-Rad). Membranes were immediately exposed to X-ray films (Super RX, Fujifilm) and films developed in a Curix 60 apparatus (Agfa, Belgium).

2.13 Preparation and analysis of proteoliposomes

2.13.1 Detergent dialysis

Micelles were prepared from lipid films of phosphatidylcholine (egg lecithin; Lipid products, Nutfield, Surry, UK). A stock solution of lipids (500 mg/ml) was diluted with 10 ml of methanol and the solvent was evaporated in a 250 ml round flask on a rotavapor (Büchi, Switzerland) at 40°C and 100 rpm. The pressure was set to 180 mbar for 10 min following by 80 mbar for 30 min and finally by 20 mbar for 1 hour. To remove the last traces of solvent, the flask was stored overnight under vacuum. The lipid film was dissolved by addition of sodium cholate (Fluka) in solution of His-CLD1 (elution fractions from the affinity purification, see Sec. 2.12.3) or in dialysis buffer (for 'control liposomes') with sodium cholate and octylglucoside (Sigma). The final concentration of lipids was 5 mg/ml with a molar ratio of 0.85 of sodium cholate to lipid. The final concentration of octylglucoside was 1 % (w/v). The ratio of protein to lipid was approximately 1:100 (w/w), which corresponds to a molar ratio of approximately 1:3000. Micelles were equilibrated for 3 hrs at RT on a rocking plate and subsequently dialysed.

The dialysis was performed in Eppendorf tubes according to the method of Overall (1987). Briefly, the cap of an Eppendorf tube was perforated with a heated Pasteur pipette to create a hole of 8 mm in diameter. 250 µl of micelles were placed into the modified tubes. A dialysis membrane (mw.-cutoff 5000; Dianorm) was placed over the tube opening and clamped in place by closing the perforated cap. The tube was inverted and fixed on a floating tube holder. Tubes were immersed in 2 l dialysis buffer (130 mM NaCl, 50 mM Na₂HPO₄/NaH₂PO₄) and care was taken to remove the air pockets trapped in the tubes. To ensure a proper dialysis, a magnetic stirrer was placed on the bottom of the vessel with dialysis buffer. The dialysis buffer was changed 3 times a day. The dialysis was run for 48 hrs. After the dialysis, the liposomes were characterized by dynamic light scattering (see Sec. 2.13.2) and subsequently loaded onto a sucrose density gradient (see Sec. 2.13.3).

To monitor the removal of detergents from micelles (without His-CLD1), 448 kBq/ml of ³H-cholic acid and 74 kBq/ml octyl ¹⁴C-β-D-glucopyranoside, respectively, were added to micelles. Samples were collected as indicated, mixed with 3 ml scintillation cocktail (Ultima Gold, Packard BioScience) and analyzed by liquid scintillation counting.

2.13.2 Dynamic light scattering

The average size and the size distribution of liposome preparations were analyzed by dynamic light scattering with a Zetasizer 3000 HSA (Malvern Instruments, UK) with a 10 mW helium neon laser (633 nm) equipped with a x-channel correlator. Dynamic light scattering was measured at 25°C in 1.5 ml disposable cuvettes (Brand). Liposomes were diluted 1:50 with dialysis buffer for the measurements. The size distribution was calculated by fitting a single exponential (cumulant fit) to the correlation function to obtain the mean size (z-average diameter) and an estimate of the width of the distribution (polydispersity index). To report correlograms, raw data from the correlator were normalized for the baseline ('far point') and scaled to obtain values ranging from 0-1.

2.13.3 Sucrose density gradient

Liposomes prepared by dialysis were mixed with 80 % (w/v) sucrose in TNE buffer (25 mM Tris, 150 mM NaCl, 5 mM EDTA, pH 7.4) to obtain a final concentration 60 % (w/v) sucrose. The sucrose gradient (11.5 ml) was prepared as follows. In a centrifuge tube, a cushion of 80 % (w/v) sucrose in TNE buffer (1.5 ml) was overlaid by 60 % (w/v) sucrose containing the liposomes (4 ml), followed by 40 %, 20 % and 5 % (w/v) sucrose in TNE buffer (2 ml each). The tube was centrifuged at 39'000 rpm (200'000 *g*) for 19 hrs at 4°C in a Beckman ultracentrifuge with SW41 Ti rotor. After the centrifugation, fractions of 1 ml were collected from the top of the tube (fractions 1 to 12). Liposomes were visible as a turbid band in the upper part of the centrifuge tube. The density of the fractions was calculated from the refractive index (Birnie and Rickwood, 1978), which was measured at 20°C with an automatic refractometer (RFM90; Bellingham and Stanley, UK). In addition, fractions were analysed by dynamic light scattering (Sec. 2.13.2).

3 Results

3.1 Morphological studies on the modulation of tight junctions

3.1.1 Calcium chelation method

A calcium depletion model was used to study the morphology of plaque and transmembrane proteins of tight junctions (TJs). The Madin Darby canine kidney (MDCK) cells (or MDCK expressing N-terminally GFP-tagged claudin-1; MDCK-GFP-CLD1) were grown on polyethylene terephthalate (PET) cell culture inserts and a short-term treatment with a calcium chelator (EGTA) was applied (for details see Sec. 2.7.4).

The influence of EGTA on the transepithelial electrical resistance (TEER) and on the localization of a TJ-plaque protein (zonula occludens-1; ZO-1) during the opening and re-formation of TJs after the addition of normal calcium-containing medium is demonstrated in Fig. 3.1. The control cells before the EGTA treatment displayed well organized 'honeycomb-like' structures typical for proteins localized at TJs. Twenty minutes after the EGTA treatment, a rapid drop of TEER could be observed. The cells were rounded up and ZO-1 was present in the membrane regions as well as in the remaining intercellular contacts between the cells. A re-distribution of ZO-1 into the cytoplasm upon the TJ-disruption occurred. Replacement of the chelation medium with the calcium-containing medium led to a gradual restoration of the TEER as well as the characteristic TJ-structures within one hour.

3.1.2 Dynamic behavior of cingulin

Cingulin is a plaque protein of TJs (Citi et al., 1988). To describe the dynamic behavior of cingulin, control samples and EGTA-treated MDCK cells were immunolabeled for cingulin, the plaque protein ZO-1 and the transmembrane protein occludin (OCLN). The cytoskeletal protein F-actin was visualized with a fluorescent derivative of phalloidin (for details see Sec. 2.8). High-resolution images were simultaneously recorded for each fluorescent channel and a colocalization analysis was performed as described in Sec. 2.8. Optical sectioning of the samples is depicted in Fig. 3.2A. The results are illustrated in Fig 3.3 and Fig 3.4.

According to the morphology of the cells treated with EGTA, we defined two regions of interest (ROIs) for the statistical analysis of co-localization. Schematic representation is shown in Fig. 3.2B. Regions of interest type I were defined as the areas of the plasma membranes and regions of interest type II as the areas of the remaining contacts (filaments) between the cells after the disruption of TJs.

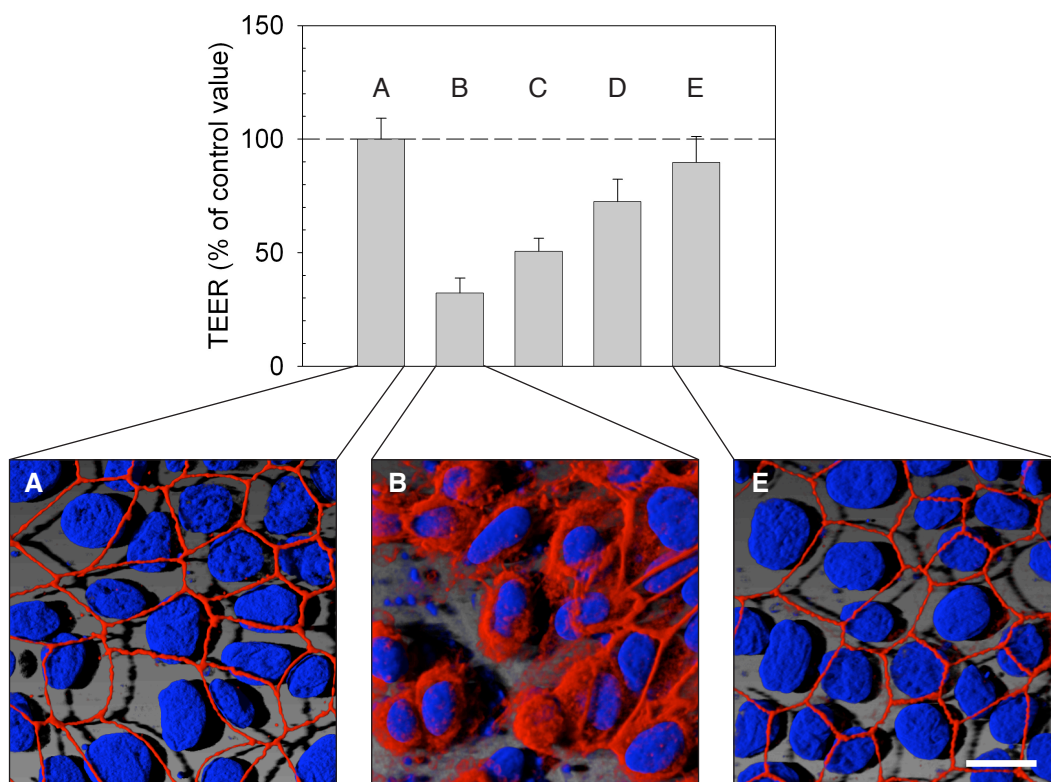


Figure 3.1: **Effect of calcium depletion on TEER and localization of ZO-1.** MDCK cells were cultured on PET inserts for 3 days and calcium chelation was performed as described in Sec. 2.7.4. At the indicated time points, TEER values were recorded and cells were fixed and labeled for ZO-1 (red) and nuclei (blue). (A) Control (w/o EGTA); (B) 20 min after EGTA treatment; (C) 20 min recovery; (D) 40 min recovery; (E) 1 hr recovery in calcium-containing medium. Error bars represent values of four cell culture inserts from a representative experiment. CLSM images are shown as 3D-reconstructions (SFP-mode). Scale bar, 15 μ m.

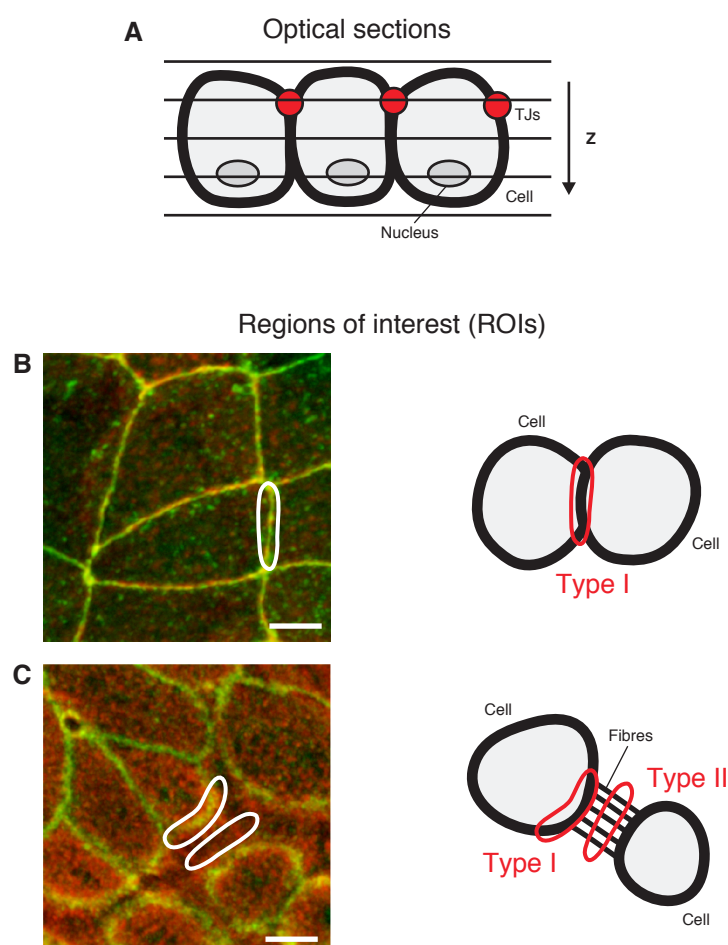


Figure 3.2: **Optical sectioning and regions of interest defined for statistical analysis of co-localization.** (A) Optical sections of $0.15\ \mu\text{m}$ for high-resolution images are numbered from the apical to the basolateral position. Regions of interest (ROIs) in the (B) control cells and (C) EGTA-treated cells. ROI type I were chosen as the area of the plasma membranes and ROI type II as the filaments remaining between cells after TJ disruption. Color code: green, cingulin; red, F-actin. Scale bar, $5\ \mu\text{m}$.

In the ROIs type I, one major co-localization peak could be observed for each protein pair, in the control cells as well as in the EGTA-treated cells (Fig. 3.4). The co-localization in the ROIs type I was not significantly changed upon the disruption of TJs by EGTA treatment and the major peak of co-localization was retained for all protein combinations. The co-localization peak shifted from layer 33 to 51 for protein pair cingulin with ZO-1, and from layer 39 to 46 for protein pair cingulin with F-actin. In contrast, for the protein pair cingulin with OCLN, the co-localization peak was not shifted. In the ROIs type II, the major peak of co-localization was retained for the combination of cingulin and OCLN, as well as for cingulin and F-actin, however, the extent of co-localization was slightly reduced, as compared to the ROI type I in the control. A different pattern was seen for the combination of cingulin and ZO-1, in which the co-localization was significantly reduced.

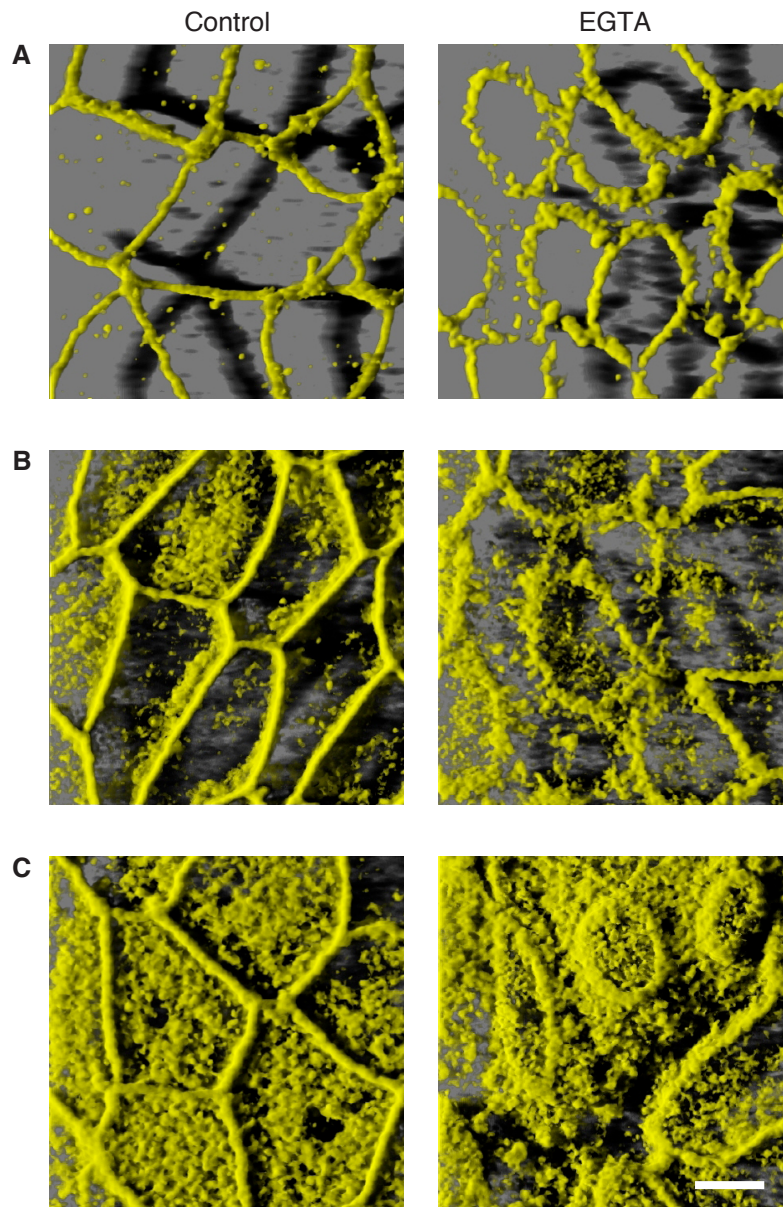


Figure 3.3: **Co-localization of cingulin with ZO-1, OCLN and F-actin.** MDCK cells were grown on PET cell culture inserts for 11 days and calcium chelation experiments were performed. Control and EGTA-treated cells were fixed and labeled for cingulin, ZO-1, OCLN and F-actin. High-resolution images were acquired by CLSM (Sec. 2.8). Co-localizations of (A) cingulin and ZO-1, (B) cingulin and OCLN, (C) cingulin and F-actin are illustrated as 3D-reconstructed (SFP-mode) micrographs. Only co-localized pixels are shown. Scale bar, 5 μm .

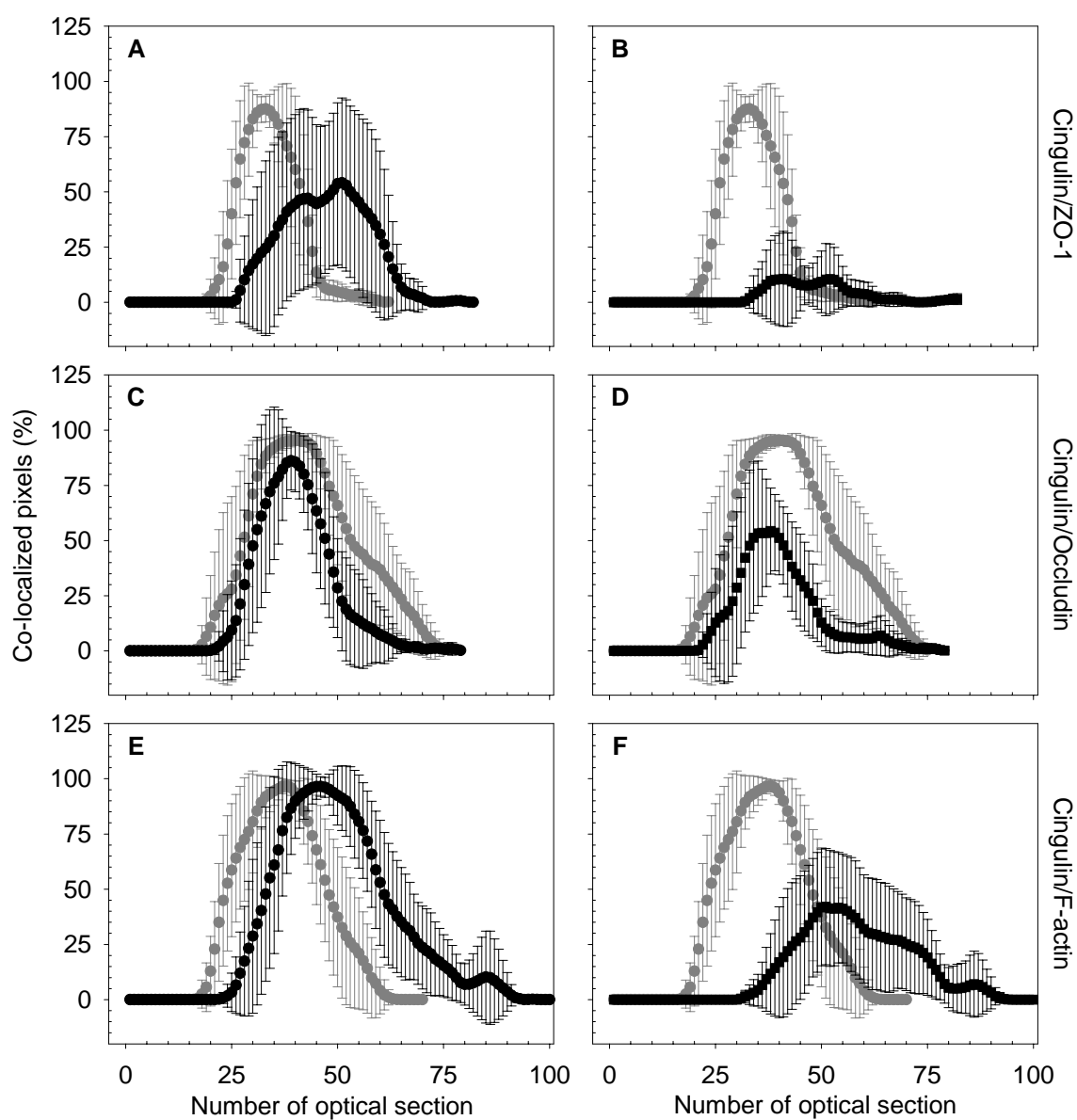


Figure 3.4: **Statistical analysis of cingulin co-localization with different TJ proteins.** From the high-resolution CLSM images, regions of interest (ROIs; see Fig. 3.2) of type I and II were selected and the number of co-localized pixels (in percent of total fluorescent pixels) of the respective fluorescent channels was calculated for each optical section (for details see Sec. 2.8). Shown are profiles of EGTA treated cells (A, C, E, black circles represent ROI type I; B, D, F, black squares represent ROI type II) and control cells (A-F, grey circles represent ROI type I). Data represent mean values and standard deviations of co-localized pixels from 10 representative ROIs. Optical sections are numbered from the apical to the basolateral position (Fig. 3.2A).

3.1.3 Dynamic behavior of GFP-tagged claudin-1

To describe the behavior of claudin-1 (CLD1) in the calcium depletion model, a GFP-tagged CLD1 (GFP-CLD1) was generated. The CLD1 sequence was tagged with GFP by subcloning of the PCR-amplified open reading frame (ORF) into the pEGFP-C1 vector (for details see Sec. 2.9.1). The identity of the resulting construct pEGFP-CLDN1 was confirmed by DNA sequencing (not shown). MDCK cells were transfected with the construct by lipid-mediated transfection and upon selection with geneticine (G418), a stable transfected cell line MDCK-GFP-CLD1 was established (for details see Sec. 2.6). The growth characteristics of the MDCK-GFP-CLD1 cell line were not changed when compared to parent MDCK cells (not shown).

Transfected cells grown on PET cell culture inserts for 3-4 days were fixed and localization of the GFP-CLD1 was investigated by CLSM (for details see Sec. 2.8). The GFP-fluorescence was located in the lateral membranes and displayed a 'honeycomb-like' structure typical for proteins localized at TJs (Fig. 3.5). The GFP-CLD1 present in the lateral membranes co-localized with labeling against endogenous transmembrane proteins of TJs, such as claudin-4 (CLD4) and OCLN, respectively. In addition, a strong GFP-signal was observed in the cytoplasm of the MDCK-GFP-CLD1 cells. The cytoplasmic localization persisted in the cultured cells from stage I to III of development (Rothen-Rutishauser et al., 1998a), i.e. up to 11 days in culture (not shown). To investigate the cytoplasmic localization of GFP-CLD1, the MDCK-GFP-CLD1 cells were subjected to labeling against the peripheral Golgi membrane protein 58K and probed with LysoTracker Red DND-99, a fluorescent acidotropic probe for labeling and tracking acidic organelles such as lysosomes (Fig. 3.5). The GFP-CLD1 co-localized partially with the fluorescent signal of LysoTracker DND-99, whereas almost no co-localization could be observed for the Golgi 58K protein. A cytoplasmic localization of CLD was also revealed in parent MDCK (non-transfected cells) when labeled for CLD4 (not shown).

To describe the dynamic behavior of GFP-CLD1 in relation to different TJ proteins, the calcium chelation method was applied (Sec. 2.7.4). Several time points were defined to follow the disruption and re-assembly of TJs: control at 0 min (before EGTA treatment), 20 min after EGTA treatment, and after addition of calcium-containing medium, every 10 min up to 1 hr recovery. At these time points, the cells were fixed and labeled for ZO-1, OCLN, CLD4 and F-actin. Results of ZO-1 staining are illustrated in Fig. 3.6. Before the EGTA treatment, a well-developed staining and co-localization of ZO-1 and GFP-CLD1 was observed in the lateral membranes. After the EGTA treatment, a clear disruption of TJs occurred due to a calcium removal. Cells were separated and remained connected by filaments that also contain F-actin (see Fig. 3.2C). In the recovery series, the cell-cell contacts re-established and this process was finished after 60 min. During the re-sealing of the contacts, the GFP-CLD1 and ZO-1 staining re-distributed from the cytoplasmic localization back to the lateral membranes. No difference in the kinetics of the re-sealing for GFP-CLD1 and ZO-1 was found. Similar dynamic behavior could be found also for other TJ proteins, such as OCLN and CLD4 (not shown).

The influence of EGTA on the GFP-CLD1 was visualized in living cells as well. Unfortunately, a bleaching of the GFP-fluorescence during the time-relapse imaging occurred and hampered a proper analysis of the dynamic behavior. The GFP-fluorescence appeared to be more stable after the fixation, and thus fixed samples were analyzed only.

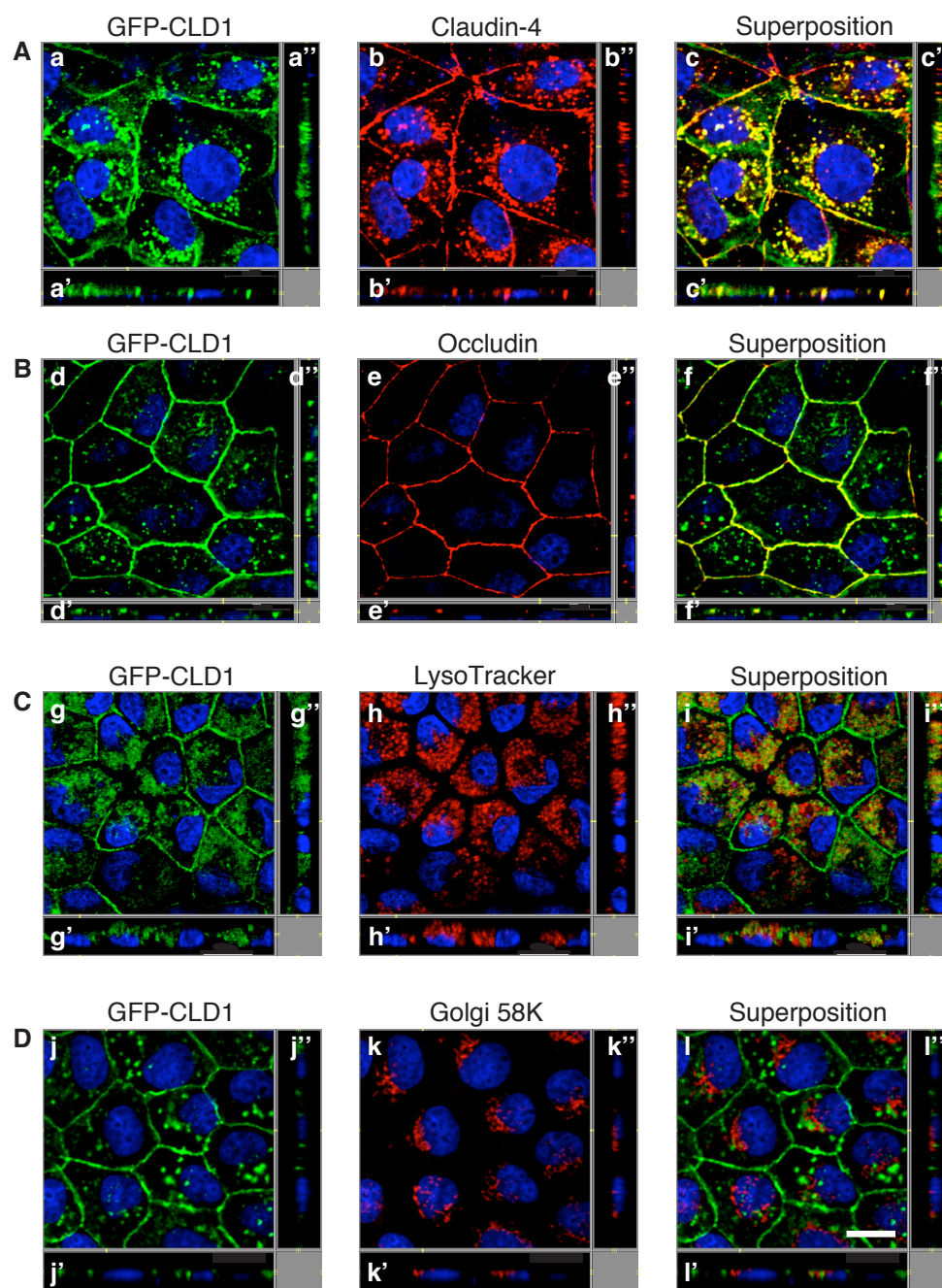
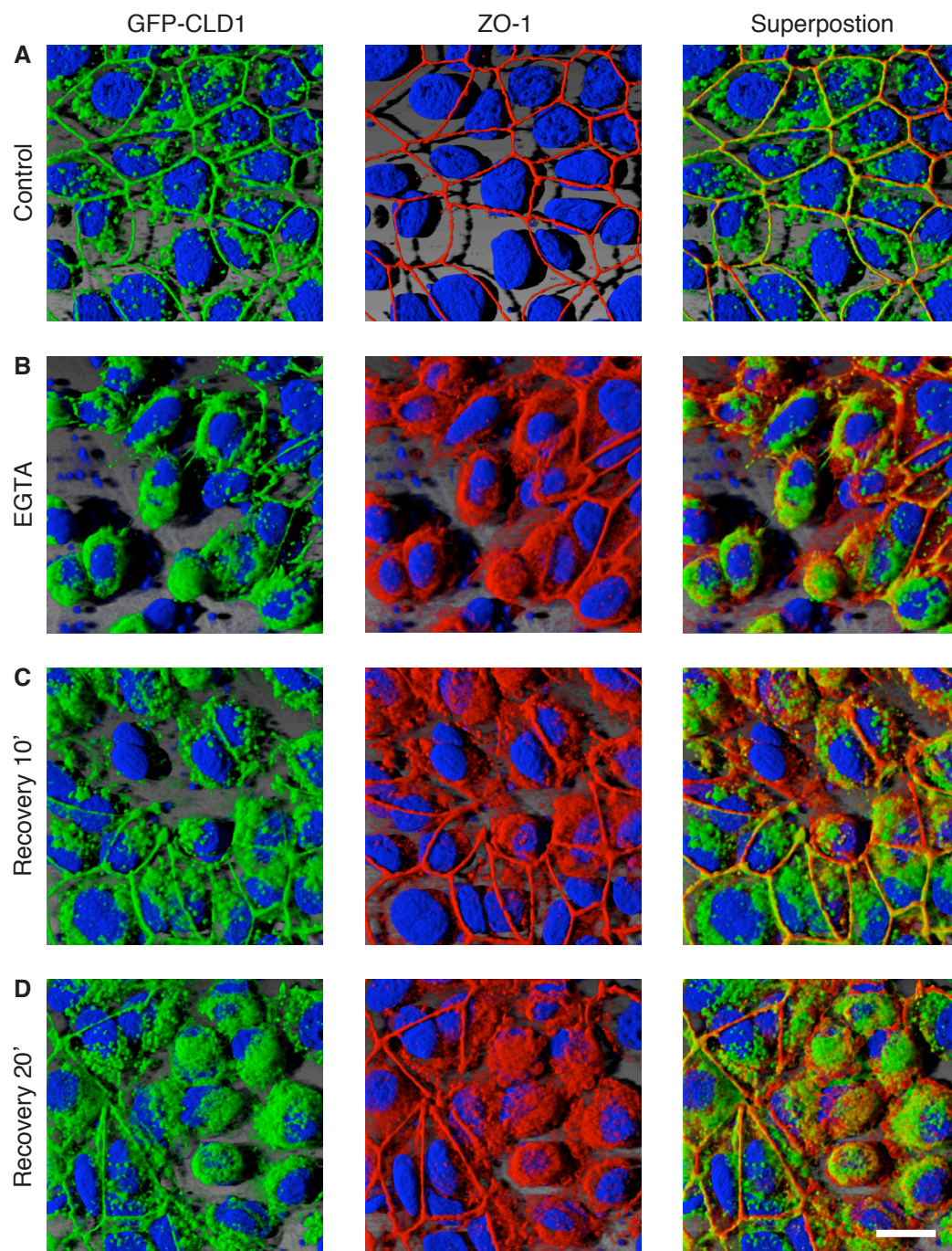


Figure 3.5: **Localization of GFP-CLD1 in transfected MDCK cells.** MDCK-GFP-CLD1 cells (for details see Sec. 2.6) were grown on PET cell culture inserts (A, B, D) or in coverglass chambers (C) for 3-4 days and prepared for CLSM as described in Sec. 2.8. Color code: (A-D, green) GFP-CLD1; (A, red) claudin-4; (B, red) occludin; (C, red) lysosomes; (D, red) Golgi apparatus; (A-D, blue) nuclei. CLSM images are shown as (a-l) xy-sections, (a'-l') xz-projections and (a''-l'') yz-projections. Scale bar, 15 μm .



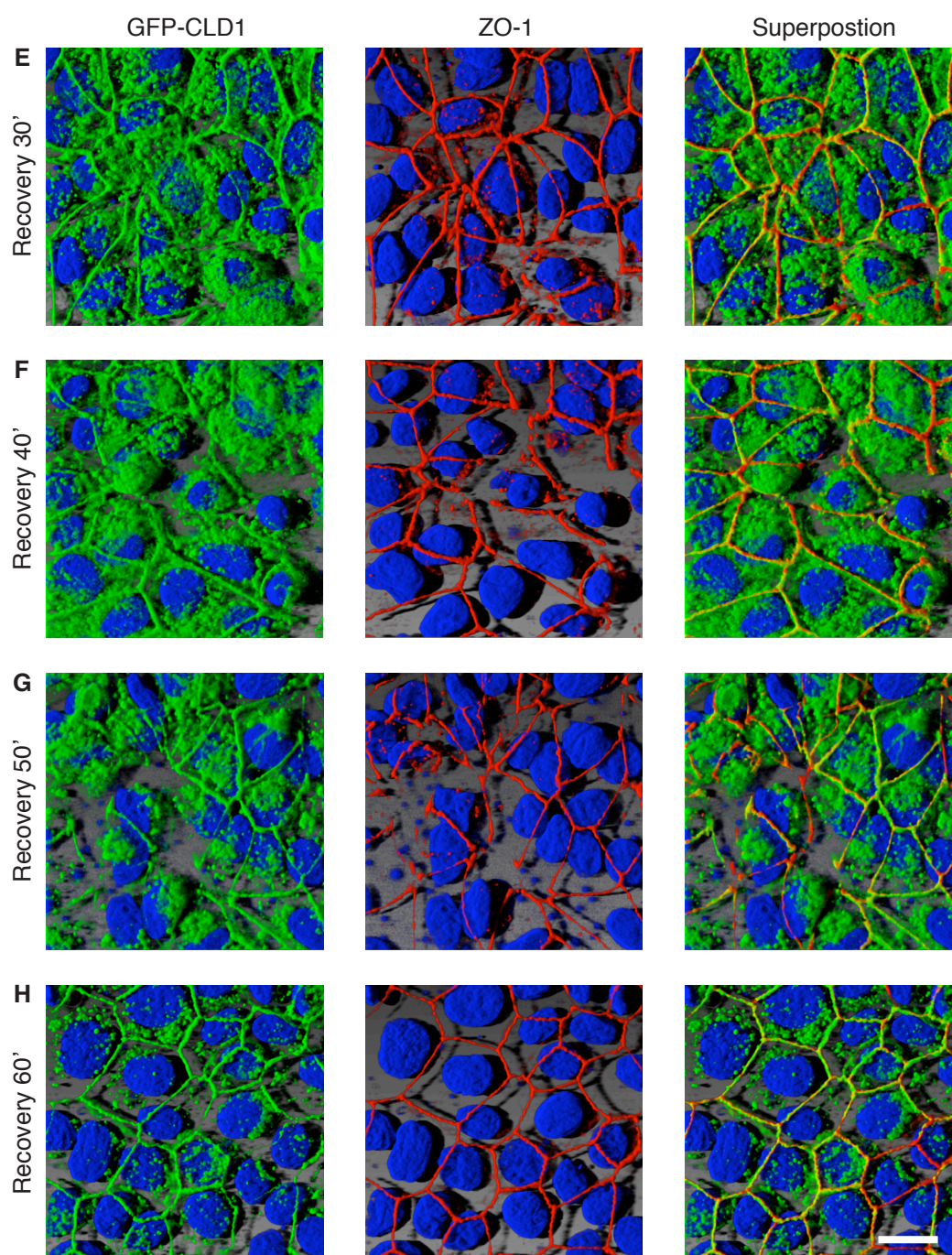


Figure 3.6: **Localization of GFP-CLD1 and ZO-1 upon disruption and re-assembly of tight junctions.** MDCK cells expressing GFP-CLD1 (green) were cultured on PET inserts for 3 days and calcium chelation was performed as described in Sec. 2.7.4. Samples were fixed and labeled for ZO-1 (red) and nuclei (blue). (A) control; (B) 20 min after EGTA treatment; (C) 10 min recovery; (D) 20 min recovery; (E) 30 min recovery; (F) 40 min recovery; (G) 50 min recovery; (H) 1 hr recovery in calcium-containing medium. CLSM images are shown as 3D-reconstructions (SFP-mode). Scale bar, 15 μ m.

3.2 Synthetic peptide homologues to claudin and occludin sequences as a strategy to modulate tight junctions

3.2.1 Influence of peptide homologues to claudin on tight junctions

We designed peptide homologues corresponding to the sequences of the first extracellular domain of human claudins (Fig. 3.7) and tested their ability to modulate TJs in MDCK cells. The peptides were designed according to the sequence of three claudins, namely claudin-1 (CLD1), claudin-2 (CLD2) and claudin-4 (CLD4). The extracellular loop was divided into three parts to obtain peptides with amino acid residues 31-49, 47-65 and 63-81, respectively. In addition, the CLD1 peptide homologue 47-65 (peptide **6**) was modified by replacing the cysteines with serine residues (peptide **14**) and by C-terminal amidation (peptide **5**), respectively.

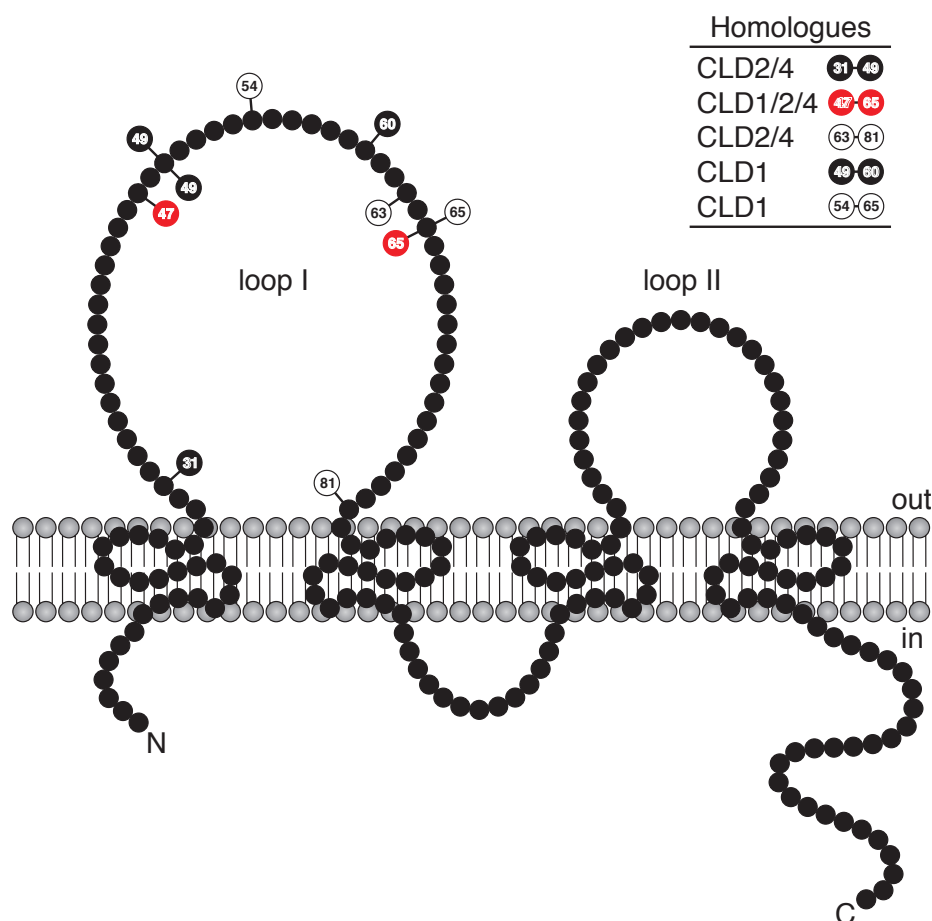


Figure 3.7: **Design of peptide homologues corresponding to the first extracellular loop of claudin.** Peptides were designed according to the sequence of three claudins (CLD1, CLD2 and CLD4) with amino acid residues 31-49, 47-65, 49-60, 54-65 and 63-81, respectively. Peptide sequences are listed in Sec. 2.2 in Tab. 2.1. Abbreviations: in, intracellular space; out, extracellular space.

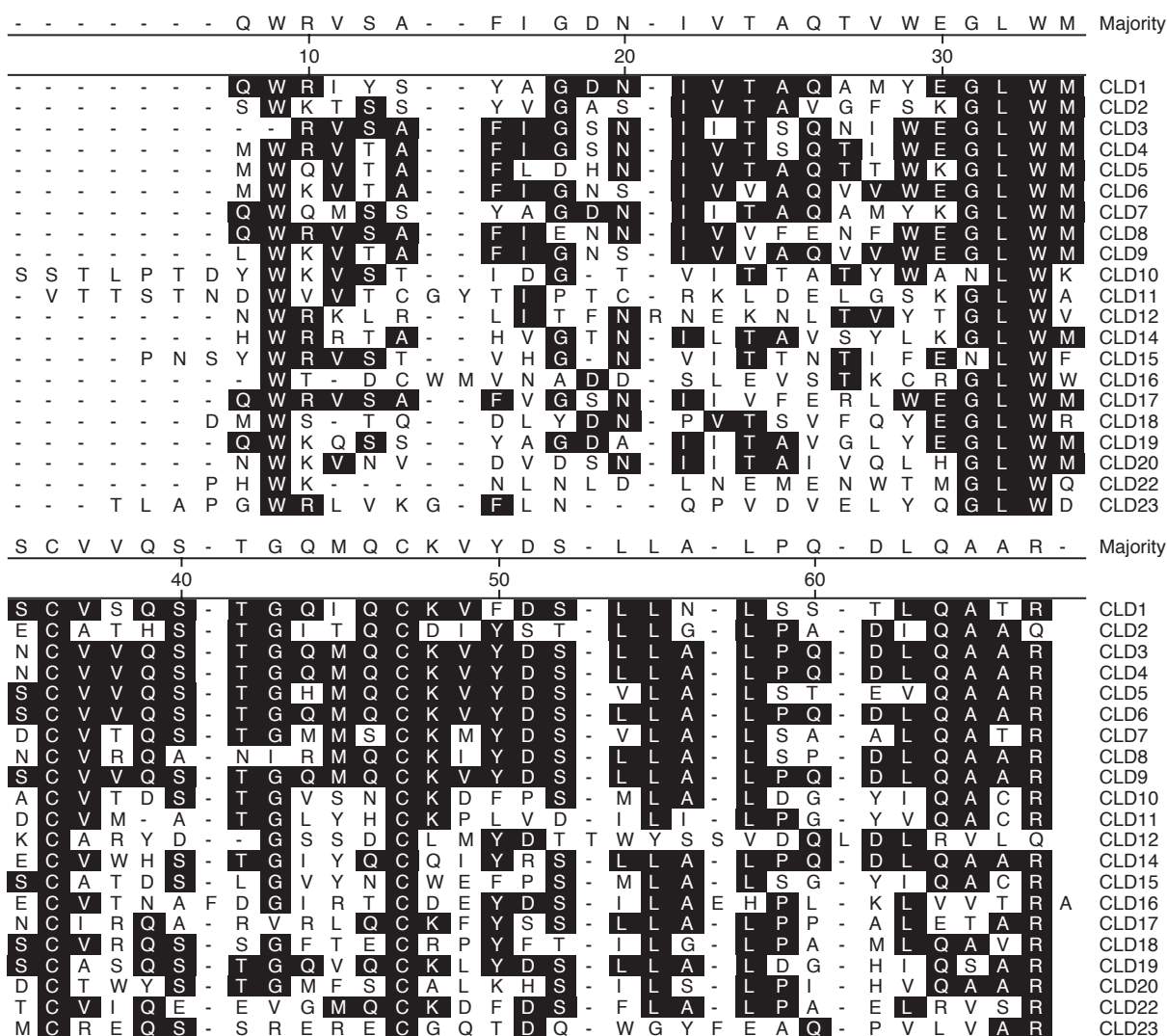


Figure 3.8: **Amino acid alignment of the first extracellular loop of claudins.** Alignment of the first extracellular loop of claudins shows high sequence similarity. Amino acids are written in one-letter code according to the IUPAC convention (IUPAC-IUB, 1984). Identical amino acids are shaded black. Sequences were retrieved from UniProtKB/Swiss-Prot database (Boeckmann et al., 2003; Wu et al., 2006) under the following accession numbers: claudin-1 (CLD1), O95832; claudin-2 (CLD2), P57739; claudin-3 (CLD3), O15551; claudin-4 (CLD4), O14493; claudin-5 (CLD5), O00501; claudin-6 (CLD6), P56747; claudin-7 (CLD7), claudin-8 (CLD8), P56748; claudin-9 (CLD9), O95484; claudin-10 (CLD10), P78369; claudin-11 (CLD11), O75508; claudin-12 (CLD12), P56749; claudin-14 (CLD14), O95500; claudin-15 (CLD15), P56746; claudin-16 (CLD16), Q9Y5I7; claudin-17 (CLD17), P56750; claudin-18 (CLD18), P56856; claudin-19 (CLD19), Q8N6F1; claudin-20 (CLD20), P56880; claudin-22 (CLD22), Q8N7P3; claudin-23 (CLD23), Q96B33. Amino acid sequence alignment was performed with the MegAlign program (DNASTAR Lasergene) using the ClustalW method (Thompson et al., 1994).

The amino acid alignment of the first extracellular loop among different claudins revealed high sequence similarity (Fig. 3.8). The motif GLWM as well as two cysteine residues within the sequence are highly conserved among claudins and might play an important role in the claudin-claudin-mediated TJ adhesion. Thus, we designed two overlapping peptide homologues of CLD1 (Fig. 3.7), with amino acid residues 49-60 (peptide **7**) and 54-65 (peptide **11**) to be tested as potential TJ-modulators. In order to improve solubility and to introduce charged amino acids, the CLD1 peptide homologue 49-60 (peptide **7**) was further modified by adding N- and C-terminal sequence tags consisting of dipeptide lysine-lysine (peptide **9**) or aspartic-aspartic acid (peptide **10**).

Due to the fact that CLD peptides were hardly soluble in cell culture medium with or without FCS, a co-solvent, DMSO or acetonitril was used as indicated. The co-solvent alone was found not to influence TEER and paracellular permeability of MDCK cells up to a concentration of 2% (not shown). After incubation with peptides, the TEER was measured and the mannitol permeation assay performed (for details see Sec. 2.7).

A representative kinetic profile of mannitol permeation across the MDCK cell monolayer is shown in Fig. 3.9. The permeation experiment with mannitol was performed under sink conditions, i.e. during the entire experiment, the concentration of mannitol in the receiver compartment did not exceed 10% of the mannitol concentration in the donor compartment. The apparent permeability coefficients were calculated as described in Sec. 2.7.3. For comparison between different experiments, the TEER and apparent permeability values were normalized to the control of the respective experiment without peptide.

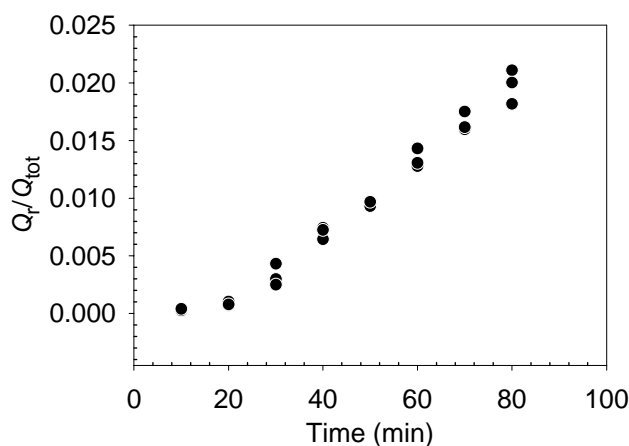


Figure 3.9: **Permeation of mannitol through the MDCK monolayer.** Permeation assay was performed with ^3H -mannitol (for details see Sec. 2.7.3) on day 5 of cell culture. Data represent values of three wells from one representative experiment. Symbols: Q_r/Q_{tot} , molar ratio of mannitol on acceptor side to the total amount of mannitol. Experimental details: seeding density, 0.5×10^5 cells/cm 2 ; 1% (v/v) DMSO; 10% (v/v) FCS.

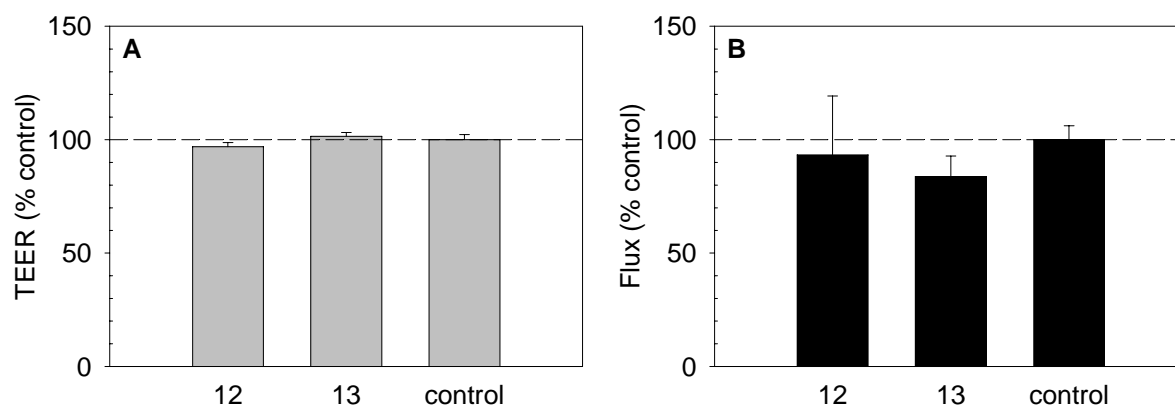


Figure 3.10: **Effect of CLD2 peptide homologues on TEER and mannitol permeability of MDCK cells.** MDCK cells grown on PET cell culture inserts for 3 days were treated with peptide **12** and **13**, respectively. (A) TEER measurements and (B) permeation of mannitol. Experimental details: seeding density, 5×10^5 cells/cm²; 0.1 mM peptide; 1% (v/v) DMSO; 10% (v/v) FCS; 50 μ M Pefabloc; 48 hrs of incubation. Error bars represent values of three cell culture inserts from one experiment.

MDCK cells grown on PET cell culture inserts were treated with peptide homologues to the CLD2 (peptide **12** and **13**, respectively). An aggregation of peptide **12** upon addition to the culture medium was observed. No significant change of TEER and mannitol permeability, respectively, was found as compared to the control without peptide (Fig. 3.10).

To test the influence of synthetic peptides on TJs at low serum concentration, in the following experiment the concentration of FCS was reduced from 10% to 1%. MDCK cells were assayed with CLD4 peptide homologue 31-49 (peptide **15**), 47-65 (peptide **16**) and 63-81 (peptide **17**), respectively (Fig. 3.11). An aggregation of peptide **15** was noticed after the addition to the culture medium. We could not observe significant changes of TEER for any of the CLD4 peptide homologue, whereas a slight increase of mannitol permeability for the CLD4 peptide homologue 47-65 (peptide **16**) and 63-81 (peptide **17**) was present. The CLD1 peptide homologues 47-65 (peptide **4** and **5**), 49-60 (peptide **7**), 54-65 (peptide **11**), respectively, did not significantly change the TEER and mannitol permeability as compared to control (not shown). Similar results were obtained when the CLD2 peptide homologue 63-81 (peptide **14**) was tested.

The sequence of several CLD peptide homologues contains one or two cysteine residues (see Tab. 2.1). The formation of disulfide bridges between peptide molecules could lead to the generation of oligomers and/or affect the conformation of the peptides. Thus, the cysteine-containing peptides were assayed with MDCK cells in the presence of 1 mM 1,2-dithiothreitol (DTT). Neither the CLD1 peptide homologue (peptide **4**), nor the CLD2 (peptide **13** and **14**, respectively) or the CLD4 (peptide **16** and **17**, respectively) peptide homologues showed a significant influence on the treated cells, as judged from TEER and mannitol permeability (Fig. 3.12). Similarly, an analogue of the CLD1 peptide homologue 47-65 containing serines instead of cysteines (peptide **6**) showed no effect on TEER and mannitol permeability (not shown).

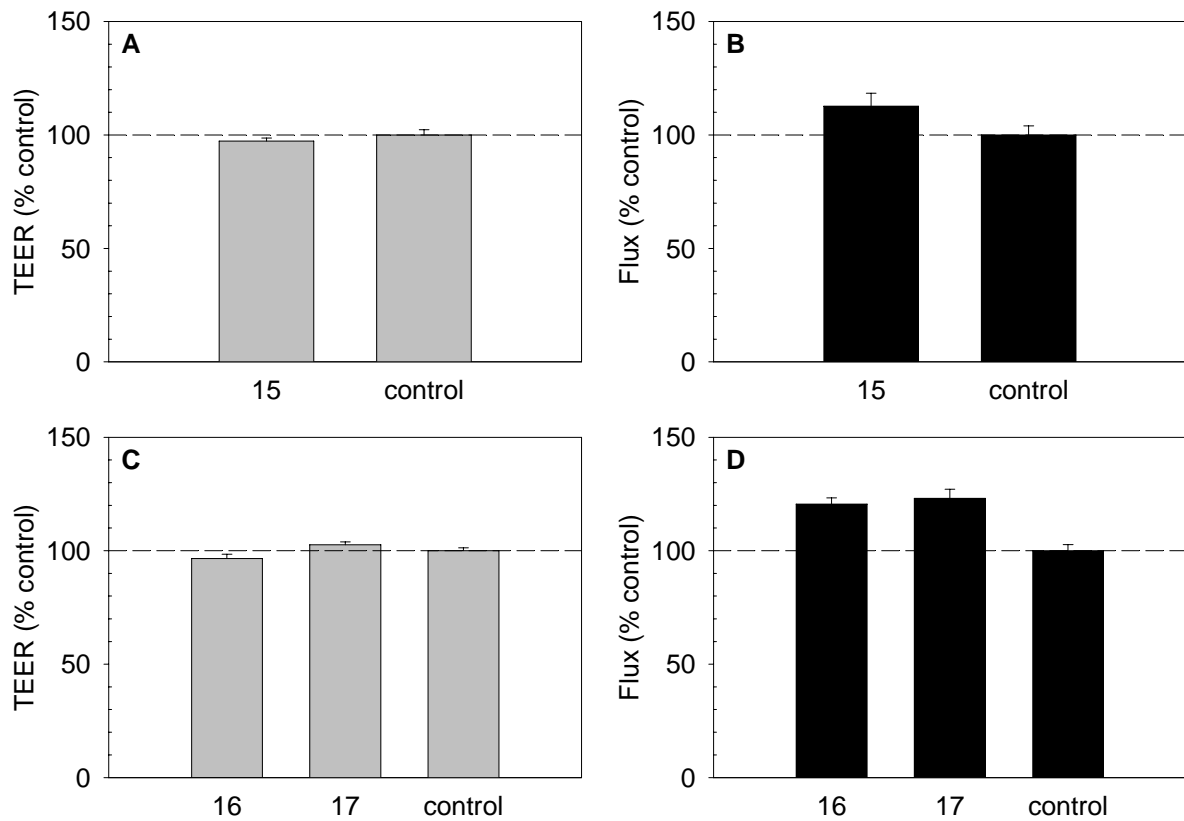


Figure 3.11: **Effect of CLD4 peptide homologues on TEER and mannitol permeability of MDCK cells.** MDCK cells grown on PET cell culture inserts for 3 days were treated with peptide **15**, **16** and **17**, respectively. (A, C) TEER measurements and (B, D) permeation of mannitol. Experimental details: seeding density, 5×10^5 cells/cm²; 0.1 mM peptide; 1% (v/v) DMSO; 1% (v/v) FCS; 50 μ M Pefabloc; 48 hrs of incubation. Error bars represent values of three cell culture inserts from one experiment.

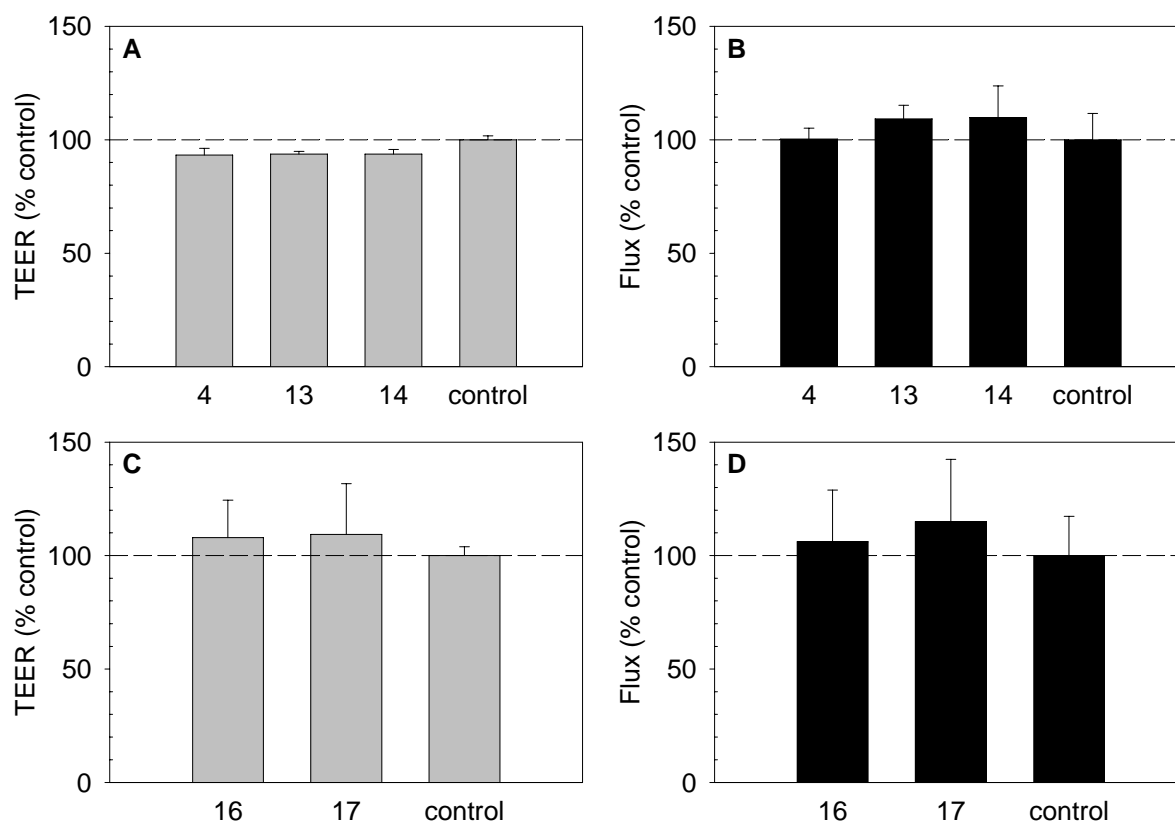


Figure 3.12: Effect of CLD1, CLD2 and CLD4 peptide homologues on TEER and mannitol permeability of MDCK cells under reducing conditions MDCK cells grown on PET cell culture inserts for 3 days were treated with peptide **4**, **13**, **14**, **16** and **17**, respectively. (A, C) TEER measurements and (B, D) mannitol permeation. Experimental details: seeding density, 5×10^5 cells/cm²; 0.1 mM peptide; 1% (v/v) DMSO; 1 mM DTT; 1% (v/v) FCS; 50 μ M Pefabloc; 48 hrs of incubation. Error bars represent values of three cell culture from one experiment.

We hypothesized, that a lower cell-seeding density and a higher peptide concentration might increase the binding probability of peptide molecules to the native claudins and trigger the opening of TJs. To test this hypothesis, MDCK cells were seeded at a 10-times lower seeding density (i.e. 0.5×10^5 cells/cm²) and the peptide concentration was increased by a factor of 3-6 as indicated. We could observe a decrease of TEER and an increase of mannitol permeability for the CLD1 (peptide **7**) and the CLD2 (peptide **12**) peptide homologues (Fig. 3.13). In contrast, peptide **8**, a scrambled peptide of the CLD1 peptide homologue 49-60 showed no effect on TEER and paracellular permeability. Similar results were obtained with the CLD1 peptide homologue 54-65 (peptide **11**) (not shown). However, the dramatic increase of the CLD1 (peptide **7**) and CLD2 (peptide **12**) peptide concentration led to a visible precipitation upon addition of the peptide to the medium, whereas peptide **8** did not precipitate. To investigate the influence of the peptide precipitates on the cell layer, the MDCK cells treated with peptide **7** were fixed, labelled for ZO-1, occludin, F-actin, and observed in the CLSM (Fig. 3.14). Massive changes

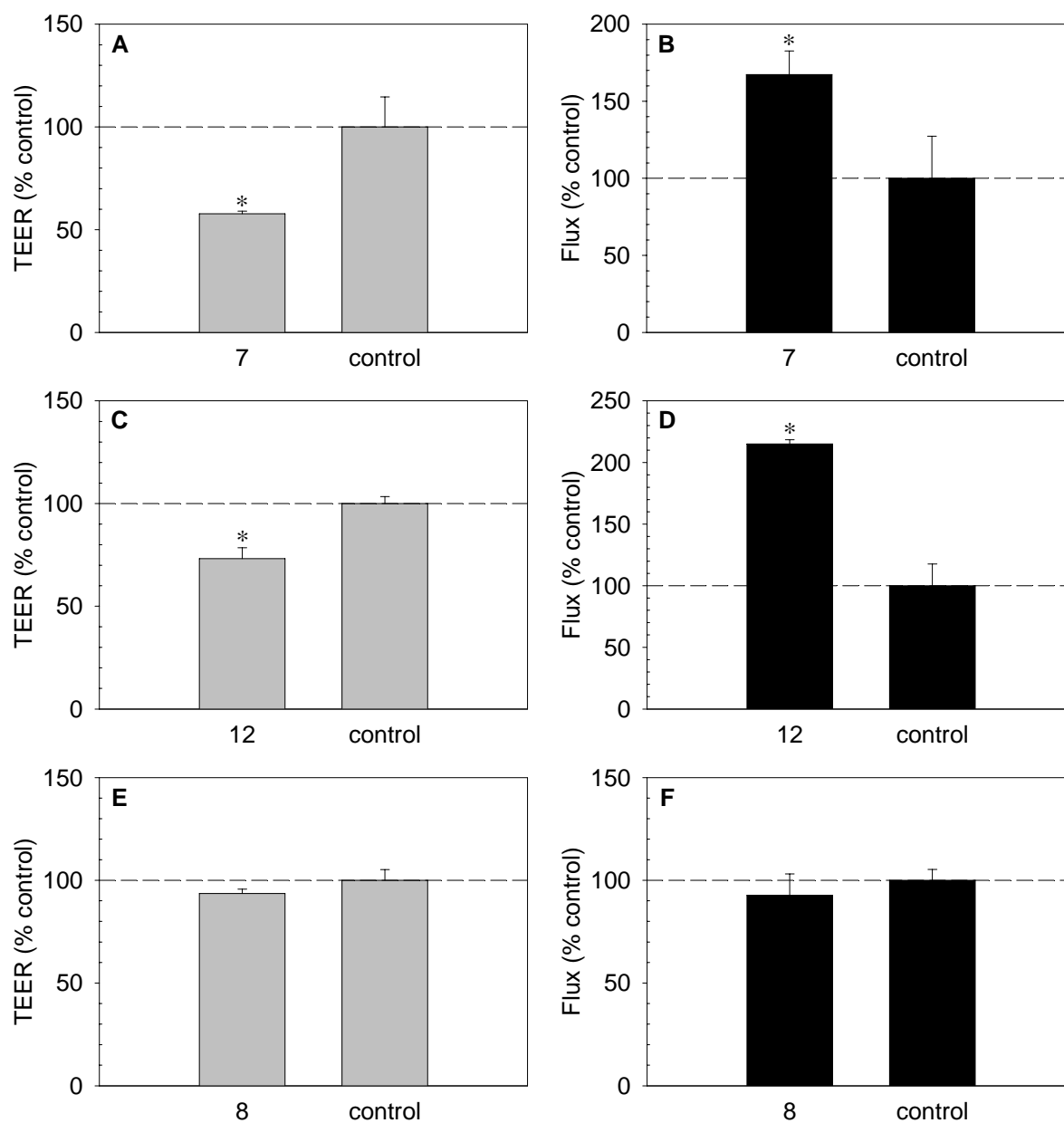


Figure 3.13: **Effect of a high concentration of CLD1 and CLD2 peptide homologues on TEER and mannitol permeability of MDCK cells.** MDCK cells grown on PET cell culture inserts for 3 days were treated with peptide **7**, **12** and **8**, respectively. (A, C, E) TEER measurements and (B, D, F) mannitol permeation. Experimental details: seeding density, 0.5×10^5 cells/cm²; 0.3 mM peptide **7** and **8**, 0.6 mM peptide **12**; 1 % (v/v) DMSO; 10 % (v/v) FCS; 50 μ M Pefabloc; 48 hrs of incubation. Error bars represent values of six cell culture inserts from two independent experiments (A-D, controls); single values from two independent experiments each including a cell culture insert (A-D, labeled with asterisk); three cell culture inserts from one experiment (E, F).

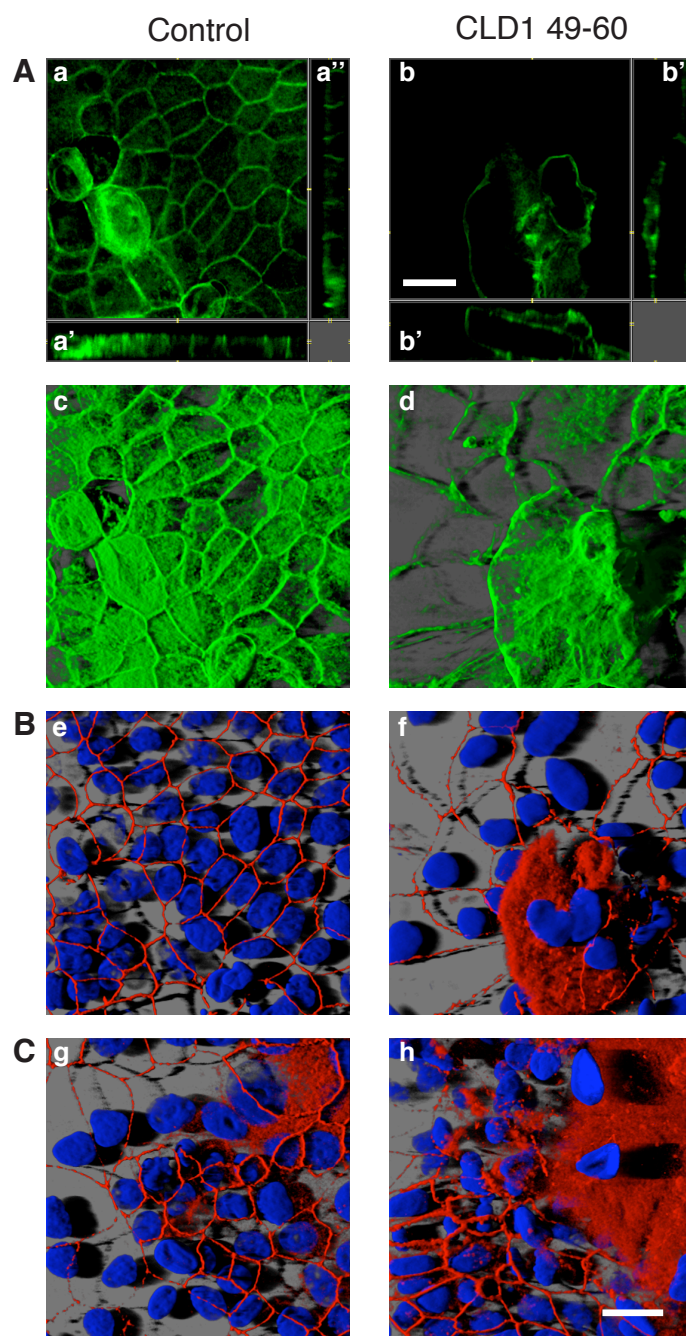


Figure 3.14: **Morphology of MDCK cells after treatment with CLD1 peptide homologue 49-60.** MDCK cells grown on PET cell culture inserts for 3 days were treated with peptide 7. Cells were fixed and samples were prepared for CLSM as described in Sec. 2.8. (A) F-actin (green), (B) ZO-1 (red), nuclei (blue), (C) occludin (red), nuclei (blue); (a, b) xy-sections, (a', b') xz-projections, (a'', b'') yz-projections, (c-h) 3D-reconstructions (SFP-mode). Experimental details: seeding density, 0.5×10^5 cells/cm²; 0.3 mM peptide; 1 % (v/v) DMSO; 10 % (v/v) FCS; 50 μ M Pefabloc; 48 hrs of incubation. Scale bar, 20 μ m.

in the cell morphology were detected. The cell layer was severely damaged, with an impaired staining of ZO-1 and occludin. To test, if the changes of TEER and permeability of mannitol caused by peptide **7** are related to the changes in the cell morphology, the peptide was assayed at a higher co-solvent concentration (DMSO or acetonitrile). Permeation studies after treatment of MDCK with peptide **7** in medium containing 2% of co-solvent showed TEER and mannitol permeability unchanged (Fig. 3.15). In addition, MDCK grown up-side-down on the cell culture insert and treated with peptide **7** (added from basolateral side only) under conditions, where peptide aggregation occurred, showed TEER values similar to the control (not shown).

To investigate the behavior of peptide **7** in solution, we carried out circular dichroism measurements to assess the secondary structure of this peptide. Circular dichroism spectra are displayed in the range between 185 and 260 nm (Fig. 3.16). The multicomponent analysis of the spectrum of peptide **7** dissolved in phosphate buffer with 5% (v/v) acetonitril indicated that the peptide adopted predominantly a disordered structure and β -strands. The spectrum

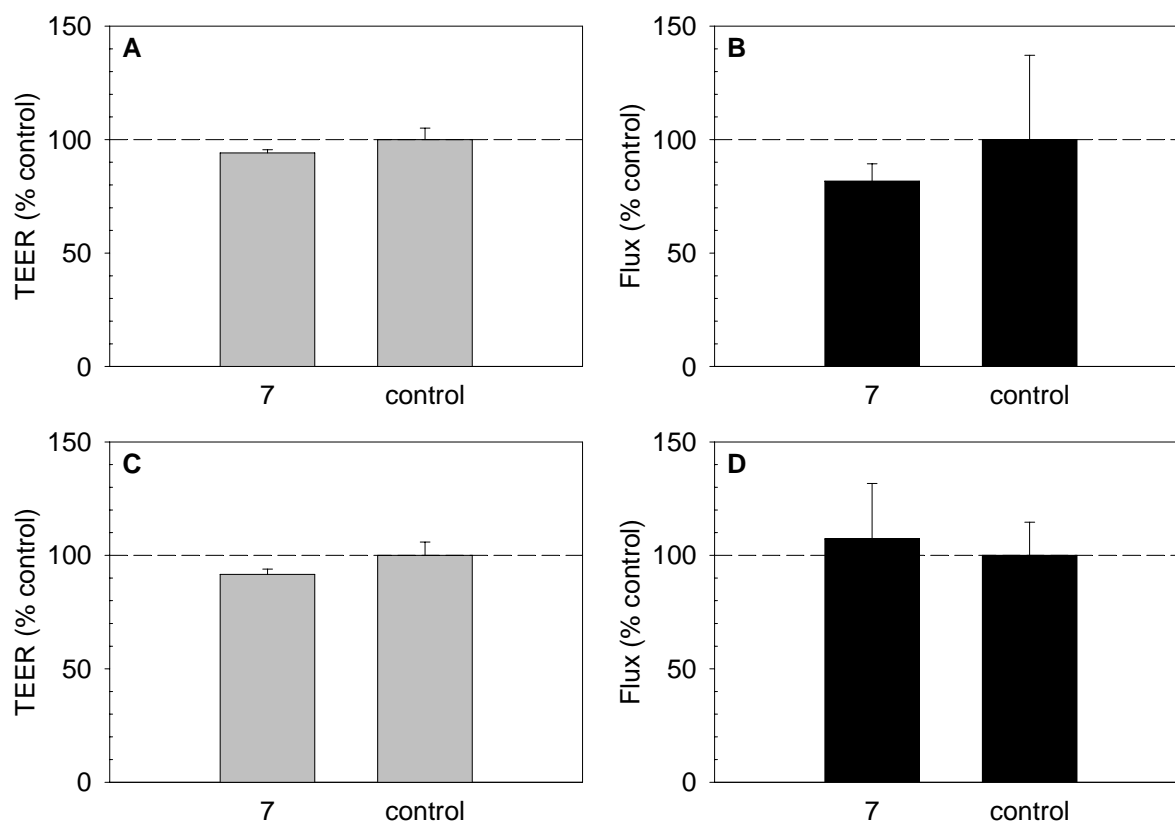


Figure 3.15: **Effect of solubilized CLD1 peptide homologue 49-60 on TEER and mannitol permeability of MDCK cells.** MDCK cells grown on PET cell culture inserts for 3 days were treated with peptide **7** in the presence of 2% DMSO (A, B) and 2% (v/v) acetonitril (C, D), respectively. (A, C) TEER measurements and (B, D) mannitol permeation. Experimental details: seeding density, 0.5×10^5 cells/cm²; 0.3 mM peptide; 10% (v/v) FCS; 50 μ M Pefabloc; 48 hrs of incubation. Error bars represent values of three cell culture inserts from one experiment.

of peptide **7** in 1, 2, 3-trifluoroethanol (TFE) revealed a double minimum at wavelengths near 210 and 222 nm, which is typical for α -helical structure. Multicomponent analysis of the spectra of peptide **7** dissolved in TFE showed that the disordered structure remains still predominant, while the α -helical portion of the sequence is increased and β -strands decreased.

In order to improve solubility and to introduce charged amino acids, peptide **7** was modified by adding N- and C-terminal sequence tags consisting of dipeptide lysine-lysine (peptide **9**) and aspartic-aspartic acid (peptide **10**), respectively. These peptides were soluble in the cell culture medium without FCS. Judging from the TEER and apparent permeability coefficients of MDCK cells treated with peptide **9** and **10**, respectively, no TJ disruption occurred (Fig. 3.17).

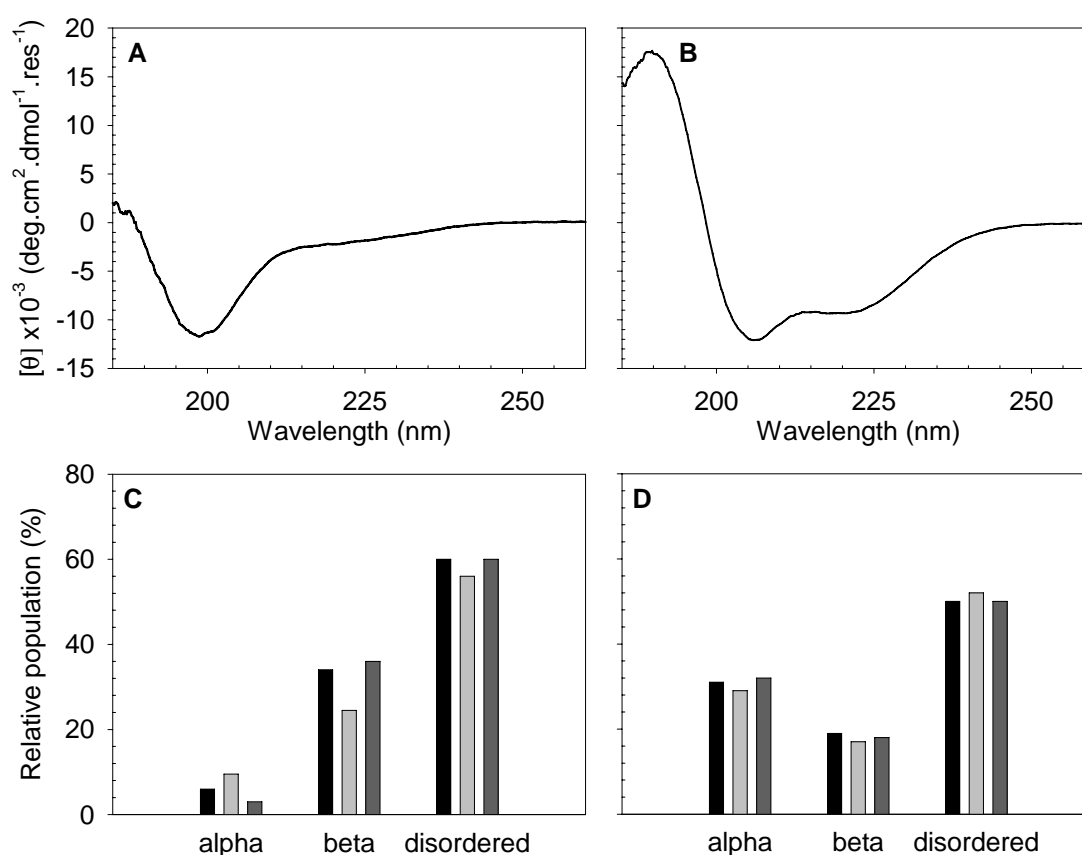


Figure 3.16: **Circular dichroism pattern of CLD1 peptide homologue 49-60.** CD spectra of peptide **7** dissolved in (A) phosphate buffer containing 5% (v/v) acetonitril, or in (B) TFE and its corresponding multicomponent analysis (C and D). Spectra were deconvoluted by means of the algorithms CONTIN/LL (black), SELCON3 (grey) and CDSSTR (dark grey). Experimental details: 37°C; 0.5 mg/ml peptide.

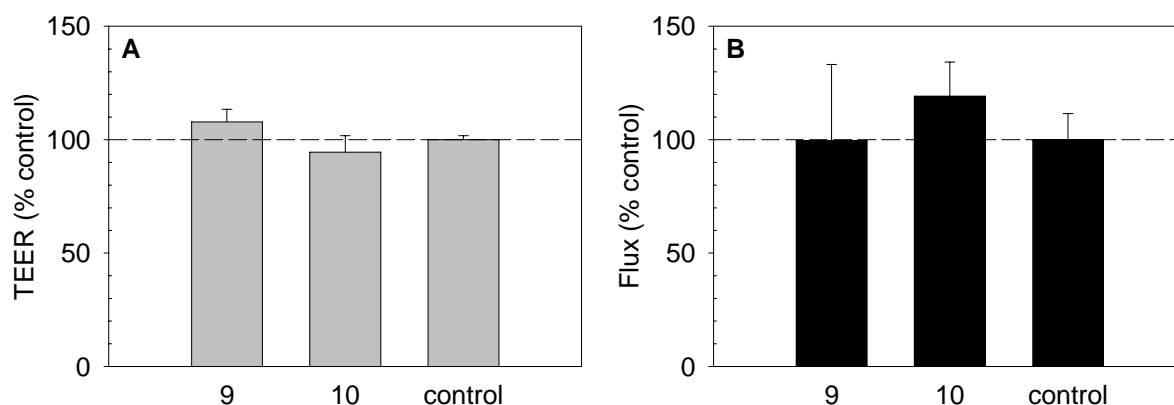


Figure 3.17: **Effect of charged CLD1 peptide homologues on TEER and mannitol permeability of MDCK cells.** MDCK cells grown on PET cell culture inserts for 5 days were treated with peptide **9** and **10**, respectively. (A) TEER measurements and (B) mannitol permeation. Experimental details: seeding density, 0.5×10^5 cells/cm²; 0.3 mM peptide; no co-solvent; no FCS; 6 hrs of incubation. Error bars represent values of three cell culture from one experiment.

3.2.2 Influence of peptide homologues to occludin on tight junctions

The need for a positive control of a TJ-modulating peptide led us test previously published occludin peptide homologues (Tavelin et al., 2003) for their ability to modulate TJs in MDCK and Caco-2 cells, respectively. We used an occludin (OCLN) peptide corresponding to the N-terminal part (close to the transmembrane domain) of the first extracellular loop of human occludin, with amino acid residues 90-103 (peptide **1**). This peptide sequence was further modified by coupling to 2-aminotetradecanoic acid (lipoamino acyl residue), resulting in peptide **2**. The lipoamino acyl residue in peptide **2** was synthesized as BOC-protected 2-aminotetradecanoic acid as described in Sec. 2.2. The identity of purified product was confirmed by NMR, mass spectrometry, elementary analysis and melting point (data not shown). In addition, to study the effects of peptide **1** on TJs by means of fluorescence microscopy, the sequence was coupled to 5(6)-carboxyfluorescein (5(6)-FAM) to obtain peptide **3**.

The solubility of occludin peptide homologues was enhanced by addition of a co-solvent (DMSO or acetonitril) as indicated. After incubation with peptides, the TEER was measured and the mannitol permeation assay performed.

The treatment of MDCK cells with 0.1 mM peptide **1** for 6 hrs did not cause relevant difference of TEER and mannitol permeation, as compared to the control (Fig. 3.18). Similar results were obtained when peptide **2** was tested (Fig. 3.18). When peptide **1** and **2**, respectively, were tested at higher concentration (0.3 mM), no effects were observed either (data not shown). Decomposition of peptide **1** during the 6-hour-incubation was found to be < 25% (data not shown).

Next, Caco-2 cells grown on PET cell culture inserts were treated with peptide **1** and **2**, respectively, at a concentration of 0.3 mM for 6 hrs (Fig. 3.19). A slight increase of TEER in

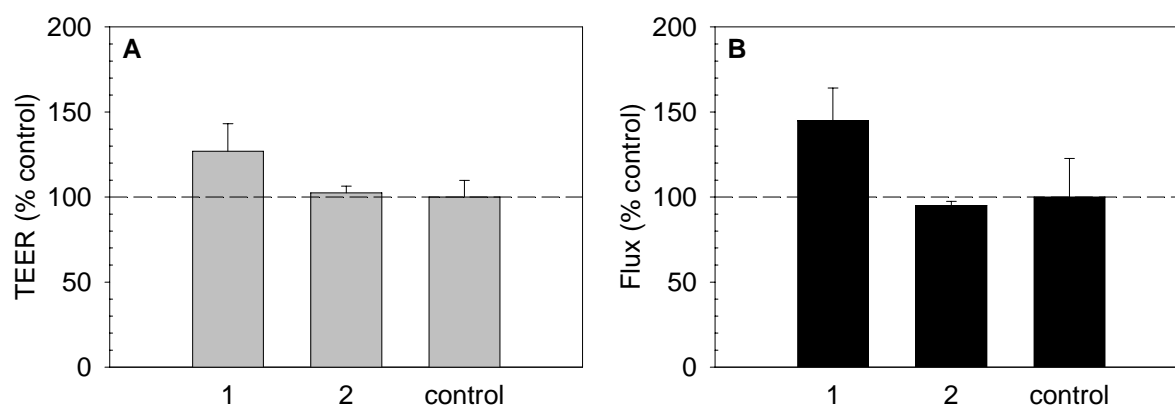


Figure 3.18: **Effect of OCLN peptide homologues on TEER and mannitol permeability of MDCK cells.** MDCK cells grown on PET cell culture inserts for 5 days were treated with peptide 1 and 2, respectively. (A) TEER measurements and (B) permeation of mannitol. Experimental details: seeding density, 0.5×10^5 cells/cm²; 0.1 mM peptide; 1% (v/v) DMSO; no FCS; 6 hrs of incubation. Error bars represent values of three cell culture from one experiment.

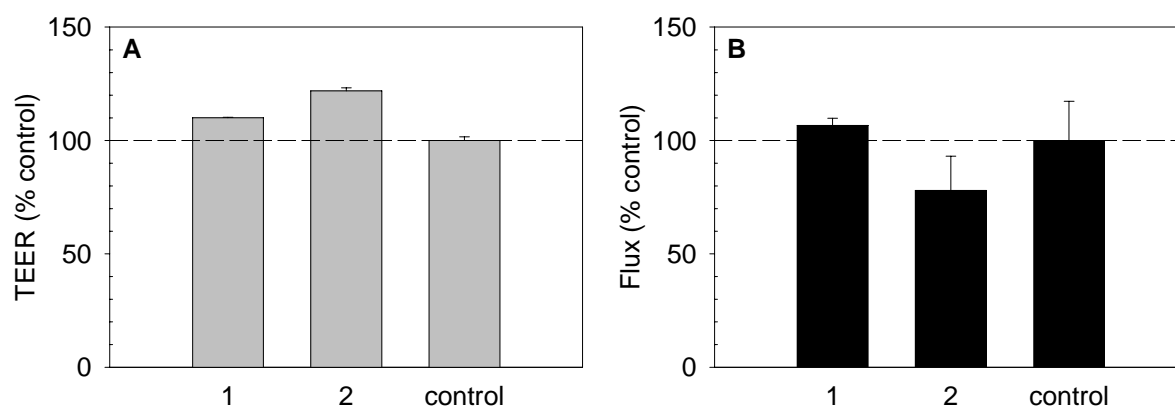


Figure 3.19: **Effect of OCLN peptide homologues on TEER and mannitol permeability of Caco-2 cells.** Caco-2 cells grown on PET cell culture inserts for 22 days were treated with peptide 1 and 2, respectively. (A) TEER measurements and (B) permeation of mannitol. Experimental details: seeding density, 4.4×10^5 cells/cm²; 0.3 mM peptide; 1% (v/v) DMSO; no FCS; 6 hrs of incubation. Error bars represent values of three cell culture inserts from one experiment.

peptide-treated cells was observed, however, no significant difference of mannitol permeability was found between peptide-treated cells and control. Similar results were obtained, when Caco-2 cells were grown on polycarbonate (PC) cell culture inserts (data not shown).

To investigate the affinity of peptide homologues of occludin to TJs, the fluorescently labeled peptide 90-103 (peptide **3**) was added to MDCK cells and the localization of the peptide was observed in living cells by means of CLSM (Fig. 3.20A). A strong fluorescence signal in a punctuate manner was found within the cytoplasm. No affinity of peptide **3** to TJs could be observed. Control cells treated with co-solvent and 5(6)-FAM displayed a slight cytoplasmatic fluorescence. A similar experiment was performed with Caco-2 cells (Fig. 3.20B). A different staining pattern was observed as compared to MDCK cells. A strong fluorescence was localized at the cell-cell border. Control cells showed a similar staining pattern as compared to the peptide-treated cells.

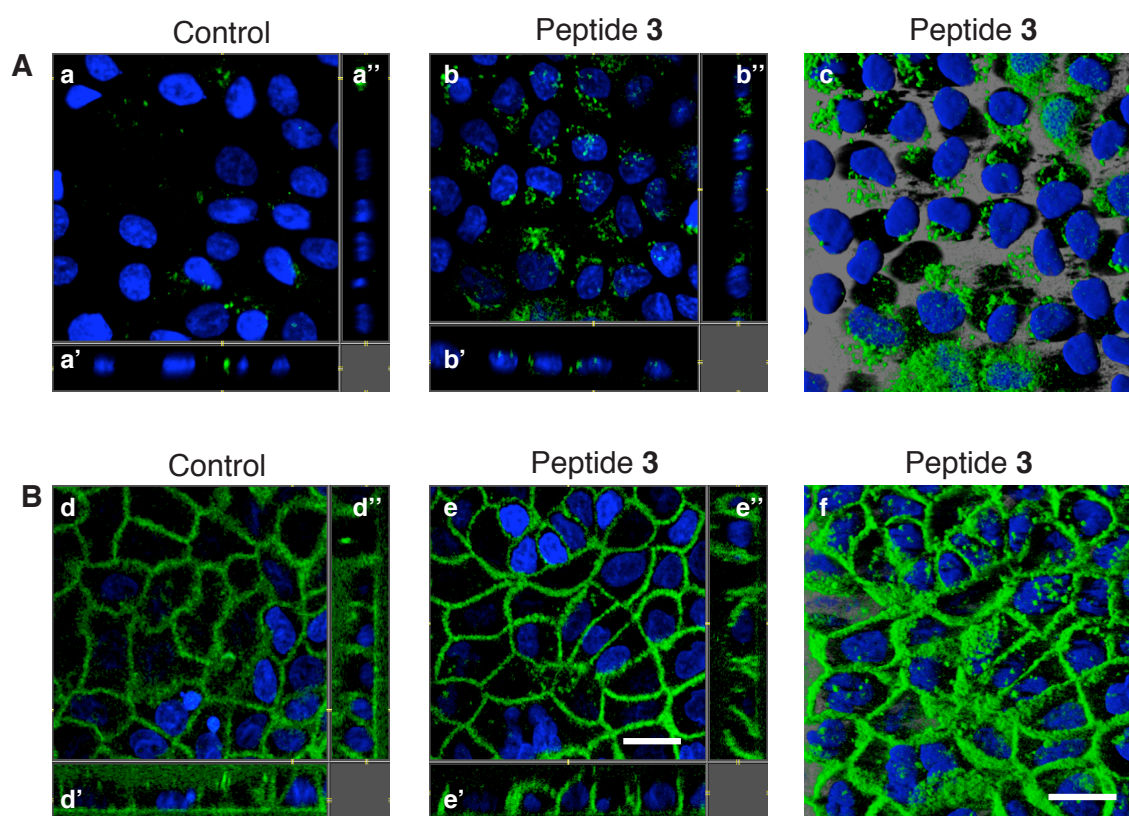


Figure 3.20: **Localization of 5(6)-FAM-labelled OCLN peptide homologue 90-103 in MDCK and Caco-2 cells.** (A) MDCK cells and (B) Caco-2 cells grown on PET cell culture inserts for 5 and 21 days, respectively, were treated with peptide **3**. Control cells were treated with 5(6)-FAM and co-solvent. Living cells were mounted after a washing step and immediately analyzed by CLSM. (a, b, d, e) xy-sections, (a', b', d', e') xz-projections, (a'', b'', d'', e'') yz-projections, (c, f) 3D-reconstructions (SFP-mode). Color code: blue, nuclei; green, fluorescence 5(6)-FAM (a, d) or fluorescence of peptide **3** (b, c, e, f), respectively. Experimental details: seeding density, 0.5 or 1×10^5 cells/cm²; 0.1 mM peptide; 0.1 mM 5(6)-FAM; 1 μ g/ml Hoechst 33342; 2% (v/v) acetonitril; no FCS; 50 μ M Pefabloc, 6 hrs of incubation. Scale bar, 20 μ m.

3.3 Development of claudin-containing proteoliposomes as an *in-vitro* model for the screening of tight junction modulators

3.3.1 Production of His-tagged claudin-1

3.3.1.1 Characterization of the insect cell line

The host cells in the baculovirus expression system are the *Spodoptera frugiperda* (Sf9) cells. Sf9 cells were cultured in suspension as described in Sec. 2.5.3. To characterize the cells, a growth curve was established. Cells seeded at a density of 0.5×10^6 per ml reached the log-phase after about 2 days. The viability of the cells in the log-phase was greater than 98 % (for details see Sec. 2.5.3). The stationary phase was reached after 5 days, with a density of about 15×10^6 cells per ml (Fig. 3.21).

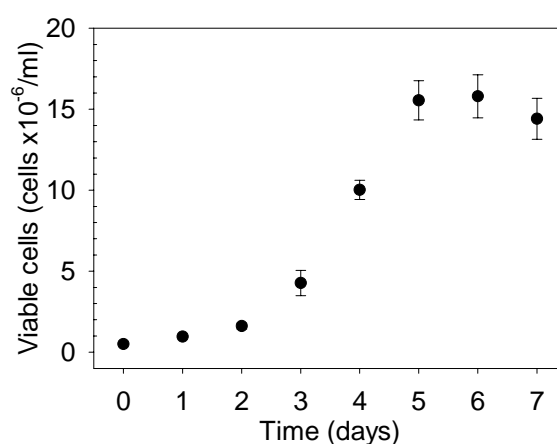


Figure 3.21: **Growth curve of Sf9 cells.** Sf9 cells were seeded at a density of 0.5×10^6 cells/ml in a 125 ml flask and incubated at 28°C with shaking. Cell counts as indicated (for details see Sec. 2.5.3). Data represent mean values and standard deviations of cell counts in triplicates from a representative experiment.

3.3.1.2 Generation of recombinant baculoviruses

The baculovirus expression system is based on the generation of recombinant baculoviruses containing the gene of interest, which are used to infect the host cell line to enable the expression of proteins under the control of a polyhedrine promoter (Ciccarone et al., 1997).

For the generation of recombinant baculoviruses for the expression of His-CLD1, the open reading frame (ORF) of human claudin-1 (CLD1) was PCR-amplified and the amplified fragment cloned into the pFastBacHT vector, downstream to the six histidine tag sequence (for details see Sec. 2.9.1). The construct was DNA sequenced to confirm the identity (not shown).

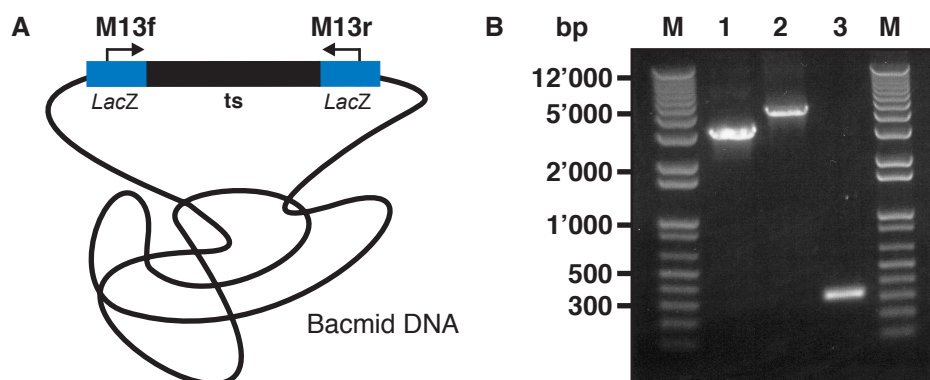


Figure 3.22: **Analysis of recombinant bacmids CLDN1 and GUS by PCR.** (A) Schematic representation of annealing of M13 primers in the transposed bacmid DNA. (B) PCR reactions to confirm transposition in the bacmid DNA were performed and amplified products were analyzed by agarose gel electrophoresis (for details see Sec. 2.11.1 and Sec. 2.9.7). Line 1, bacmid CLDN1; line 2, bacmid GUS; line 3, non-transposed bacmid. Abbreviations: M, DNA marker; M13f, M13 forward primer; M13r, M13 reverse primer; ts, transposed sequence from pFastBacHTB-CLDN1 and pFastBac1-GUS, respectively.

A baculovirus shuttle vector containing the ORF of CLDN1 (bacmid CLDN1) was generated by a transformation of DH10Bac competent bacteria (for details see Sec. 2.10.3). Similarly, the pFastBac1-GUS construct was used to generate a baculovirus shuttle vector coding for the expression of β -glucuronidase (bacmid GUS). The expression of β -glucuronidase was chosen as a control for the efficiency of the bacmid transfection to Sf9 cells.

The baculovirus shuttle vector contains a sequence encoding the *LacZ* α peptide (Ciccarone et al., 1997), the expression of which is disrupted upon a transposition. White colonies containing the transposed bacmid were picked and the successful transposition confirmed by a PCR reaction with M13 forward and M13 reverse primer (Fig. 3.22). If transposition occurred, annealing of primers in the disrupted *LacZ* gene of the bacmid led to an amplification of the transposed sequence. Single bands with the expected size for amplicons from bacmid CLDN1 (line 1; expected size \sim 3100 bp), bacmid GUS (line 2; expected size \sim 4200 bp) and non-transposed bacmid (line 3; expected size \sim 300 bp) were observed. By using a combination of M13 primer and CLDN1 gene specific primer, amplified fragments from bacmid CLDN1 revealed the expected sizes as well (not shown).

Purified bacmid DNA was introduced to Sf9 cells by a lipid-mediated transfection as described in Sec. 2.11.2. Successful transfection was recognized by morphological changes typical for an infection of insect cells with nuclear polyhedrosis viruses, i.e. an increased cell diameter and cease of growth. Signs of infection were observed for cells transfected with bacmid CLDN1 as well as with bacmid GUS. Control cells (without bacmid) showed normal growth (Fig. 3.23). The cell toxicity of the transfection reagent was found to be minimal (not shown). To confirm the successful transfection, cells transfected with bacmid GUS were assayed for the expression of β -glucuronidase *in-situ*. The cleavage product resulting from the enzymatic processing of X-glucuronide (5-bromo-4-chloro-3-indolyl- β -D-glucuronic acid) by the expressed β -glucuronidase caused the transfected cells to turn blue. The overall transfection efficiency for

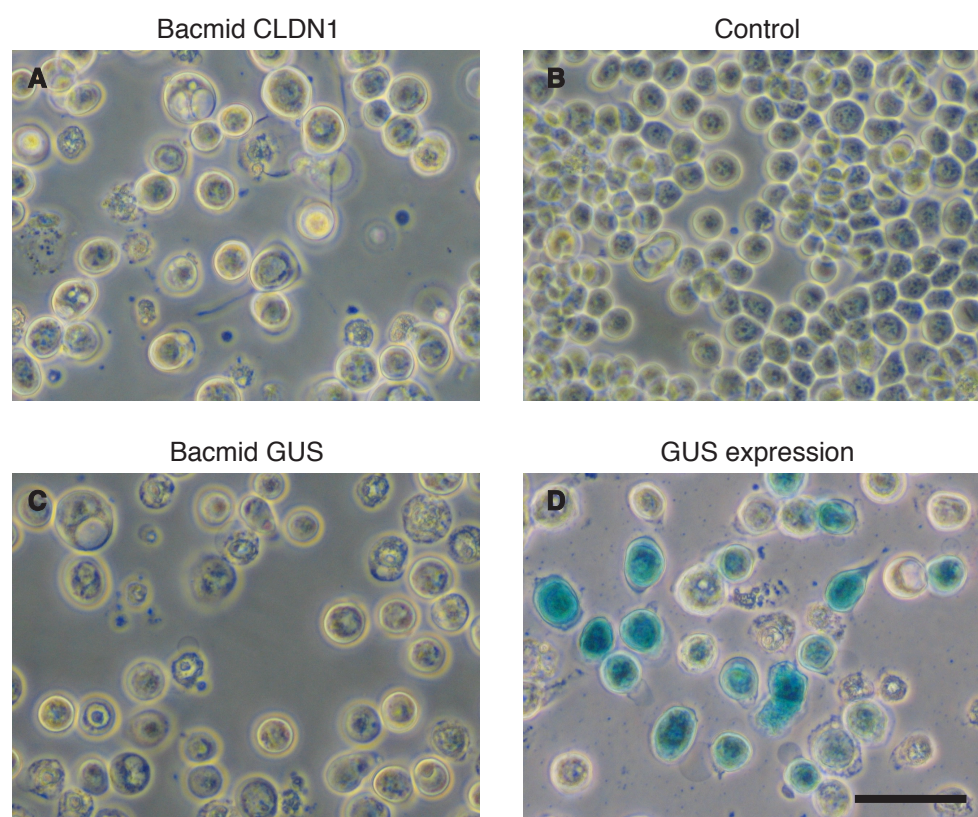


Figure 3.23: **Sf9 cells transfected with bacmids CLDN1 and GUS.** Sf9 cells were transfected with (A) bacmid CLDN1 and (C, D) bacmid GUS. (B) Control cells (without bacmid DNA). The cells were incubated for 3 days at 28°C (details see Sec. 2.11.2). (D) Cells transfected with bacmid GUS were assayed for β -glucuronidase (GUS) expression *in-situ* (details see Sec. 2.11.5.1). Images were taken with a PowerShot G5 digital camera (Canon) under a light microscope (Zeiss). Scale bar, 50 μ m.

bacmid GUS was approximately 30-40 %, as estimated from cell counts in the light microscope at low magnification.

Recombinant baculoviruses released into the medium were collected and amplified to obtain viral stocks of higher titer (for details see Sec. 2.11.3). In general, 8 amplification rounds resulted in a viral stock with a titer of about 1×10^8 pfu per ml (data not shown).

3.3.1.3 Expression and purification of His-CLD1

Insect Sf9 cells were infected with amplified baculoviral stock coding for the expression of His-CLD1. Infected cultures stopped to grow immediately (Fig. 3.24A) as well as morphological changes typical for an infection by baculoviruses. Two days after the infection, samples of infected cells were analyzed for the presence of the recombinant His-CLD1 by immunocytochemistry, as well as by SDS-PAGE and Western blot. Confocal micrographs revealed the His-CLD1 localized as 'patch-like' structures, which filled the infected cells (Fig. 3.24B). On the Western blot, a band around 22 kDa was detected with the mouse anti-claudin-1 antibody

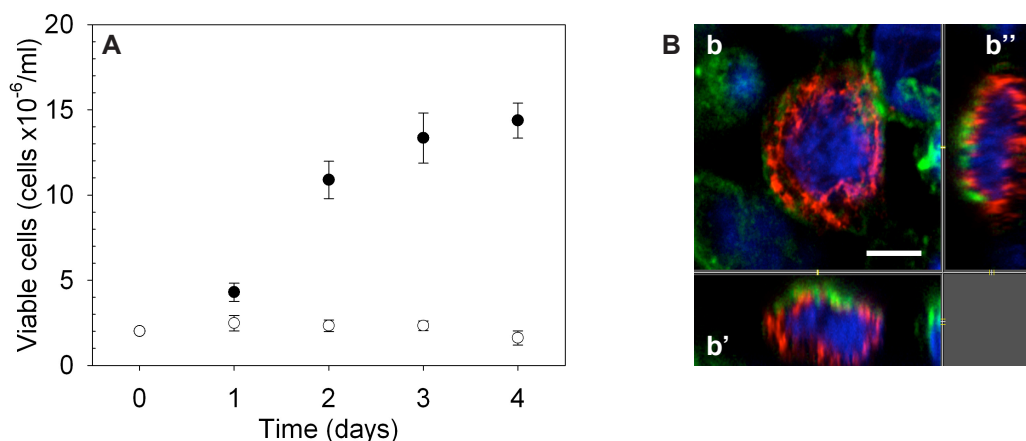


Figure 3.24: **Characteristics of CLDN1-baculovirus-infected Sf9 cells.** (A) Growth curve of Sf9 cells infected with amplified CLDN1-baculoviral stock (open symbols) and control cells (closed symbols). Cells were infected in suspension culture at MOI 3 as described in Sec. 2.11.5.2. Data represent mean values and standard deviations of cell counts in triplicates from a representative experiment. (B) CLSM image of infected Sf9 cells (blue, nuclei; red, anti-claudin-1; green, F-actin). (b) xy-section, (b') xz-projection, (b'') yz-projection. Infection of attached cells at MOI 20; cells were fixed after 2 days and prepared for CLSM as described in Sec. 2.8. Scale bar, 7 μm.

(Fig. 3.25A). The protein was undetectable in the non-infected control cells. The presence of His-tag in the CLD1 was confirmed by an immunoblot with anti-His tag antibody (not shown).

To investigate the optimal multiplicity of infection (MOI) and time course of protein expression, cells were infected at MOI 3, 5 and 10, respectively. Samples were taken after 2, 3 and 4 days and analyzed by immunoblotting. The expression level of His-CLD1 did not differ among the different MOIs and incubation times (Fig. 3.25B).

For a large scale expression of His-CLD1, insect cells were infected in suspension at MOI 3 for 2 days. After homogenization of the cells, the His-CLD1-containing membrane fragments were prepared in a two-step centrifugation (for details see Sec. 2.12.2). Samples of pellets and supernatants were taken as indicated and analyzed by immunoblot with anti-claudin-1 antibody (Fig. 3.26). Crude membranes contained His-CLD1, however, roughly one third of the total His-CLD1 was lost during the preparation, mainly in the low-speed centrifugation step.

Crude membranes were solubilized by octylglucoside and the purification of His-CLD1 was performed by affinity chromatography (see Sec. 2.12.3). Analysis of fractions by an immunoblot with claudin-1 antibody showed the expected purification pattern (Fig. 3.27), i.e. His-CLD1 was captured on the column (line 2) and eluted with the first three fractions of the elution step (lines 8, 9, 10). However, a silver stain of the elution fractions revealed additional bands at higher molecular weights than His-CLD1 (Fig 3.28). The yield from one purification was only 0.1 mg, which represents 0.01 % of the total protein amount from 2×10^9 cells (corresponding to 1000 ml of infected culture).

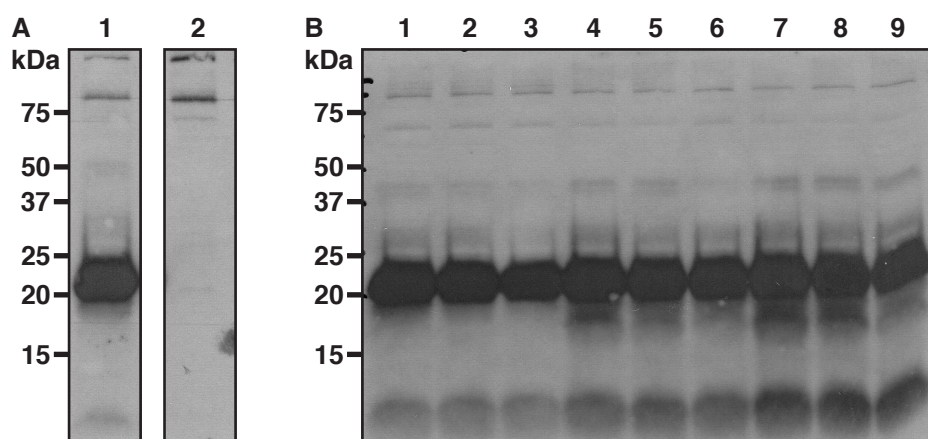


Figure 3.25: **Expression of His-CLD1 in Sf9 cells.** Sf9 cells were seeded at a density of 2×10^6 viable cells/ml in and infected with CLDN1 recombinant baculoviral stock at MOI 3, 5 and 10. After 2, 3 and 4 days of incubation, cell lysates were analysed by immunoblot with anti-claudin-1 antibody as described in Sec. 2.12.6. (A) line 1, infected cells; line 2, non-infected cells; (B) line 1-3, infected cells at MOI 3 after 2, 3, 4 days; line 4-6, infected cells at MOI 5 after 2, 3, 4 days; line 7-9, infected cells at MOI 10 after 2, 3, 4 days.

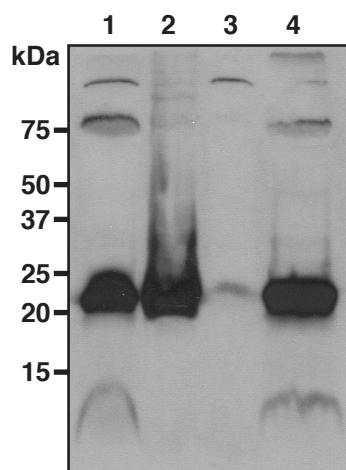


Figure 3.26: **Isolation of crude membranes containing His-CLD1.** Crude membranes were prepared by homogenization of infected Sf9 cells and stepwise centrifugation (for details see Sec. 2.12.2). Pellets and supernatants were analyzed by immunoblot with anti-claudin-1 antibody. The slots were loaded with 0.05 % v/v of St1 (St2) or with 0.1 % v/v of Pt1 and crude membranes. Line 1, supernatant St1; line 2, pellet Pt1; line 3, supernatant St2; line 4, crude membranes.

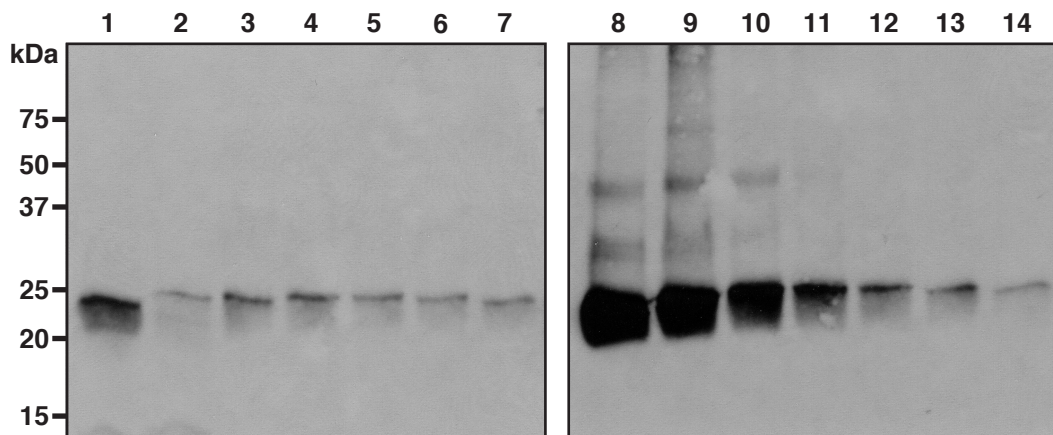


Figure 3.27: **Purification of His-CLD1 by affinity chromatography.** Crude membrane fractions from infected cells were solubilized by octylglucoside and purification was performed as described in Sec. 2.12.3. Fractions were analysed by immunoblot with anti-claudin-1 antibody. Line 1, cleared lysate; line 2, flow-through; line 3-7, wash steps; line 8-14; elution steps.

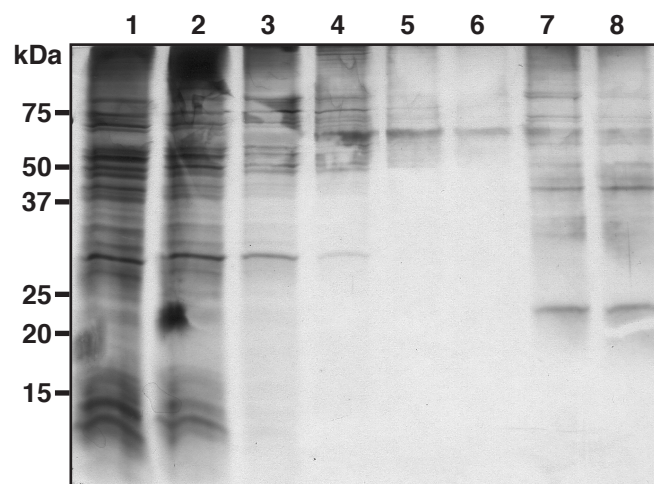


Figure 3.28: **Purification of His-CLD1 by affinity chromatography.** Crude membrane fractions from infected cells were solubilized by octylglucoside and purification was performed as described in Sec. 2.12.3. Fractions were analysed by SDS-PAGE and silver staining. Line 1, cleared lysate; line 2, flow-through; line 3-6, wash steps; line 7-8; elution steps.

3.3.2 Preparation and characterization of His-CLD1-proteoliposomes

The purified His-CLD1 was reconstituted into phosphatidyl choline (PhC) liposomes to test for a possible interaction between the reconstituted proteins. Liposomes without His-CLD1 ('control liposomes') were used for comparison. His-CLD1-proteoliposomes were prepared by detergent dialysis (for details see Sec. 2.13.1). Micelles containing His-CLD1 (protein to lipid ratio 1:100 w/w) were prepared by addition of purified His-CLD1 and sodium cholate to the PhC lipid film, and the dialysis run for 48 hrs at RT. Liposomes were detected after overnight dialysis (not shown). After 48 hrs of dialysis, the average mean hydrodynamic diameter of His-CLD1-proteoliposomes was 66.6 nm with a polydispersity factor 0.09 corresponding to a size variance of 30% assuming a monomodal distribution. The intensity size distribution profile for a proteoliposome preparation is shown in Fig. 3.29. The average mean hydrodynamic diameter of control liposomes prepared by dialysis was 61.9 nm and the polydispersity factor below 0.04 corresponding to a size variance of 20% assuming a monomodal distribution.

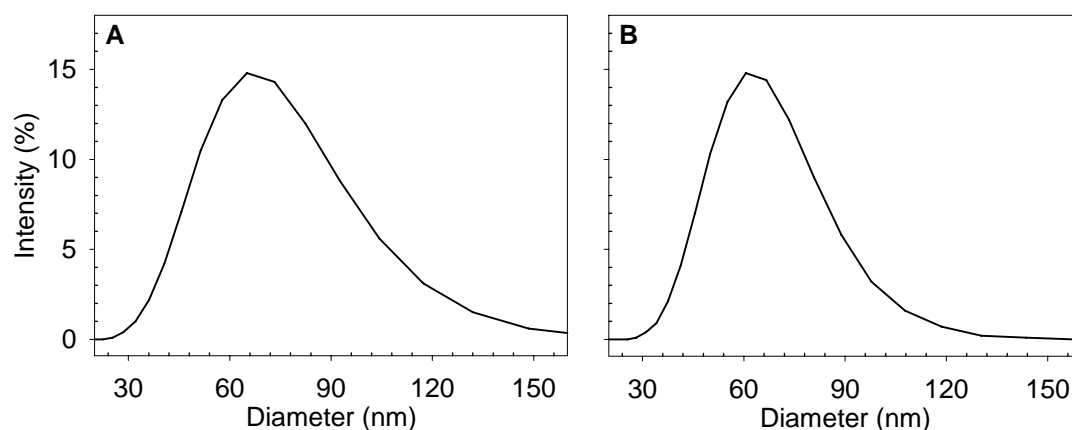


Figure 3.29: **Size distribution profiles of liposomes and His-CLD1-proteoliposomes prepared by dialysis.** Size distribution profiles of (A) His-CLD1-proteoliposomes and (B) control liposomes (without His-CLD1). The size distribution was measured by dynamic light scattering (see Sec. 2.13.2). Representative size distribution profiles are shown.

To investigate the interaction between reconstituted proteins, the correlogram of the proteoliposomes was acquired by the dynamic laser scattering technique (for details see Sec. 2.13.2). In the correlogram, correlation coefficients are plotted as a function of time. A noise in the baseline of the correlogram is a sign for the presence of aggregates. As shown in Fig. 3.30, the baseline in the correlogram of the proteoliposomal preparation was flat. No difference could be observed between correlograms of His-CLD1-proteoliposomes and control liposomes.

To characterize the dialysis system, the kinetics of the detergent removal from PhC micelles were investigated by addition of ^3H -cholic acid and ^{14}C -octylglucoside, respectively (Fig. 3.31). After 48 hrs of dialysis, the concentration of cholic acid was about 1.5% of the initial concentration, which corresponds to a residual detergent concentration of 111 nM. The concentration

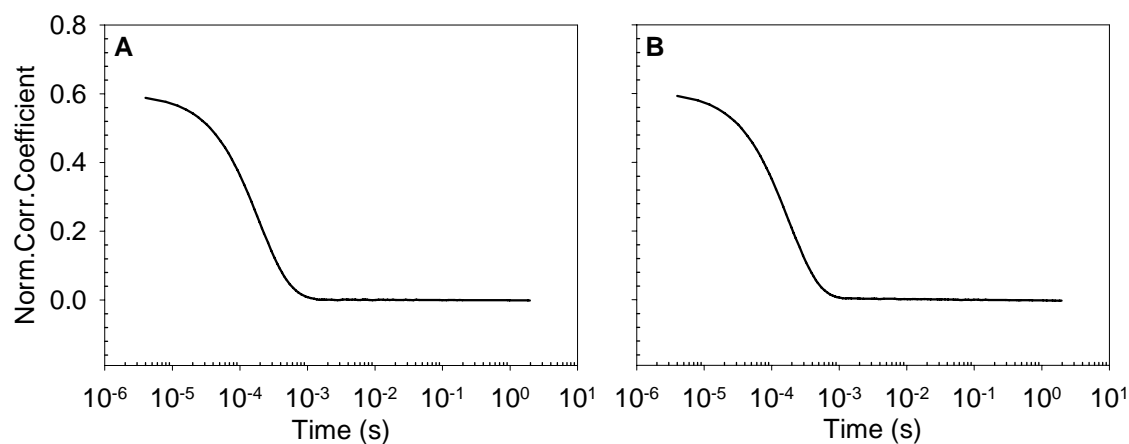


Figure 3.30: **Correlograms of His-CLD1-proteoliposomes and control liposomes prepared by dialysis.** Correlograms of (A) His-CLD1-proteoliposomes and (B) control liposomes (without His-CLD1) were acquired by dynamic light scattering (see Sec. 2.13.2). Normalized values of correlation coefficients are plotted. Representative correlograms are shown.

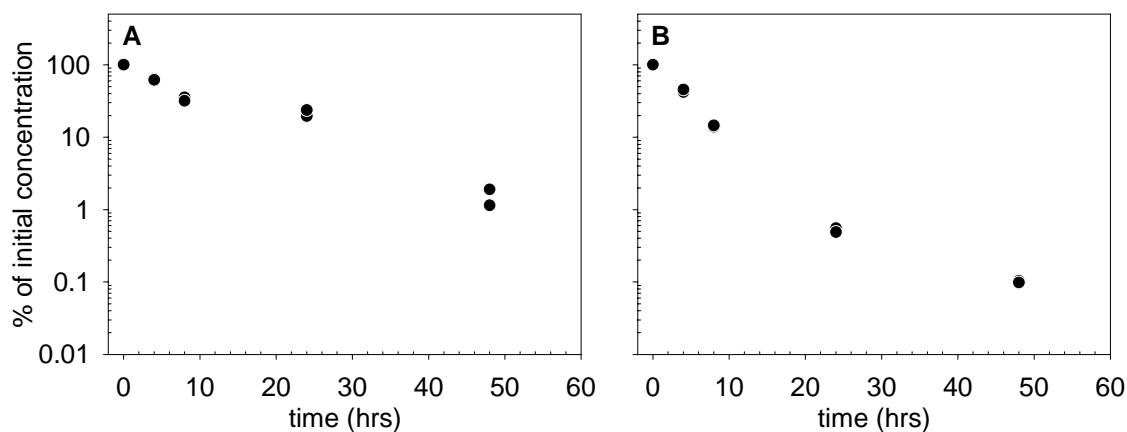


Figure 3.31: **Kinetics of detergent removal during dialysis.** Removal of (A) ^3H -cholic acid and (B) octyl ^{14}C - β -D-glucopyranoside from PhC liposomes. Liposomes were prepared from micelles by dialysis (for details see Sec. 2.13.1). Data are duplicates from a representative experiment.

of octylglucoside was about 0.1 % of the initial concentration, which corresponds to a residual detergent concentration of 34 nM. The removal of octylglucoside from PhC micelles was faster as compared to cholic acid, according to the respective critical micellar concentrations.

To confirm the reconstitution of His-CLD1 into the liposomes, proteoliposomes were loaded onto a sucrose density gradient (for details see Sec. 2.13.3). After the density centrifugation, the gradient was fractionated and the density of each fraction determined from the refractive indices (Fig. 3.32). The proteoliposomes were visible as a turbid band in the upper part of the centrifuge tube, corresponding to a density range between 1.05 and 1.07 g/cm³. The density fractions were subsequently analysed by SDS-PAGE and immunoblotting with anti claudin-1 antibody (Fig. 3.33). His-CLD1 was mainly localized in fractions 1 to 4. No His-CLD1 was detected in the high density fractions (7-12), where non-reconstituted protein would accumulate.

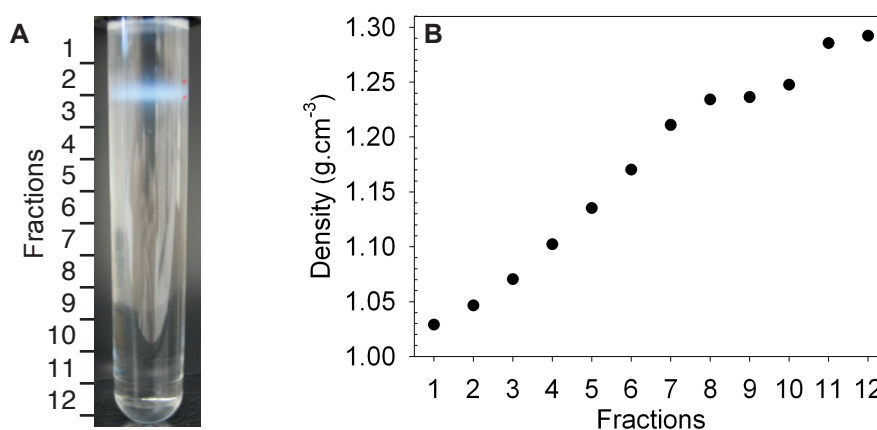


Figure 3.32: **Sucrose density gradient of His-CLD1-proteoliposomes.** (A) Sucrose gradient of His-CLD1-proteoliposomes; proteoliposomes are visible as a white band between fraction 2 and 3. (B) Density profile of fractions collected from the sucrose gradient. Sucrose density gradients were formed after centrifugation at 200'000 *g* for 19 hrs (for details see in Sec. 2.13.3). The gradient was fractionated from the top, the refractive index of each fraction was measured and the density calculated as described in Sec. 2.13.3. A representative density profile is shown.

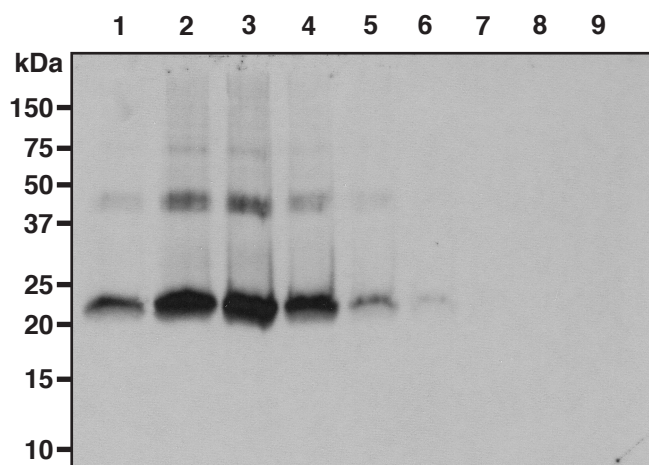


Figure 3.33: **Confirmation of His-CLD1 reconstitution into proteoliposomes.** Fractions from the density gradient (see Sec. 2.13.3) were analysed for the presence of His-CLD1 by SDS-PAGE and immunoblot with anti-claudin-1 antibody (see Sec. 2.12.6). Line 1-6, fractions 1-6; line 7, pooled fractions 7 and 8; line 8, pooled fractions 9 and 10; line 9, pooled fractions 11 and 12.

4 Discussion

4.1 Morphological studies on the modulation of tight junctions

In order to learn more about the behavior of single TJ proteins upon the TJ modulation, we applied the calcium depletion method in the cell culture of MDCK cells. We have chosen cingulin and claudin-1 (CLD1) as the representatives for the plaque and transmembrane proteins of TJs, respectively, and investigated their dynamic behavior in relation to other TJ proteins, and to the cytoskeletal protein F-actin by CLSM. According to the morphology of the cells after the calcium chelation, we defined two regions of interest (ROI) for the co-localization analysis. The membrane areas (ROI type I) and the filaments remaining between the cells after the TJ opening (ROI type II). Statistical analysis of the CLSM data revealed one major peak of co-localization for cingulin with zonula occludens-1 (ZO-1), occludin (OCLN) and F-actin, respectively, under the normal calcium conditions. After calcium depletion, this pattern was not significantly changed in the membrane regions, and the maximum of co-localization shifted to a more basal position for the protein pair cingulin with ZO-1 and F-actin, respectively, due to changes in geometry of cells (rounding up). In the regions of filaments, the co-localization was slightly reduced for protein pair cingulin with OCLN and F-actin, respectively. In contrast, the co-localization of cingulin with ZO-1 was significantly reduced. With the GFP-CLD1, we observed no significant differences between the kinetics of the TJ re-formation, as judged from the labeling for ZO-1, CLD4 and F-actin.

It is well established that TJs rapidly dissociate and become leaky when calcium is removed from the culture medium. Conversely, readdition of calcium makes TJ proteins reassemble and reseal the barrier (Martinez-Palomo et al., 1980; Bhat et al., 1993; Armitage et al., 1994). To demonstrate the opening of TJs by calcium depletion, we measured TEER and analyzed the morphology of ZO-1 by CLSM. The depletion of the extracellular calcium by EGTA induced a rapid decrease of the TEER (to 30% of the initial values) and opening of TJs with a partial internalization of ZO-1. The TEER value and the characteristic staining pattern of ZO-1 were restored within one hour after the addition of the normal calcium-containing medium, suggesting a fully reversible re-assembly of TJs. It was previously reported, that reorganization of the actin cytoskeleton mediates the disassembly of the apical junctional complex during the calcium chelation method, leading to a clathrin-mediated internalization of the junctional proteins such as ZO-1, CLD4, OCLN and E-cadherin (Ivanov et al., 2004a,b). The proteins were observed to enter early endosomes followed by a movement to an unique storage compartment, from which the proteins could recycle back to the apical junctional complex.

Under the normal calcium concentration, cingulin co-localized in the membrane regions with ZO-1, OCLN and F-actin, respectively. After the EGTA treatment, the extent of the co-localization in the membrane regions was not significantly changed. Cingulin has previously been shown to co-localize with ZO-1 and OCLN, respectively, in the lateral membranes of epithelial cells (Stevenson et al., 1989; Langbein et al., 2002). In addition, binding of cingulin to ZO-1, OCLN and F-actin, respectively, was demonstrated by biochemical methods, such as immunoprecipitation and pull-down assays (Cordenonsi et al., 1999a,b; D'Atri and Citi, 2001). No cytoplasmic localization of cingulin under normal calcium conditions was reported. Only, after the depletion of extracellular calcium in MDCK cells, an internalization of cingulin was described (Citi, 1992). We have observed a cytoplasmic localization of cingulin, occludin and F-actin, respectively, prior as well as after the calcium chelation. In contrast, ZO-1 protein showed a different behavior. In the control cells, no cytoplasmic localization of ZO-1 was observed, whereas after the calcium chelation an internalization of ZO-1 occurred. The internalization was dependent on the age of the cells. When 3 day-old cells were treated with EGTA, a cytoplasmic distribution of ZO-1 after the TJ opening was observed. In contrast, the 11 day-old cells showed to be insensitive to the calcium induced internalization of ZO-1. In the co-localization study with cingulin, we used cells after 11 days in culture, and thus no cytoplasmic co-localization of cingulin with ZO-1 was present either in the control cells or in the cells after the calcium chelation.

Interestingly, when we compare a co-localization of ZO-1 with F-actin and OCLN, respectively, to the co-localization of cingulin with F-actin and OCLN, respectively, we find differences although both cingulin and ZO-1 are typical plaque proteins of TJs. The ZO-1 protein was reported to co-localize in the membrane regions with OCLN, CLD1 and F-actin, respectively, revealing one prominent peak of co-localization (Rothen-Rutishauser et al., 1998a), similarly as the co-localization profile of cingulin with F-actin and OCLN, respectively, in the membrane regions. However, after the EGTA treatment, the extent of co-localization of ZO-1 with OCLN was reduced to 15% of the control value, whereas the co-localization increased 2 to 3-fold in the case of the pair ZO-1 and F-actin (Rothen-Rutishauser et al., 1998a). We found that the cingulin co-localization with OCLN and F-actin, respectively, was not changed in the membrane regions and decreased only slightly in the regions of filaments. A detailed analysis of the images revealed the presence of cingulin and ZO-1 in the filaments connecting the cells after the TJ opening, but the proteins did not co-localize. This result suggests, that the binding between cingulin and ZO-1 is disrupted after the separation of the adjacent cells. In addition, the extent of co-localization for cingulin and ZO-1 with F-actin, respectively, after the TJ opening was also different, although both proteins do have an intimate interaction with F-actin (Fanning et al., 1998; Wittchen et al., 1999; D'Atri and Citi, 2001). It has been shown, that in cingulin-depleted MDCK cells the barrier function of TJs was not affected (Guillemot and Citi, 2006). In contrast, MDCK cells lacking ZO-1 and ZO-2 fail to form TJs and the re-expression of ZO-1 alone is sufficient to restore the barrier (Umeda et al., 2006). These findings provide evidence for a different role of cingulin and ZO-1 in the TJs.

To further explore the kinetics of TJ re-assembly, MDCK cells were transfected with green fluorescent protein-tagged claudin-1 (GFP-CLD1). The GFP-CLD1 localized to the lateral membranes and to the cytoplasm of the transfected MDCK cells. This cytoplasmic staining co-

localized partially with a probe for lysosomes, whereas no co-localization was found with a marker for the Golgi apparatus. Cytoplasmic localization of CLDs (CLD1 and CLD4) was also observed in the non-transfected MDCK cells. It is well known that genetically encoded fluorescent tags can perturb the behavior of the acceptor protein or even induce cell toxicity (Kosemund et al., 2000; Meyer et al., 2007; Agbulut et al., 2007). An intracellular localization of the GFP-fused CLD1 was previously observed in MDCK cells (Rueffer and Gerke, 2004; Shen and Turner, 2005), however, with a lesser intensity as compared to our MDCK-GFP-CLD1 cells. In other cases, a proper targeting of TJ proteins fused to GFP was reported (Furuse et al., 1998a; Riesen et al., 2002). The GFP fusion protein with CLD3 was shown to be endocytosed during the re-modeling of the TJs (Matsuda et al., 2004). Thus, it is well possible that the cytoplasmic GFP-CLD1 in the transfected cells represents a recycled portion of the protein, which is targeted to the lysosomes.

In the lateral membranes of the transfected MDCK cells, the GFP-CLD1 co-localized with endogenous TJ proteins CLD4 and OCLN, respectively. The GFP-CLD1 fluorescence in the cell-cell contacts was bright and no use of a gene-expression enhancer, such as sodium butyrate (Tanaka et al., 1991) was required. However, we failed to investigate the influence of EGTA in living cells in the CLSM, because bleaching occurred during the recovery study. This behavior was unexpected, since the CLD1 was fused to a red-shifted variant of the wild-type (wt) GFP, the fluorescence of which is 35-fold more intense than the wt GFP (Cormack et al., 1996). In addition, this enhanced GFP variant (EGFP) contains more than 190 silent mutations that create an ORF composed almost entirely of preferred human codons, which have been shown to increase the expression of GFP in mammalian cells (Haas et al., 1996; Yang et al., 1996). Some photobleaching has been described for the wt GFP when excited near to its major excitation peak at 340-390 nm or 395-440 nm (Chalfie et al., 1994), but we used an argon laser line of 488 nm. At this wavelength, the EGFP has been shown to photobleach about two-fold faster than the wt GFP (Patterson et al., 1997). On the other hand, the photobleaching of the EGFP is five-fold slower than the one of fluorescein (Patterson et al., 1997).

The paraformaldehyde-fixed samples showed a stable GFP-CLD1 fluorescence and allowed us to study the kinetics of the resealing in relation to other proteins, such as ZO-1, CLD4 and F-actin. However, the analysis of the re-assembly after the EGTA treatment revealed no differences between the kinetics of the re-formation for the respective proteins. Apparently none of the studied proteins does have an 'initialization function' to start the re-formation of the new cell-cell contacts. The identification of proteins involved in the early phase of the re-sealing would allow to target those proteins and control the TJ opening. This could only be achieved with real-time CLSM using relatively stable fluorescence markers.

Currently, a number of fluorescent tags is available to enable a simultaneous observation of 4 to 5 proteins in living cells (Chudakov et al., 2005). In addition, by a combination of fluorescent tags, the advantage of fluorescence resonance energy transfer (FRET) can be taken. Blasig et al. (2006) expressed the cyan fluorescent protein (CFP)- and yellow fluorescent protein (YFP)-tagged OCLN (and also CFP- and YFP-CLD5) in living HEK cells to demonstrate an interaction of the proteins. Since FRET typically occurs if the distance of the two fluorophores is ≤ 6 nm (Sekar and Periasamy, 2003), the use of such a technique to study the dynamics of TJs is limited, because the distance between the two plasma membranes of the adjacent

cells is too large to result in a FRET signal. Thus, only the dynamics of the proteins within the same plasma membrane could be studied. Dynamic behavior of individual CLD1 strands was previously described in L-fibroblasts transfected with GFP-CLD1 (Sasaki et al., 2003). The CLD strands were randomly broken and annealed, and dynamically associated with each other. Authors failed to describe the dynamic behavior of GFP-CLD1 in polarized epithelial cells, because of the high density of the protein in the TJs which hampered the visualization of individual TJ strands.

To conclude, we have applied the CLSM to study the dynamic behavior of cingulin and GFP-CLD1 in MDCK cells. The studies on localization and co-localization of TJ proteins provide us with important information about the morphology of these proteins in the state of disassembly and re-assembly of TJs. However, since the resolution of the confocal microscope is around 200 nm, we cannot study a direct interaction of the TJ proteins. For many paracellular permeation enhancers, a contraction of the perijunctional actomyosin ring occurs parallel with an increased TJ permeability and results often in cellular toxicity (Ward et al., 2000). Thus, observation of the actin cytoskeleton in the CLSM help us to evaluate the safety of new permeation enhancers. In addition, the understanding of mechanism of the TJ opening and re-sealing would allow a development of more specific and perhaps more effective methods to promote drug absorption.

4.2 Synthetic peptide homologues to claudin and occludin sequences as a strategy to modulate tight junctions

Peptides emulating the sequence of the TJ-sealing protein occludin (OCLN) were suggested as a novel strategy for enhancing the paracellular permeation of poorly absorbed drugs (Wong and Gumbiner, 1997). Hence claudins are currently believed to be responsible for the sealing mechanism of TJs, we aimed to identify CLD peptides with a TJ-modulating potential. We included two peptide homologues to OCLN that had been described to modulate TJs in epithelial cells (Tavelin et al., 2003) as a positive control for our assays. To assess the effects of peptides on the cell layer, we used TEER measurements, a mannitol permeation assay and CLSM. The TEER and the permeation of mannitol, a marker for paracellular diffusion, allowed us to monitor the actual state of TJs. The CLSM provided information about the morphology of the cells and allowed us to study the distribution and the binding of a fluorescent peptide homologue to the TJs. To find optimal conditions for a TJ-modulating activity, we varied several critical factors in the assays, such as the concentration of foetal calf serum (FCS) in cell cultures, the oxidation-reduction state of peptides, the seeding density of the cultured cells and the peptide concentration for incubation.

The CLD2 peptide homologues tested in the presence of 10% (v/v) FCS did not influence the TJs as shown with TEER and mannitol permeation. Lowering of the serum concentration to 1% (v/v) did not change the result. None of tested peptide homologues (CLD1, CLD2 and CLD4) could selectively open the TJs. This indicates that TJ modulation was not hindered by a non-specific binding of the respective peptides to FCS. In previous studies, the peptides displayed a TJ-modulating activity on cell cultures either in presence (Wong and Gumbiner, 1997) or absence of FCS (Tavelin et al., 2003).

The sequence of several CLD peptide homologues contains one or two cysteine residues. We hypothesized, that a formation of disulfide bridges between the peptides could disturb the possible interaction with the native CLDs. However, the cysteine-containing CLD1, CLD2 and CLD4 peptide homologues assayed in the presence of a reducing agent (DTT) were also not able to open the TJs of the MDCK cells. In addition, an analogue of the CLD1 peptide homologue 47-65 containing serines instead of cysteines (peptide **6**) was also tested and did not show an effect on TEER and mannitol permeability. Claudin-5 (CLD5) is the predominant claudin in the blood-brain barrier and was suggested to be directly responsible for the tightness of this barrier (Nitta et al., 2003). It has been previously shown, that the expression of CLD5 in MDCK cells (lacking endogenous CLD5) resulted in a five-fold increase of the TEER (Wen et al., 2004). Mutations of cysteines in the extracellular domain of CLD5 abolish its ability to increase the TEER when transfected to MDCK cells, and a mutation of a cysteine in the loop I (position 64) strikingly increased the paracellular flux of monosaccharides. Also, the second extracellular loop of OCLN contains two conserved cysteine residues (Furuse et al., 1993). Interestingly, an OCLN-loop-II peptide modified on cysteines with the acetamidomethyl groups was able to disrupt TJs in a cell culture model, whereas unmodified peptide was ineffective (Wong and Gumbiner, 1997). Authors reported that the modification of cysteines increased

the hydrophilicity of the peptide and prevented a formation of oligomers as observed on SDS-PAGE. In contrast, others reported TJ-modulating effects of OCLN peptides with unmodified cysteine residues (Nusrat et al., 2005; Chung et al., 2001). The results from the above mentioned studies suggest a crucial role of cysteines in the formation of the TJs, however, it is not clear whether the cysteine residues contribute to the TJ-modulating effect of peptides homologues.

It was previously reported, that the permeation-enhancing effect of an OCLN peptide homologue depends on the growth state of the cells (Wong and Gumbiner, 1997). For newly-formed monolayers that had not yet reached the maximum TEER, the effects were much more pronounced than with stationary monolayers. Thus, we hypothesized that a lowering of the cell density in the assay may increase the binding probability of peptides to CLDs located in TJs and trigger the TJ-opening. An increase of the peptide concentration should also enhance this process. However, due to the limited solubility of the CLD peptide homologues, higher concentrations of peptide **7** and **12** (0.3 and 0.6 mM, respectively) led to the formation of peptide aggregates upon addition of the peptides to the culture medium. Theoretically, these could function as a slow-releasing depot that would deliver peptides directly at the cell-cell contacts. Indeed, when assayed for 48 hrs at 10-fold lower cell density and at the higher peptide concentration, a decrease of TEER and an increase of mannitol permeability for the CLD1 (peptide **7**) and the CLD2 (peptide **12**) peptide homologue were observed. These results suggested a TJ-modulating effect. However, CLSM revealed massive morphological changes in the peptide **7**-treated cells. This damage led most probably to the apparent TJ-modulating effect. This was indeed the case, as we confirmed in further experiments. In a first approach, MDCK cells were grown up-side-down on the cell culture inserts and treated for 48 hrs with peptide **7** under conditions, where aggregation occurred, but the aggregates were not deposited on the cell layer. The TEER remained high at values similar to the ones obtained without peptide. In a second approach, a short-term (6 hrs) incubation with the peptide, precipitates failed to affect the TEER and the mannitol flux of the MDCK cells. Finally, a re-designed assay to test peptide **7** at higher co-solvent concentration (i.e. conditions, where no visible aggregation occurred) also showed no effects on the TEER and mannitol permeation. The results of these experiments confirmed the non-specific influence of the peptide aggregates on the cell monolayer.

Surprisingly, the CLD2 homologue 31-49 (peptide **12**) aggregated at lower concentration (0.1 mM) thereby causing no change of the mannitol permeability after 48 hrs of incubation. A similar behavior to the peptide **12** was observed for the CLD4 homologue 31-49 (peptide **15**). The grand average hydropathy index (GRAVY) may be used to predict the overall hydrophobicity of proteins and peptides (Kyte and Doolittle, 1982). The higher the index the more hydrophobic the peptides tend to be. Interestingly, for the CLD peptide homologues with amino acid residues 31-49 (peptide **12** and **15**) and 49-60 (peptide **7**), respectively, higher GRAVY indices were predicted as compared to the other CLD homologues. We speculate, that the amount and the shape of the aggregates may have had a different influence on the cell layer. Thus, a higher peptide concentration led to more pronounced aggregation, which induced the cell damage. Peptide association and aggregation were reported in several studies performed with peptide homologues to OCLN (Tavelin et al., 2003; Nusrat et al., 2005). Poor solubility of the TJ-modulating-peptides of OCLN was mentioned only in one study (Wong and Gumbiner,

1997), however, a co-solvent was used by many of the authors (Vietor et al., 2001; Chung et al., 2001; Nusrat et al., 2005; Tavelin et al., 2003). Poor solubility for the peptides homologues of the first extracellular loop of CLD1 was also observed (Mrsny, 2007).

Changes in the morphology (CLSM) or expression (Western blot) of the endogenous TJ proteins were also reported in previous studies performed with peptide homologues to OCLN. A peptide emulating the whole second extracellular domain of OCLN decreased the amount of OCLN present at the TJs of A6 *Xenopus* kidney cells (Wong and Gumbiner, 1997). Vietor et al. (2001) tested the same OCLN peptide, and reported a similar decrease of OCLN in the TJs of mouse mammary EpH4 cells. In addition, the peptide treatment led to the formation of multilayered, unpolarized cell clusters. Interestingly, these clusters very much resemble the morphology we observed after the treatment with CLD peptide aggregates. When a single dose of a peptide homologue to OCLN was administered to adult rats intratesticularly, the germ cells started to be depleted from the seminiferous epithelium within 8-16 days (Chung et al., 2001). Moreover, the peptides corresponding to the second extracellular loop of OCLN led to a strong desorganization of the staining pattern for CLD1, OCLN, F-actin, ZO-1 and JAM in the human epithelial cell line T84, as observed by CLSM (Nusrat et al., 2005). The TJ-modulating effects for the peptide homologues to the first extracellular loop of OCLN were associated with a more diffuse OCLN staining in the CLSM, as compared to the control without peptide, but the expression level of OCLN did not change, as demonstrated by Western blot (Tavelin et al., 2003).

We hypothesized that an introduction of hydrophilic amino acids to the hydrophobic sequences will not only increase solubility, but also support the interaction of peptides with charged residues present in native CLDs in TJs, and thus possibly enhance permeability. The tags consisting of lysines and aspartic acids, respectively, increased the peptide solubility (peptide **9** and **10**), however, no TJ-modulating effect was observed.

The proposed extracellular loops of CLDs could potentially have an interaction not only extracellularly and at the cell surface, but also within the hydrophobic lipid bilayer. For instance, the TJ-proteins ZO-1 and OCLN have been shown to have an intimate association with the cholesterol- and sphingomyelin-enriched lipid microdomains known as lipid rafts (Nusrat et al., 2000b). We examined therefore the circular dichroism spectra of the CLD1 peptide homologue 49-60 (peptide **7**). A solvent-dependent conformational change was observed, when the peptide was moved from a hydrophilic to a hydrophobic environment. The relative portion of the α -helix increased from around 10% in the hydrophilic environment (buffer) to 30% in the lipid-like environment (TFE). This result is in agreement with previous reports, showing that TFE stabilizes the α -helical structures of proteins and peptide fragments (Shiraki et al., 1995; Lehrman et al., 1990). Such a conformational change as observed with peptide **7** was reported for an OCLN peptide homologue that showed modulating effects on TJs (Nusrat et al., 2005). It has been suggested that the TJ-modulating activity of the peptide homologues may be facilitated by the association with lipids in the cell membranes (Mrsny, 2005). However, in contrast to findings of Nusrat et al. (2005), the ability of peptide **7** to undergo solvent-dependent changes was not associated with a TJ-modulating activity.

Protein-protein interactions are often mediated by small protein-recognition motifs, so called 'hot spots', where the key anchor residues are arranged in a particular three-dimensional struc-

ture. Such recognition motifs are mostly α -helices, then β -sheets, left-handed polyproline II helices and peptide chain turns (sites where a peptide chain reverses its overall direction) (Che et al., 2006). Numerous studies indicate, that by mimicking the secondary structures one can regulate the protein functions (Berg, 2003; Davis et al., 2007). Thus, it could be speculated, that a stable peptide conformation would contribute to an interaction of peptides with the native OCLN or CLD, and thus to a TJ-modulating activity. An estimation of the secondary structure of human CLD1 and OCLN suggests that particular segments of the extracellular domains may be in α -helical or β -sheet structures (Mrsny, 2005). However, since the peptide **7** adopted predominantly a disordered structure, it might not possess the potential to mediate such interactions with the native CLDs. Neither the exact CLD-CLD interaction nor the 3D-structure of CLD are known, which make it impossible to rationally design peptides (and peptidomimetics) or small molecules capable of modulating the TJ function.

Externally supplied peptides may have difficulties to access the critical components of TJs. The calcium switch protocol induces a disassembly of TJs (Martinez-Palomo et al., 1980). Thus, peptides added during a calcium switch protocol should have a better access to the TJ components (Nusrat et al., 2005) and, alternatively, upon the addition of calcium the re-sealing of the TJ structures could be hindered, if the peptide had a sufficient affinity for the corresponding target proteins. However, the peptide homologues to CLD1 and CLD2 (peptide **7** and **13**) failed to interfere with the re-sealing of the TJs after calcium replacement (not shown). In contrast, several short peptide homologues of OCLN were shown to induce such effects (Lacaz-Vieira et al., 1999).

Peptide homologues to the first (Wong and Gumbiner, 1997; Vietor et al., 2001; Chung et al., 2001; Blaschuk et al., 2002; Nusrat et al., 2005) or second (Van Itallie and Anderson, 1997; Lacaz-Vieira et al., 1999; Tavelin et al., 2003; Everett et al., 2006) extracellular domain of OCLN were previously shown to modulate the TJs *in-vitro*, as well as *in-vivo*. The striking differences between the published data and ours led us to test two peptide homologues to OCLN. The OCLN peptide homologue 90-103 (peptide **1**) and its derivative coupled to the lipoamino acid (peptide **2**) were synthesized and tested under similar conditions as described by Tavelin et al. (2003). In contrast to their report, both peptides failed to modulate TJs in the assay with MDCK and Caco-2 cells, respectively. It is important to note that Tavelin et al. (2003) only found increased mannitol permeation with peptide **1** when added from both sides of the cell culture insert. When applied from the apical side only, no effects were observed. Authors claim that the reason for the lack of the effect from the apical side was a rapid enzymatic degradation of the peptide and a formation of peptide aggregates. The TJ-modulating effect of peptide **1** from the basolateral side of the cell culture was explained by a better accessibility of the aggregates to the TJs from this side of the cell layer. Tavelin and colleagues further showed that conjugation of the peptide **1** to the lipoamino acid protected the peptide against the enzymatic degradation and reduced the tendency of the peptide to form aggregates. The peptide conjugate was also active if only added from the apical side. For the TJ-modulating effect, however, a cleavage of the lipoamino acyl residue was required to release the free peptide **1**. We found only a minor decomposition (< 25%) of peptide **1** during the incubation with MDCK cells. Since MDCK cells are less metabolically active than Caco-2, and the peptide **1** is the actual effective molecule, we would expect a significant effect of the peptide **1** when applied to the MDCK cells from both

sides of the cell culture insert. Similarly, peptide **2** should display an effect when assayed with Caco-2, because the brush border enzymes would release the free peptide **1**. The fact that the peptide **1** released from the peptide **2** can undergo aggregation in the same way as the non-conjugated homologue is not discussed by the authors.

The Caco-2 cells were previously shown to have distinct growth characteristics depending on the cell culture support (Rothen-Rutishauser et al., 2000). Cells formed monolayers on polycarbonate (PC) filters and mixed mono- and multilayers on polyethylene terephthalate (PET) filters. In multilayers, TJs were not restricted to the most apical cell layer, but also appeared in lower layers. Since the Caco-2 multilayers might be less sensitive to the peptides, we also assayed the OCLN peptides with Caco-2 cells grown on PC filters. However, we found no difference between the two supports.

To explore the binding of peptide **1** morphologically, we assayed its fluorescent derivative in the CLSM. No TJ-specific binding was observed in MDCK and in Caco-2 cells, respectively. With the MDCK cells the peptide was clearly localized in the cytoplasm, suggesting endocytotic uptake. To exclude the possibility that bound peptide was internalized, we performed an experiment where the incubation time was shortened from 6 hrs to 30 min only. However, we only observed a non-specific labeling of the cells. After a prolonged washing step, the fluorescence signal of the peptide disappeared. These data show that the peptide was not able to associate with the TJ structures. If the TJ-modulating effects were mediated by the binding of the parent peptide to the native TJs, we would expect a binding of the fluorescent peptide as well. However, we cannot exclude, that the FITC moiety could have changed the peptide properties, and thus block the association with TJs.

The sequence similarity of the dog and human OCLN is more than 90 %, as calculated with the Lipman-Pearson method (MegAlign program, DNASTAR Lasergene). Peptide **1** differs in 3 amino acids between the dog and human sequence (Met vs. Leu, Gly vs. Ser and Ile vs. Val), which corresponds to a sequence similarity of 78.6 %. However, two of the non-identical amino acids belong to the same group of amino acids concerning their hydrophobicity (Voet and Voet, 1995). Thus, the lack of the TJ-modulating effect for peptide **1** and **2** in our assay with the dog cell line (MDCK) is unlikely to be due to the species-related differences.

It is interesting to note, that the effective concentrations of different peptide homologues to OCLN required for a significant TJ-modulating effect differ among the published data by a factor of 1500. The concentration of peptide **1** tested in our assays was 0.1 mM and 0.3 mM, which corresponds to a two and six-fold higher concentration, respectively, than the minimal effective concentration of this peptide in the original publication of Tavelin et al. (2003). Thus, the lack of the effect due to the insufficient peptide concentration can be excluded.

In summary, in our hands the approach to modulate TJs with peptides emulating the sequences of the extracellular loops of CLDs was inefficient and associated with non-specific effects of peptide aggregates. Our data concerning the ability of peptide homologues to the first extracellular loop of OCLN did not support the findings of Tavelin et al. (2003). It has to be pointed out, that a poor peptide solubility was of major concern. The problem of the peptide aggregation was only marginally addressed in the previous studies. It may well be, that for some of the TJ-modulating effects reported, non-specific interactions similar to those we observe with CLD peptide homologues were involved. It seems, that the hydrophobicity of the

sequences plays an important role in the formation of TJs, since less hydrophobic peptides did not aggregate but failed to induce the TJ-opening. A contradiction can also be found between the results reported for the peptide homologues corresponding the first and second extracellular loop of OCLN. It is possible, that the striking differences observed in these various studies were due to different cell cultures and peptide preparations. For example, the tendency of peptide homologues of OCLN to aggregate was observed to be supplier-dependent (Tavelin, 2004). In addition, we have to consider several other important issues for the use of this strategy to enhance absorption. First, peptides *per se* have a low metabolic stability and are rapidly degraded by proteolytic enzymes. More frequent dosing and larger doses would be needed to obtain the required concentration *in-vivo*. For example, to reach an *in-vivo* concentration of 0.1 mM for a 20-amino acid peptide intended to modulate TJs of the blood-brain barrier, we would need to inject a single dose of approximately 1 g assuming that the peptide distributes only in the systemic circulation and no degradation by serum proteases occurs. Although, high doses are generally well tolerated, the ability to make them cost effectively represents a serious problem (Latham, 1999). Strategies to improve the peptide metabolic stability are, however, available (Pauletti et al., 1997; Kieber-Emmons et al., 1997) and would certainly be required for the TJ-modulating peptides. Second, the TJ-opening might improve the delivery of poorly absorbed drugs, but the potential for absorption of undesirable materials such as endotoxins may have important clinical consequences. This issue is not easy to handle and would need a subtle tuning of the temporary opening. Third, many researches including us applied the peptide homologues from both, apical and basolateral side of the cell cultures, whereas the pharmacological agents are generally applied to the apical (luminal) side of epithelia. Therefore, an apical TJ-modulating activity would be a prerequisite for further development of this strategy. Finally, we should consider that the paracellular route represents only a small fraction of the epithelial surface area, and thus a limitation to reach the required drug concentration (Mrsny, 2005).

4.3 Development of claudin-containing proteoliposomes as an *in-vitro* model for the screening of the tight junction modulators

Claudin molecules are believed to be responsible for the sealing mechanism of TJs. The current model of TJs suggests that the extracellular domains of CLDs interact homotypically or heterotypically to bridge the paracellular space (Koval, 2006). We hypothesized, that a simple *in-vitro* model of TJs based on those interactions would be useful to screen for novel permeation enhancers. For this purpose, we expressed the human His-CLD1 in the baculovirus expression system and we used an immobilized metal-affinity chromatography to purify the protein from the membrane fractions. To reconstitute the His-CLD1 into phosphatidyl choline (PhC) liposomes, we applied the detergent dialysis method. We showed a successful reconstitution of His-CLD1 into the liposomes, however, we did not observe an interaction between the reconstituted proteins, i.e. no aggregation of liposomes.

The His-CLD1 was expressed in insect cells by using the baculovirus expression system. The protein was localized intracellularly and was targeted to membranes. This protein was purified and used to prepare proteoliposomes. The issue regarding the yield in the expression system will be discussed later.

The detergent dialysis method used for the reconstitution of His-CLD1 into proteoliposomes is a method especially suited for the removal of the detergents with a high critical micellar concentration (CMC), such as octylglucoside (Helenius et al., 1979). We first attempted to prepare the detergent-lipid micelles with octylglucoside only. The dialysis of these micelles, however, resulted in a massive lipid aggregation. In contrast, when we used a mixture of octylglucoside with sodium cholate, we obtained very well defined liposomes with respect to the size and homogeneity. It is possible, that in the case of the lipid-detergent micelles prepared by octylglucoside only, the removal of the detergent is too fast to yield in defined liposomes. In fact, the dialysis of radiolabeled detergents from micelles revealed that the rate of octylglucoside removal was nearly twice as fast as of sodium cholate. Thus, the addition of sodium cholate contributed to controllable conditions.

Because the amount of purified His-CLD1 was limited, the residual amounts of detergents were analyzed in pure PhC liposomes. We assume that the removal of the detergents from the His-CLD1-proteoliposomes would be similar, since it has been shown that the presence of an integral membrane protein, such as the major human erythrocyte MN-glycoprotein, had only minor effects on the retention of detergents by the reconstituted liposomes (Allen et al., 1980). The residual detergent concentration of cholate and octylglucoside in liposomes after 48 hrs of dialysis was 111 and 34 nM, respectively. This results in an approximate ratio of 1 molecule of cholate per 57'000 molecules of phosphatidyl choline and 20 molecules of His-CLD1, respectively, and 1 molecule of octylglucoside per 186'000 molecules of phosphatidyl choline and 65 molecules of His-CLD1, respectively. Bile salts and octylglucoside were reported to enhance the paracellular permeation of mannitol (Lindhardt and Bechgaard, 2003; Tirumalasetty and Eley, 2006), however, in a concentration that is more than 130-fold and 290-fold higher than

the residual concentration of cholate and octylglucoside, respectively. We thus speculate that the residual detergent concentrations are far too low to influence the reconstituted proteins in the liposomes.

Beside the detergent dialysis, also other methods such as an adsorption of the detergent onto hydrophobic beads or dilution of detergent below the CMC are widely used to remove detergents (Schubert, 2003). However, a significant adsorption of lipids to the beads was reported with the absorption method (Phillippot et al., 1983; Ueno et al., 1984). The dilution method is problematic as well, due to the need of re-concentration of the proteoliposomes and, additionally, a considerable amount of residual detergents is left in the preparations (Rigaud and Levy, 2003). Also other strategies are available to prepare proteoliposomes, such as by sonication and freeze-thawing or by the use of organic solvents. These methods are often harmful to membrane proteins (Rigaud and Levy, 2003), and thus the detergent dialysis is the method of choice.

The reconstitution efficiency of His-CLD1 into the proteoliposomes was determined by an isopycnic centrifugation of the proteoliposomes on a sucrose gradient. The Western blot of the fractions from the density gradient revealed that the His-CLD1 was mainly localized in the lipid-containing fractions, corresponding to a density range between 1.05 and 1.07 g/cm³. Beside the 22 kDa-band of His-CLD1, additional bands corresponding to dimers of His-CLD1 were also observed. We have already seen these dimers during the affinity purification of His-CLD1 from the Sf9 crude membranes. In addition, we detect such dimers also when the endogenous CLD1 is solubilized by octylglucoside from MDCK cells (not shown). This suggests that His-CLD1 can form SDS-resistant dimers when solubilized in octylglucoside. SDS-resistant oligomers are routinely seen with other membrane proteins similar to CLD, such as connexins (Rhee et al., 1996). Also, His-CLD4 expressed in insect cells was reported to form higher molecular weight oligomers (from dimers up to hexamers), when solubilized in perfluoro-octanoic acid, and these oligomers were SDS-resistant (Mitic et al., 2003). Contrary to our result, authors showed that His-CLD4 solubilized in octylglucoside existed as monomer and localized to low density fractions when loaded onto a sucrose density gradient. This is rather surprising, since soluble proteins are reported to be located at higher densities in density gradients (Carlson et al., 1978; Findlay and Evans, 1987). The fact that Mitic et al. (2003) observed His-CLD4 in low density fractions may be due to the residual lipids bound to the protein after the solubilization from membranes. Since the final concentration of octylglucoside in the density gradient was below the CMC, the localization of His-CLD4 in the low density fractions is unlikely due to the presence of mixed micelles of octylglucoside with the protein. If proteoliposomes are loaded onto a density gradient, non-reconstituted proteins are located at the bottom of the gradient (Rigaud et al., 1988; Levy et al., 1992), i.e. at higher density fractions. Thus, the presence of the His-CLD1 in the low density fractions must be due to the reconstitution in the proteoliposomes. It would be interesting to analyze the efficiency of the His-CLD1 reconstitution by freeze-fracture electron microscopy and compare the result with a freeze-fracture image of an epithelium (or CLD-transfected fibroblasts), to gain information if an artificial formation of TJ was achieved.

To characterize the proteoliposomes, we used dynamic laser light scattering. As shown on correlograms, no association of liposomes to larger structures was observed. These results

suggest that the protein-protein interactions between the re-constituted His-CLD1 may be too weak to mediate adhesion. If the hydrophobic interactions had been responsible for the interaction of the extracellular domains of the TJ-transmembrane proteins, we would rather have expected a strong interaction between the proteins. An example of such an interaction may be given by the gap junction protein connexin (Sosinsky and Nicholson, 2005). Connexin has the same topology as CLD and OCLN, bearing two extracellular loops and four transmembrane domains (Milks et al., 1988). Six molecules of connexin engage to form a connexon-hemichannel, and two connexons interact with the extracellular loops to form a gap junction channel between the adjacent cells (Makowski et al., 1977). Hydrophobic interactions play a significant role in the connexon-connexon interaction. To split the interaction between the connexon-hemichannels in the isolated rat liver gap junctions, relatively harsh conditions (combination of 8 M urea, chelating agents and higher temperature) are needed (Ghoshroy et al., 1995), suggesting a rather strong interaction.

Alternatively, the molar ratio of protein to lipid (1:3000, i.e. ~ 2000 claudin molecules per liposome) in our experiment could be too low to mediate the interactions between the reconstituted proteins. Based on experiments with the symmetry of protein orientation in the proteoliposomes (Sharom et al., 1993), we most probably have 50% of His-CLD1's oriented with their extracellular loops outward the proteoliposome, and 50% in the opposite direction, displaying their C- and N-terminal ends. Thus, theoretically, only the half of the reconstituted protein is available for the binding. An increase in the protein concentration should be definitely the next step to investigate the His-CLD1 proteoliposomal system.

The dynamic laser scattering to detect aggregates or associates is a 'yes-or-no' method and has its limitation. It is not possible to quantify the amount of the aggregated particles. Different methods are available to study the adhesion mechanisms of proteins in a semi-quantitative or even quantitative way (Vedula et al., 2005). These methods are mainly cell-based methods, but could be modified for use with the CLD1-proteoliposomes. For example, McClay et al. (1981) labeled a set of cells with a radioactive phosphorus and, subsequently, incubated those cells with a cell monolayer on a microtiter plate. After a certain time, the plate was inverted and centrifuged at different speeds. Following this, the bottom of the plate was cut and quantified by liquid scintillation. The centrifugal speed needed to separate 50% of the bound cells gives a rough estimate of the force of adhesion between the cells. Such a method could be modified for proteoliposomes. A set of proteoliposomes immobilized on a solid surface would be incubated with proteoliposomes loaded with e.g. radiolabeled phospholipids, to enable a sensitive detection.

Recently, the development of the atomic force microscopy (AFM) has even made it possible to resolve forces at the level of a single molecular interaction. A number of methods is available to functionalize the AFM cantilever to immobilize cells, liposomes and proteins of interest (Benoit and Gaub, 2002; Vedula et al., 2005; Jass et al., 2000). The cantilever deflection due to its interaction with a substrate is converted into the force. Several hundred of so called 'force curves' are recorded and analyzed to obtain the quantitative values for the interactions. The cadherin-cadherin interactions in a solution were probed by this method (Baumgartner et al., 2000). To measure an association between the proteoliposomes and to screen for molecules disturbing the adhesion by the AFM technology would be challenging, since liposomes are fluid

and dynamic systems (Casals et al., 2003).

Apart from the screening of molecules binding to the CLD extracellular loops, our system would be suitable to explore the interaction between different CLDs in order to refine the current model of TJs. For this purpose, liposomes would be reconstituted with single or several CLDs and the association between the liposomes mediated by the extracellular loops could be measured by surface plasmon resonance (SPR). As discussed previously, 50 % of the reconstituted proteins display the extracellular loops and 50 % the N- and C-terminal ends. The interaction between the termini of two proteins would contribute to the measured associations. To address this problem, it would be needed to simplify the structure of the CLDs to the respective extracellular loops. The sequence of the loops would be tagged by e.g. biotin moiety on its N- and C-termini, to enable a streptavidine-mediated binding on the surface of liposomes and the SPR chip, respectively.

To conclude, we successfully re-constituted the His-CLD1 into the phosphatidyl choline liposomes. Dynamic laser scattering did not reveal interaction of the extracellular domains between the reconstituted proteins. These results, however, have to be considered as a pilot. The expression and reconstitution protocols must be optimized to enable a development of this assay. The first step should be the optimization of the protein expression.

In the baculovirus system, the efficiency of an infection and subsequent protein expression depends on optimal cell growth conditions (Bradley, 1990; Geisse and Kocher, 1999). In our hands, the Sf9 cells exhibited a doubling time of about 22 hrs in the logarithmic growth phase, which is comparable to what has been reported for a Sf9 suspension culture in serum-free medium (Rhiel et al., 1997). Thus, the low expression was not due to the non-standardized cell culture.

To express the His-CLD1, the cells were infected with baculoviruses in suspension culture at multiplicity of infection (MOI) of 3. One day post-infection, the cell growth did not continue and the cell density remained constant for another 3 days. This is in contrast to Rhiel et al. (1997), who reported a significant decrease in the cell density (Sf9) already 48 hrs post-infection, by using a multiplicity of infection (MOI) approximately 15-times lower than we used. A decrease in the cell density of infected Sf9 cells was also shown in a shaker flask culture, when infected between MOI 0.1 to 10 with a baculovirus coding for the expression of β -galactosidase (Radford et al., 1997). We observed that the expression level of His-CLD1 did not differ among the different MOIs and incubation times. In previous studies with recombinant baculoviruses coding for the expression of β -galactosidase (expressed intracellularly in Sf9 cells), the product yields were also relatively insensitive to the MOI (Murhammer and Goochee, 1988; Schopf et al., 1990; Kioukia et al., 1995; Radford et al., 1997). In contrast, Licari and Bailey (1991) reported that higher MOI's led to higher product yields.

Another aspect for optimization of the His-CLD1 production is the purification from crude membranes. To solubilize proteins we used octyl β -D-glucopyranoside, a nonionic detergent, that has been extensively utilized for solubilization of membrane proteins (Hammond and Zarenda, 1996). Octylglucoside was not able to dissolve the membrane fractions completely and a small insoluble fraction remained. Indeed, octylglucoside was reported to extract only around 32 % of the total protein from the Sf9 membrane fractions as compared to SDS, the standard of 100 % extraction (Mitic et al., 2003). Others also reported a low efficiency of octyl-

glucoside to extract membrane proteins, such as P-glycoprotein, from the membrane fractions of Sf9 (Taylor et al., 2001). However, octylglucoside is a mild and non-denaturing detergent that allows membrane proteins to be solubilized without affecting their structural features (Seddon et al., 2004). In addition, its compatibility with immobilized metal-affinity purification and the possibility of a removal by dialysis (Rosevear et al., 1980; Gonzalez-Ros et al., 1981) is of big advantage as compared to other detergents. The low yield of His-CLD1 in the purification cannot be attributed to the partial loss of His-CLD1 in the preparation of crude membranes or to the low protein extraction efficiency of octylglucoside, but rather to the low expression level in insect cells. This hypothesis is supported by checking the immunolabeling of His-CLD1 in infected cells by the CLSM. Only low number of cells expressing His-CLD1 was observed (not shown). The yield of the purification could be optimized by enhancing the infection efficiency and utilizing another affinity tag for the purification. Several studies have documented an enhanced protein production following a co-transfection with baculoviruses expressing chaperone proteins, which are known to aid in the folding and modification of newly synthesized proteins (Higgins et al., 2003; Kato et al., 2005; Fourneau et al., 2004; Zhang et al., 2003). Also, a significant increase in the expression levels has been reported after addition of various DNA elements to the virus, such as the 21 bp segment from 5' untranslated regions of a lobster tropomyosin cDNA (Sano et al., 2002). The position of the His-tag is also important for the protein expression and purification (Lee and Altenberg, 2003; Arnau et al., 2006). However, CLDs were produced with both N- and C-terminal His-tags. Mitic et al. (2003) used a C-terminal deca-His-tag to express and purify large amounts of CLD4 in Sf9 cells. Hoevel et al. (2002) expressed and purified CLD1 tagged with a N-terminal hexa-His-tag, also from Sf9 cells. Thus, the position of the tag in the case of CLDs seems to be rather irrelevant. A combination of several tags is considered to be of advantage for a protein purification (Waugh, 2005; Arnau et al., 2006). The option to express the His-CLD1 in a different expression system must be considered.

5 Outlook

In this work, we proposed the use of proteoliposomes reconstituted with claudins as a screening assay for molecules able to bind to the extracellular loop of CLDs. An increase in the amount of His-CLD1 to be reconstituted shall be the next step to investigate the proteoliposomal system. To achieve this goal, the protocols regarding the expression and purification must be further optimized to obtain high yield of purified protein.

This assay would be suited to explore the interactions between the claudins in order to enable the development of specific permeation enhancers. Provided that a significant and reproducible association of proteoliposomes occurs, it would be interesting to test the influence of pH and ionic strength on the association. The characterization of the proteoliposomes regarding these factors would provide us with information if the interaction is also charge dependent. Further, peptides or peptidomimetics with defined secondary structures would be tested to investigate, whether the interaction between the extracellular loops is conformation dependent. Positive result would provide us with a starting point for design of molecules specifically interacting with the extracellular domains of claudins that would possibly represent a new class of permeation enhancers. Indication that claudins are promising targets for permeation enhancement has been previously demonstrated with a non-toxic permeation enhancement in rats by using the C-terminal domain of *Clostridium perfringens* toxin that tightly interact with extracellular domains of claudin-3 and claudin-4. These findings support the approach of targeting claudins to enhance drug delivery of hydrophilic drugs.

References

- Agbulut, O., Huet, A., Niederlander, N., Puceat, M., Menasche, P., and Coirault, C. (2007). Green fluorescent protein impairs actin-myosin interactions by binding to the actin-binding site of myosin. *Journal of Biological Chemistry*, 282(14):10465–71.
- Aijaz, S., Balda, M. S., and Matter, K. (2006). Tight junctions: molecular architecture and function. *International Review of Cytology*, 248:261–98.
- Allen, T. M., Romans, A. Y., Kercret, H., and Segrest, J. P. (1980). Detergent removal during membrane reconstitution. *Biochimica et Biophysica Acta*, 601(2):328–42.
- Amasheh, S., Meiri, N., Gitter, A. H., Schöneberg, J., Mankertz, J., Schulzke, D. J., and Fromm, M. (2002). Claudin-2 expression induces cation-selective channels in tight junctions of epithelial cells. *Journal of Cell Science*, 115(24):4969–4976.
- Ambudkar, S. V. (1995). Purification and reconstitution of functional human P-glycoprotein. *Journal of Bioenergetics and Biomembranes*, 27(1):23–9.
- Anderberg, E. K. and Artursson, P. (1993). Epithelial transport of drugs in cell culture. VIII: Effects of sodium dodecyl sulfate on cell membrane and tight junction permeability in human intestinal epithelial (Caco-2) cells. *Journal of Pharmaceutical Sciences*, 82(4):392–8.
- Anderson, J. M. (2001). Molecular structure of tight junctions and their role in epithelial transport. *News in Physiological Sciences*, 16:126–30.
- Anderson, J. M., Van Itallie, C. M., and Fanning, A. S. (2004). Setting up a selective barrier at the apical junction complex. *Current Opinion in Cell Biology*, 16(2):140–5.
- Ando-Akatsuka, Y., Saitou, M., Hirase, T., Kishi, M., Sakakibara, A., Itoh, M., Yonemura, S., Furuse, M., and Tsukita, S. (1996). Interspecies diversity of the occludin sequence: cDNA cloning of human, mouse, dog, and rat-kangaroo homologues. *Journal of Cell Biology*, 133(1):43–7.
- Andreeva, A. Y., Krause, E., Muller, E. C., Blasig, I. E., and Utepbergenov, D. I. (2001). Protein kinase C regulates the phosphorylation and cellular localization of occludin. *Journal of Biological Chemistry*, 276(42).
- Armitage, W. J., Juss, B. K., and Easty, D. L. (1994). Response of epithelial (MDCK) cell junctions to calcium removal and osmotic stress is influenced by temperature. *Cryobiology*, 31(5):453–60.

- Arnau, J., Lauritzen, C., Petersen, G. E., and Pedersen, J. (2006). Current strategies for the use of affinity tags and tag removal for the purification of recombinant proteins. *Protein Expression and Purification*, 48(1):1–13.
- Artursson, P., Palm, K., and Luthman, K. (1996). Caco-2 monolayers in experimental and theoretical predictions of drug transport. *Advanced Drug Delivery Reviews*, 22:67–84.
- Artursson, P., Ungell, A. L., and Lofroth, J. E. (1993). Selective paracellular permeability in two models of intestinal absorption: cultured monolayers of human intestinal epithelial cells and rat intestinal segments. *Pharmaceutical Research*, 10(8):1123–9.
- Audus, K. L., Bartel, R. L., Hidalgo, I. J., and Borchardt, R. T. (1990). The use of cultured epithelial and endothelial cells for drug transport and metabolism studies. *Pharmaceutical Research*, 7(5):435–51.
- Aungst, B. J. (2000). Intestinal permeation enhancers. *Journal of Pharmaceutical Sciences*, 89(4):429–442.
- Balda, M. S. and Anderson, J. M. (1993). Two classes of tight junctions are revealed by ZO-1 isoforms. *American Journal of Physiology*, 264(4 Pt 1):C918–24.
- Balda, M. S., Gonzalez-Mariscal, L., Matter, K., Cereijido, M., and Anderson, J. M. (1993). Assembly of the tight junction: the role of diacylglycerol. *Journal of Cell Biology*, 123(2):293–302.
- Balda, M. S. and Matter, K. (1998). Tight junctions. *Journal of Cell Science*, 111(Pt 5):541–7.
- Balda, M. S. and Matter, K. (2000). The tight junction protein ZO-1 and an interacting transcription factor regulate ErbB-2 expression. *The EMBO Journal*, 19(9):2024–33.
- Balda, M. S., Whitney, J. A., Flores, C., Gonzalez, S., Cereijido, M., and Matter, K. (1996). Functional dissociation of paracellular permeability and transepithelial electrical resistance and disruption of the apical-basolateral intramembrane diffusion barrier by expression of a mutant tight junction membrane protein. *Journal of Cell Biology*, 134(4):1031–49.
- Balkovetz, D. F. (2006). Claudins at the gate: determinants of renal epithelial tight junction paracellular permeability. *American Journal of Physiology. Renal Physiology*, 290(3):F572–9.
- Bamforth, S. D., Kniesel, U., Wolburg, H., Engelhardt, B., and Risau, W. (1999). A dominant mutant of occludin disrupts tight junction structure and function. *Journal of Cell Science*, 112 (Pt 12):1879–88.
- Banerjee, R. K. and Datta, A. G. (1983). Proteoliposome as the model for the study of membrane-bound enzymes and transport proteins. *Molecular and Cellular Biochemistry*, 50(1):3–15.

- Barker, G. and Simmons, N. L. (1981). Identification of two strains of cultured canine renal epithelial cells (MDCK cells) which display entirely different physiological properties. *Quarterly Journal of Experimental Physiology*, 66(1):61–72.
- Baumgartner, W., Hinterdorfer, P., Ness, W., Raab, A., Vestweber, D., Schindler, H., and Drenckhahn, D. (2000). Cadherin interaction probed by atomic force microscopy. *Proceedings of the National Academy of Sciences of the United States of America*, 97(8):4005–10.
- Bazzoni, G., Martinez-Estrada, O. M., Orsenigo, F., Cordenonsi, M., Citi, S., and Dejana, E. (2000). Interaction of junctional adhesion molecule with the tight junction components ZO-1, cingulin, and occludin. *Journal of Biological Chemistry*, 275(27):20520–6.
- Ben-Yosef, T., Belyantseva, I. A., Saunders, T. L., Hughes, E. D., Kawamoto, K., Van Itallie, C. M., Beyer, L. A., Halsey, K., Gardner, D. J., Wilcox, E. R., Rasmussen, J., Anderson, J. M., Dolan, D. F., Forge, A., Raphael, Y., Camper, S. A., and Friedman, T. B. (2003). Claudin 14 knockout mice, a model for autosomal recessive deafness DFNB29, are deaf due to cochlear hair cell degeneration. *Human Molecular Genetics*, 12(16):2049–61.
- Benoit, M. and Gaub, H. E. (2002). Measuring cell adhesion forces with the atomic force microscope at the molecular level. *Cells Tissues Organs*, 172(3):174–89.
- Berg, T. (2003). Modulation of protein-protein interactions with small organic molecules. *Angewandte Chemie*, 42(22):2462–81.
- Bhat, M., Toledo-Velasquez, D., Wang, L., Malanga, C. J., Ma, J. K., and Rojanasakul, Y. (1993). Regulation of tight junction permeability by calcium mediators and cell cytoskeleton in rabbit tracheal epithelium. *Pharmaceutical Research*, 10(7):991–7.
- Birnie, G. D. and Rickwood, D. (1978). *Centrifugal separations in molecular and cell biology*. Butterworths, London.
- Blaschuk, O. W., Oshima, T., Gour, B. J., Symonds, J. M., Park, J. H., Kevil, C. G., Trocha, S. D., Michaud, S., Okayama, N., Elrod, J. W., Alexander, J. S., and Sasaki, M. (2002). Identification of an occludin cell adhesion recognition sequence. *Inflammation*, 26(4):193–8.
- Blasig, I. E., Winkler, L., Lassowski, B., Mueller, S. L., Zuleger, N., Krause, E., Krause, G., Gast, K., Kolbe, M., and Piontek, J. (2006). On the self-association potential of transmembrane tight junction proteins. *Cellular and Molecular Life Sciences*, 63(4):505–14.
- Boeckmann, B., Bairoch, A., Apweiler, R., Blatter, M. C., Estreicher, A., Gasteiger, E., Martin, M. J., Michoud, K., O'Donovan, C., Phan, I., Pilbout, S., and Schneider, M. (2003). The SWISS-PROT protein knowledgebase and its supplement TrEMBL in 2003. *Nucleic Acids Research*, 31(1):365–70.
- Bollag, D. M., Rozycki, M. D., and Edelman, S. J. (1996). *Protein methods*. Wiley-Liss, New York, 2nd edition.

- Boulenc, X., Marti, E., Joyeux, H., Roques, C., Berger, Y., and Fabre, G. (1993). Importance of the paracellular pathway for the transport of a new bisphosphonate using the human Caco-2 monolayers model. *Biochemical Pharmacology*, 46(9):1591–600.
- Bradley, M. K. (1990). Overexpression of proteins in eukaryotes. *Methods in Enzymology*, 182:112–32.
- Braun, A., Hämmerle, S., Suda, K., Rothen-Rutishauser, B., Günthert, M., Krämer, S. D., Wunderli-Allenspach, H., and Braun, A. (2000). Cell cultures as tools in biopharmacy. *European Journal of Pharmaceutical Sciences*, 11 Suppl 2:S51–60.
- Briske-Anderson, M. J., Finley, J. W., and Newman, S. M. (1997). The influence of culture time and passage number on the morphological and physiological development of Caco-2 cells. *Proceedings of the Society for Experimental Biology and Medicine*, 214(3):248–57.
- Calderon, V., Lazaro, A., Contreras, R. G., Shoshani, L., Flores-Maldonado, C., Gonzalez-Mariscal, L., Zampighi, G., and Cereijido, M. (1998). Tight junctions and the experimental modifications of lipid content. *Journal of Membrane Biology*, 164(1):59–69.
- Cardellini, P., Davanzo, G., and Citi, S. (1996). Tight junctions in early amphibian development: detection of junctional cingulin from the 2-cell stage and its localization at the boundary of distinct membrane domains in dividing blastomeres in low calcium. *Developmental Dynamics*, 207(1):104–13.
- Carlson, S. S., Wagner, J. A., and Kelly, R. B. (1978). Purification of synaptic vesicles from elasmobranch electric organ and the use of biophysical criteria to demonstrate purity. *Biochemistry*, 17(7):1188–99.
- Casals, E., Verdaguer, A., Tonda, R., Galan, A., Escolar, G., and Estelrich, J. (2003). Atomic force microscopy of liposomes bearing fibrinogen. *Bioconjugate Chemistry*, 14(3):593–600.
- Cereijido, M. and Anderson, J. M. (2001). *Tight junctions*. CRC Press, New York, 2nd edition.
- Cereijido, M., Robbins, E. S., Dolan, W. J., Rotunno, C. A., and Sabatini, D. D. (1978). Polarized monolayers formed by epithelial cells on a permeable and translucent support. *Journal of Cell Biology*, 77(3):853–80.
- Chalfie, M., Tu, Y., Euskirchen, G., Ward, W. W., and Prasher, D. C. (1994). Green fluorescent protein as a marker for gene expression. *Science*, 263(5148):802–5.
- Chan, W. and Chan, W. C. (2000). *Fmoc solid phase peptide synthesis. A practical approach*. Oxford University Press, Nottingham.
- Chao, A. C., Vu Nguyen, J., Broughall, M., Griffin, A., Fix, J. A., and Daddona, P. E. (1999). In vitro and in vivo evaluation of effects of sodium caprate on enteral peptide absorption and on mucosal morphology. *International Journal of Pharmaceutics*, 191:15–24.

- Che, Y., Brooks, B. R., and Marshall, G. R. (2006). Development of small molecules designed to modulate protein-protein interactions. *Journal of Computer-Aided Molecular Design*, 20(2):109–30.
- Chen, Y. H., Lu, Q., Goodenough, D. A., and Jeansonne, B. (2002). Nonreceptor tyrosine kinase c-Yes interacts with occludin during tight junction formation in canine kidney epithelial cells. *Molecular Biology of the Cell*, 13(4):1227–37.
- Cho, M. J., Thompson, D. P., Cramer, C. T., Vidmar, T. J., and Scieszka, J. F. (1989). The Madin Darby canine kidney (MDCK) epithelial cell monolayer as a model cellular transport barrier. *Pharmaceutical Research*, 6(1):71–7.
- Chudakov, D. M., Lukyanov, S., and Lukyanov, K. A. (2005). Fluorescent proteins as a toolkit for in vivo imaging. *Trends in Biotechnology*, 23(12):605–13.
- Chung, P. N., Mruk, D., Mo, M., Lee, M. W., and Cheng, C. Y. (2001). A 22-amino acid synthetic peptide corresponding to the second extracellular loop of rat occludin perturbs the blood-testis barrier and disrupts spermatogenesis reversibly in vivo. *Biology of Reproduction*, 65:1340–1351.
- Ciccarone, V. C., Polayes, D., and Luckow, V. A. (1997). Generation of recombinant baculovirus DNA in *E. coli* using a baculovirus shuttle vector. In *Methods in molecular medicine*. Humana Press, Totowa, New Jersey.
- Citi, S. (1992). Protein kinase inhibitors prevent junction dissociation induced by low extracellular calcium in MDCK epithelial cells. *Journal of Cell Biology*, 117(1):169–78.
- Citi, S. and Denisenko, N. (1995). Phosphorylation of the tight junction protein cingulin and the effects of protein kinase inhibitors and activators in MDCK epithelial cells. *Journal of Cell Science*, 108(Pt 8):2917–26.
- Citi, S., Sabanay, H., Jakes, R., Geiger, B., and Kendrick-Jones, J. (1988). Cingulin, a new peripheral component of tight junctions. *Nature*, 333(6170):272–6.
- Citi, S., Sabanay, H., Kendrick-Jones, J., and Geiger, B. (1989). Cingulin: characterization and localization. *Journal of Cell Science*, 93(Pt 1):107–22.
- Colegio, O., Van Itallie, C. M., McCrea, H. J., Rahner, C., and Anderson, J. M. (2002). Claudins create charge-selective channels in the paracellular pathway between epithelial cells. *American Journal of Physiology. Cell Physiology*, 283(1):C142–7.
- Colegio, O. R., Van Itallie, C., Rahner, C., and Anderson, J. M. (2003). Claudin extracellular domains determine paracellular charge selectivity and resistance but not tight junction fibril architecture. *American Journal of Physiology. Cell Physiology*, 284(6):C1346–54.
- Cordenonsi, M., D'Atri, F., Hammar, E., Parry, A. D. D., Kendrick-Jones, J., Shore, D., and Citi, S. (1999a). Cingulin contains globular and coiled-coil domains and interacts with ZO-1, ZO-2, ZO-3, and myosin. *Journal of Cell Biology*, 147(7):1569–1581.

- Cordenonsi, M., Turco, F., D'Atri, F., Hammar, E., Meggio, F., and Citi, S. (1999b). *Xenopus laevis* occludin. Identification of in vitro phosphorylation sites by protein kinase CK2 and association with cingulin. *European Journal of Biochemistry*, 264:374–384.
- Cormack, B. P., Valdivia, R. H., and Falkow, S. (1996). FACS-optimized mutants of the green fluorescent protein (GFP). *Gene*, 173(1 Spec No):33–8.
- Dahl, G., Nonner, W., and Werner, R. (1994). Attempts to define functional domains of gap junction proteins with synthetic peptides. *Biophysical Journal*, 67(5):1816–22.
- D'Atri, F. and Citi, S. (2001). Cingulin interacts with F-actin in vitro. *FEBS letters*, 507:21–24.
- D'Atri, F., Nadalutti, F., and Citi, S. (2002). Evidence for a functional interaction between cingulin and ZO-1 in cultured cells. *Journal of Biological Chemistry*, 277(31):27757–64.
- Davis, J. M., Tsou, L. K., and Hamilton, A. D. (2007). Synthetic non-peptide mimetics of alpha-helices. *Chemical Society Reviews*, 36(2):326–34.
- de Oliveira, S. S., de Oliveira, I. M., De Souza, W., and Morgado-Diaz, J. A. (2005). Claudins upregulation in human colorectal cancer. *FEBS Letters*, 579(27):6179–85.
- de Oliveira, S. S. and Morgado-Diaz, J. A. (2007). Claudins: multifunctional players in epithelial tight junctions and their role in cancer. *Cellular and Molecular Life Sciences*, 64(1):17–28.
- Dragsten, P. R., Blumenthal, R., and Handler, J. S. (1981). Membrane asymmetry in epithelia: is the tight junction a barrier to diffusion in the plasma membrane? *Nature*, 294(5843):718–22.
- Duizer, E., van der Wulp, C., Versantvoort, C. H., and Groten, J. P. (1998). Absorption enhancement, structural changes in tight junctions and cytotoxicity caused by palmitoyl carnitine in Caco-2 and IEC-18 cells. *Journal of Pharmacology and Experimental Therapeutics*, 287(1):395–402.
- Ebihara, C., Kondoh, M., Hasuike, N., Harada, M., Mizuguchi, H., Horiguchi, Y., Fujii, M., and Watanabe, Y. (2006). Preparation of a claudin-targeting molecule using a C-terminal fragment of *Clostridium perfringens* enterotoxin. *Journal of Pharmacology and Experimental Therapeutics*, 316(1):255–60.
- Ebnet, K., Schulz, C. U., Meyer Zu Brickwedde, M. K., Pendl, G. G., and Vestweber, D. (2000). Junctional adhesion molecule interacts with the PDZ domain-containing proteins AF-6 and ZO-1. *Journal of Biological Chemistry*, 275(36):27979–88.
- Erdlenbruch, B., Jendrossek, V., Eibl, H., and Lakomek, M. (2000). Transient and controllable opening of the blood-brain barrier to cytostatic and antibiotic agents by alkylglycerols in rats. *Experimental Brain Research*, 135(3):417–22.

- Everett, R. S., Vanhook, M. K., Barozzi, N., Toth, I., and Johnson, L. G. (2006). Specific modulation of airway epithelial tight junctions by apical application of an occludin peptide. *Molecular Pharmacology*, 69(2):492–500.
- Eytan, G. D. (1982). Use of liposomes for reconstitution of biological functions. *Biochimica et Biophysica Acta*, 694(2):185–202.
- Fanning, A. S., Jameson, B. J., Jesaitis, L. A., and Anderson, J. M. (1998). The tight junction protein ZO-1 establishes a link between the transmembrane protein occludin and the actin cytoskeleton. *Journal of Biological Chemistry*, 273(45):29745–53.
- Fanning, A. S., Little, B. P., Rahner, C., Utepbergenov, D., Walther, Z., and Anderson, J. M. (2007). The unique-5 and -6 motifs of ZO-1 regulate tight junction strand localization and scaffolding properties. *Molecular Biology of the Cell*, 18(3):721–31.
- Fanning, A. S., Mitic, L. L., and Anderson, J. M. (1999). Transmembrane proteins in the tight junction barrier. *Journal of the American Society of Nephrology*, 10(6):1337–45.
- Farquhar, M. G. and Palade, G. E. (1963). Junctional complexes in various epithelia. *Journal of Cell Biology*, 17:375–412.
- Farshori, P. and Kachar, B. (1999). Redistribution and phosphorylation of occludin during opening and resealing of tight junctions in cultured epithelial cells. *Journal of Membrane Biology*, 170(2):147–56.
- Fasano, A. (1998). Modulation of intestinal permeability: an innovative method of oral drug delivery for the treatment of inherited and acquired human diseases. *Molecular Genetics and Metabolism*, 64(1):12–8.
- Fesenko, I., Kurth, T., Sheth, B., Fleming, T. P., Citi, S., and Hausen, P. (2000). Tight junction biogenesis in the early *Xenopus* embryo. *Mechanisms of Development*, 96(1):51–65.
- Findlay, J. B. C. and Evans, W. H., editors (1987). *Biological membranes: a practical approach*. IRL Press, Oxford.
- Fleming, T. P., Hay, M., Javed, Q., and Citi, S. (1993). Localisation of tight junction protein cingulin is temporally and spatially regulated during early mouse development. *Development*, 117:1135–44.
- Fourneau, J. M., Cohen, H., and van Endert, P. M. (2004). A chaperone-assisted high yield system for the production of HLA-DR4 tetramers in insect cells. *Journal of immunological methods*, 285(2):253–64.
- Fujibe, M., Chiba, H., Kojima, T., Soma, T., Wada, T., Yamashita, T., and Sawada, N. (2004). Thr203 of claudin-1, a putative phosphorylation site for MAP kinase, is required to promote the barrier function of tight junctions. *Experimental Cell Research*, 295(1):36–47.

- Fujita, K., Katahira, J., Horiguchi, Y., Sonoda, N., Furuse, M., and Tsukita, S. (2000). Clostridium perfringens enterotoxin binds to the second extracellular loop of claudin-3, a tight junction integral membrane protein. *FEBS Letters*, 476(3):258–61.
- Funke, L., Dakoji, S., and Bretz, D. S. (2005). Membrane-associated guanylate kinases regulate adhesion and plasticity at cell junctions. *Annual Review of Biochemistry*, 74:219–45.
- Furuse, M. (2002). Claudin-based tight junctions are crucial for the mammalian epidermal barrier: a lesson from claudin-1-deficient mice. *Journal of Cell Biology*, 156:1099–1111.
- Furuse, M., Fujita, K., Hiiragi, T., Fujimoto, K., and Tsukita, S. (1998a). Claudin-1 and -2: novel integral membrane proteins localizing at tight junctions with no sequence similarity to occludin. *Journal of Cell Biology*, 141(7):1539–50.
- Furuse, M., Furuse, K., Sasaki, H., and Tsukita, S. (2001). Conversion of zonulae occludentes from tight to leaky strand type by introducing claudin-2 into Madin-Darby canine kidney I cells. *Journal of Cell Biology*, 153(2):263–72.
- Furuse, M., Hirase, T., Itoh, M., Nagafuchi, A., Yonemura, S., and Tsukita, S. (1993). Occludin: a novel integral membrane protein localizing at tight junctions. *Journal of Cell Biology*, 123(6 Pt 2):1777–88.
- Furuse, M., Itoh, M., Hirase, T., Nagafuchi, A., Yonemura, S., and Tsukita, S. (1994). Direct association of occludin with ZO-1 and its possible involvement in the localization of occludin at tight junctions. *Journal of Cell Biology*, 127(6 Pt 1):1617–26.
- Furuse, M., Sasaki, H., Fujimoto, K., and Tsukita, S. (1998b). A single gene product, claudin-1 or -2, reconstitutes tight junction strands and recruits occludin in fibroblasts. *Journal of Cell Biology*, 143(2):391–401.
- Furuse, M., Sasaki, H., and Tsukita, S. (1999). Manner of interaction of heterogeneous claudin species within and between tight junction strands. *Journal of Cell Biology*, 147(4):891–903.
- Garrod, D., Chidgey, M., and North, A. (1996). Desmosomes: differentiation, development, dynamics and disease. *Current Opinion in Cell Biology*, 8(5):670–8.
- Gaush, C. R., Hard, W. L., and Smith, T. F. (1966). Characterization of an established line of canine kidney cells (MDCK). *Proceedings of the Society for Experimental Biology and Medicine*, 122(3):931–5.
- Geisse, S. and Kocher, H. P. (1999). Protein expression in mammalian and insect cell systems. *Methods in Enzymology*, 306:19–42.
- Ghassemifar, M. R., Sheth, B., Papenbrock, T., Leese, H. J., Houghton, F. D., and Fleming, T. P. (2002). Occludin TM4(-): an isoform of the tight junction protein present in primates lacking the fourth transmembrane domain. *Journal of Cell Science*, 115(Pt 15):3171–80.

- Ghoshroy, S., Goodenough, D. A., and Sosinsky, G. E. (1995). Preparation, characterization, and structure of half gap junctional layers split with urea and EGTA. *Journal of Membrane Biology*, 146(1):15–28.
- Gibbons, W. A., Huges, R. A., Charalambous, M., Christodoulou, M., Szeto, A., Aulabaugh, A. E., Mascagni, P., and Toth, I. (1990). Synthesis, resolution and structural elucidation of lipidic amino acids and their homo- and hetero-oligomers. *Liebig's Annals of Chemistry*, 1990:1175–1183.
- Gonzalez-Mariscal, L., Betanzos, A., and Avila-Flores, A. (2000). MAGUK proteins: structure and role in the tight junction. *Seminars in Cell and Developmental Biology*, 11(4):315–24.
- Gonzalez-Mariscal, L., Betanzos, A., Nava, P., and Jaramillo, B. E. (2003). Tight junction proteins. *Progress in Biophysics and Molecular Biology*, 81:1–44.
- Gonzalez-Mariscal, L., Islas, S., Contreras, R. G., Garcia-Villegas, M. R., Betanzos, A., Vega, J., Diaz-Quinonez, A., Martin-Orozco, N., Ortiz-Navarrete, V., Cereijido, M., and Valdes, J. (1999). Molecular characterization of the tight junction protein ZO-1 in MDCK cells. *Experimental Cell Research*, 248(1):97–109.
- Gonzalez-Ros, J. M., Paraschos, A., Farach, M. C., and Martinez-Carrion, M. (1981). Characterization of acetylcholine receptor isolated from *Torpedo californica* electroplax through the use of an easily removable detergent, beta-D-octylglucopyranoside. *Biochimica et Biophysica Acta*, 643(2):407–20.
- Goodenough, D. A., Goliger, J. A., and Paul, D. L. (1996). Connexins, connexons, and intercellular communication. *Annual Review of Biochemistry*, 65:475–502.
- Gottardi, C. J., Arpin, M., Fanning, A. S., and Louvard, D. (1996). The junction-associated protein, zonula occludens-1, localizes to the nucleus before the maturation and during the remodeling of cell-cell contacts. *Proceedings of the National Academy of Sciences of the United States of America*, 93(20):10779–84.
- Gottschalk, I., Lagerquist, C., Zuo, S. S., Lundqvist, A., and Lundahl, P. (2002). Immobilized-biomembrane affinity chromatography for binding studies of membrane proteins. *Journal of Chromatography B*, 768(1):31–40.
- Gow, A., Southwood, C. M., Li, J. S., Pariali, M., Riordan, G. P., Brodie, S. E., Danias, J., Bronstein, J. M., Kachar, B., and Lazzarini, R. A. (1999). CNS myelin and Sertoli cell tight junction strands are absent in *Osp/claudin-11* null mice. *Cell*, 99(6):649–59.
- Guillemot, L. and Citi, S. (2006). Cingulin regulates claudin-2 expression and cell proliferation through the small GTPase RhoA. *Molecular Biology of the Cell*, 17(8):3569–77.
- Guillemot, L., Hammar, E., Kaister, C., Ritz, J., Caille, D., Jond, L., Bauer, C., Meda, P., and Citi, S. (2004). Disruption of the cingulin gene does not prevent tight junction formation but alters gene expression. *Journal of Cell Science*, 117(Pt 22):5245–56.

- Gumbiner, B., Lowenkopf, T., and Apatira, D. (1991). Identification of a 160-kDa polypeptide that binds to the tight junction protein ZO-1. *Proceedings of the National Academy of Sciences of the United States of America*, 88(8):3460–4.
- Gumbiner, B. M. (1996). Cell adhesion: the molecular basis of tissue architecture and morphogenesis. *Cell*, 84(3):345–57.
- Haas, J., Park, E. C., and Seed, B. (1996). Codon usage limitation in the expression of HIV-1 envelope glycoprotein. *Current Biology*, 6(3):315–24.
- Hamazaki, Y., Itoh, M., Sasaki, H., Furuse, M., and Tsukita, S. (2002). Multi-PDZ domain protein 1 (MUPP1) is concentrated at tight junctions through its possible interaction with claudin-1 and junctional adhesion molecule. *Journal of Biological Chemistry*, 277(1):455–61.
- Hammond, J. R. and Zarenda, M. (1996). Effect of detergents on ligand binding and translocation activities of solubilized/reconstituted nucleoside transporters. *Archives of Biochemistry and Biophysics*, 332(2):313–22.
- Harada, M., Kondoh, M., Ebihara, C., Takahashi, A., Komiya, E., Fujii, M., Mizuguchi, H., Tsunoda, S., Horiguchi, Y., Yagi, K., and Watanabe, Y. (2007). Role of tyrosine residues in modulation of claudin-4 by the C-terminal fragment of Clostridium perfringens enterotoxin. *Biochemical Pharmacology*, 73(2):206–14.
- Haskins, J., Gu, L., Wittchen, E. S., Hibbard, J., and Stevenson, B. R. (1998). ZO-3, a novel member of the MAGUK protein family found at the tight junction, interacts with ZO-1 and occludin. *Journal of Cell Biology*, 141(1):199–208.
- Helenius, A., McCaslin, D. R., Fries, E., and Tanford, C. (1979). Properties of detergents. *Methods in Enzymology*, 56:734–49.
- Herve, J. C., Bourmeyster, N., and Sarrouilhe, D. (2004). Diversity in protein-protein interactions of connexins: emerging roles. *Biochimica et Biophysica Acta*, 1662(1-2):22–41.
- Hidalgo, I. J. and Li, J. (1996). Carrier-mediated transport and efflux mechanisms in Caco-2 cells. *Advanced Drug Delivery Reviews*, 22:53–66.
- Higgins, M. K., Demir, M., and Tate, C. G. (2003). Calnexin co-expression and the use of weaker promoters increase the expression of correctly assembled Shaker potassium channel in insect cells. *Biochimica et Biophysica Acta*, 1610(1):124–32.
- Hirase, T., Kawashima, S., Wong, E. Y., Ueyama, T., Rikitake, Y., Tsukita, S., Yokoyama, M., and Staddon, J. M. (2001). Regulation of tight junction permeability and occludin phosphorylation by RhoA-p160ROCK-dependent and -independent mechanisms. *Journal of Biological Chemistry*, 276(13):10423–31.

- Ho, N., Raub, T., Burton, P., Barsuhn, C., Adson, A., Audus, K., and Borchardt, R. (2000). Quantitative approaches to delineate passive transport mechanisms in cell culture monolayers. In *Transport processes in pharmaceutical systems*. Marcel Dekker.
- Hoevel, T., Macek, R., Mundigl, O., Swisshelm, K., and Kubbies, M. (2002). Expression and targeting of the tight junction protein CLDN1 in CLDN1-negative human breast tumor cells. *Journal of Cellular Physiology*, 191(1):60–8.
- Hrycyna, C. A., Ramachandra, M., Pastan, I., and Gottesman, M. M. (1998). Functional expression of human P-glycoprotein from plasmids using vaccinia virus-bacteriophage T7 RNA polymerase system. *Methods in Enzymology*, 292:456–73.
- Hunter, J., Jepson, M. A., Tsuruo, T., Simmons, N. L., and Hirst, B. H. (1993). Functional expression of P-glycoprotein in apical membranes of human intestinal Caco-2 cells. Kinetics of vinblastine secretion and interaction with modulators. *Journal of Biological Chemistry*, 268(20):14991–7.
- Iacobuzio-Donahue, C. A., Maitra, A., Shen-Ong, G. L., van Heek, T., Ashfaq, R., Meyer, R., Walter, K., Berg, K., Hollingsworth, M. A., Cameron, J. L., Yeo, C. J., Kern, S. E., Goggins, M., and Hruban, R. H. (2002). Discovery of novel tumor markers of pancreatic cancer using global gene expression technology. *American Journal of Pathology*, 160(4):1239–49.
- Ikenouchi, J., Furuse, M., Furuse, K., Sasaki, H., Tsukita, S., and Tsukita, S. (2005). Tricellulin constitutes a novel barrier at tricellular contacts of epithelial cells. *Journal of Cell Biology*, 171(6):939–45.
- Irvine, J. D., Takahashi, L., Lockhart, K., Cheong, J., Tolan, J. W., Selick, H. E., and Grove, R. (1999). MDCK (Madin-Darby Canine Kidney) cells: a tool for membrane permeability screening. *Journal of Pharmaceutical Sciences*, 88(1):28–32.
- Itoh, M., Furuse, M., Morita, K., Kubota, K., Saitou, M., and Tsukita, S. (1999a). Direct binding of three tight junction-associated MAGUKs, ZO-1, ZO-2, and ZO-3, with the COOH termini of claudins. *Journal of Cell Biology*, 147(6):1351–63.
- Itoh, M., Morita, K., and Tsukita, S. (1999b). Characterization of ZO-2 as a MAGUK family member associated with tight as well as adherens junctions with a binding affinity to occludin and alpha catenin. *Journal of Biological Chemistry*, 274(9):5981–6.
- Itoh, M., Nagafuchi, A., Yonemura, S., Kitani-Yasuda, T., Tsukita, S., and Tsukita, S. (1993). The 220-kD protein colocalizing with cadherins in non-epithelial cells is identical to ZO-1, a tight junction-associated protein in epithelial cells: cDNA cloning and immunoelectron microscopy. *Journal of Cell Biology*, 121(3):491–502.
- IUPAC-IUB (1984). Joint commission on biochemical nomenclature (JCBN). Nomenclature and symbolism for amino acids and peptides. Recommendations 1983. *European Journal of Biochemistry*, 138(1):9–37.

- Ivanov, A. I., McCall, I. C., Parkos, C. A., and Nusrat, A. (2004a). Role for actin filament turnover and a myosin II motor in cytoskeleton-driven disassembly of the epithelial apical junctional complex. *Molecular Biology of the Cell*, 15(6):2639–51.
- Ivanov, A. I., Nusrat, A., and Parkos, C. A. (2004b). Endocytosis of epithelial apical junctional proteins by a clathrin-mediated pathway into a unique storage compartment. *Molecular Biology of the Cell*, 15(1):176–88.
- Jass, J., Tjarnhage, T., and Puu, G. (2000). From liposomes to supported, planar bilayer structures on hydrophilic and hydrophobic surfaces: an atomic force microscopy study. *Biophysical Journal*, 79(6):3153–63.
- Jeansonne, B., Lu, Q., Goodenough, D. A., and Chen, Y. H. (2003). Claudin-8 interacts with multi-PDZ domain protein 1 (MUPP1) and reduces paracellular conductance in epithelial cells. *Cellular and Molecular Biology*, 49(1):13–21.
- Jesaitis, L. A. and Goodenough, D. A. (1994). Molecular characterization and tissue distribution of ZO-2, a tight junction protein homologous to ZO-1 and the Drosophila discs-large tumor suppressor protein. *Journal of Cell Biology*, 124(6):949–61.
- Kachar, B. and Reese, T. S. (1982). Evidence for the lipidic nature of tight junction strands. *Nature*, 296(5856):464–6.
- Kam, Y., Kim, D. Y., Koo, S. K., and Joe, C. O. (1998). Transfer of second messengers through gap junction connexin 43 channels reconstituted in liposomes. *Biochimica et Biophysica Acta*, 1372(2):384–8.
- Kamboj, R. K., Garipey, J., and Siu, C. H. (1989). Identification of an octapeptide involved in homophilic interaction of the cell adhesion molecule gp80 of Dictyostelium discoideum. *Cell*, 59(4):615–25.
- Katahira, J., Inoue, N., Horiguchi, Y., Matsuda, M., and Sugimoto, N. (1997). Molecular cloning and functional characterization of the receptor for Clostridium perfringens enterotoxin. *Journal of Cell Biology*, 136(6):1239–47.
- Kato, T., Murata, T., Usui, T., and Park, E. Y. (2005). Improvement of the production of GFPuv-beta1,3-N-acetylglucosaminyltransferase 2 fusion protein using a molecular chaperone-assisted insect-cell-based expression system. *Biotechnology and Bioengineering*, 89(4):424–33.
- Kawabe, H., Nakanishi, H., Asada, M., Fukuhara, A., Morimoto, K., Takeuchi, M., and Takai, Y. (2001). Pilt, a novel peripheral membrane protein at tight junctions in epithelial cells. *Journal of Biological Chemistry*, 276(51):48350–5.
- Keon, B. H., Schafer, S., Kuhn, C., Grund, C., and Franke, W. W. (1996). Symplekin, a novel type of tight junction plaque protein. *Journal of Cell Biology*, 134(4):1003–18.

- Kieber-Emmons, T., Murali, R., and Greene, M. I. (1997). Therapeutic peptides and peptidomimetics. *Current Opinion in Biotechnology*, 8:435–441.
- Kioukia, N., Nienow, A. W., Emery, A. N., and al Rubeai, M. (1995). Physiological and environmental factors affecting the growth of insect cells and infection with baculovirus. *Journal of Biotechnology*, 38(3):243–51.
- Kitajiri, S., Miyamoto, T., Mineharu, A., Sonoda, N., Furuse, K., Hata, M., Sasaki, H., Mori, Y., Kubota, T., Ito, J., Furuse, M., and Tsukita, S. (2004). Compartmentalization established by claudin-11-based tight junctions in stria vascularis is required for hearing through generation of endocochlear potential. *Journal of Cell Science*, 117(Pt 21):5087–96.
- Kominsky, S. L., Argani, P., Korz, D., Evron, E., Raman, V., Garrett, E., Rein, A., Sauter, G., Kallioniemi, O. P., and Sukumar, S. (2003). Loss of the tight junction protein claudin-7 correlates with histological grade in both ductal carcinoma in situ and invasive ductal carcinoma of the breast. *Oncogene*, 22(13):2021–33.
- Kondoh, M., Masuyama, A., Takahashi, A., Asano, N., Mizuguchi, H., Koizumi, N., Fujii, M., Hayakawa, T., Horiguchi, Y., and Watanbe, Y. (2005). A novel strategy for the enhancement of drug absorption using a claudin modulator. *Molecular Pharmacology*, 67(3):749–56.
- Kosemund, K., Geiger, I., and Paulsen, H. (2000). Insertion of light-harvesting chlorophyll a/b protein into the thylakoid topographical studies. *European Journal of Biochemistry*, 267(4):1138–45.
- Koval, M. (2006). Claudins—key pieces in the tight junction puzzle. *Cell Communication and Adhesion*, 13(3):127–38.
- Kramer, F., White, K., Kubbies, M., Swisshelm, K., and Weber, B. H. (2000). Genomic organization of claudin-1 and its assessment in hereditary and sporadic breast cancer. *Human Genetics*, 107(3):249–56.
- Krämer, S. D., Abbot, N. J., and Begley, D. J. (2001). Biological models to study blood-brain barrier permeation. In *Pharmacokinetic Optimization in Drug Research: Biological, Physicochemical and Computational Strategies*. Wiley-VCH, Weinheim.
- Kumar, N. M. and Gilula, N. B. (1996). The gap junction communication channel. *Cell*, 84(3):381–8.
- Kyte, J. and Doolittle, R. F. (1982). A simple method for displaying the hydropathic character of a protein. *Journal of Molecular Biology*, 157(1):105–32.
- Lacaz-Vieira, F., Jaeger, M. M., Farshori, P., and Kachar, B. (1999). Small synthetic peptides homologous to segments of the first external loop of occludin impair tight junction resealing. *Journal of Membrane Biology*, 168(3):289–97.

- Laemmli, U. K. (1970). Cleavage of structural proteins during the assembly of the head of bacteriophage T4. *Nature*, 227(5259):680–5.
- Langbein, L., Grund, C., Kuhn, C., Praetzel, S., Kartenbeck, J., Brandner, J. M., Moll, I., and Franke, W. W. (2002). Tight junctions and compositionally related junctional structures in mammalian stratified epithelia and cell cultures derived therefrom. *European Journal of Cell Biology*, 81(8):419–35.
- Latham, P. W. (1999). Therapeutic peptides revisited. *Nature Biotechnology*, 17(8):755–757.
- Lechner, F., Sahrbacher, U., Suter, T., Frei, K., Brockhaus, M., Koedel, U., and Fontana, A. (2000). Antibodies to the junctional adhesion molecule cause disruption of endothelial cells and do not prevent leukocyte influx into the meninges after viral or bacterial infection. *The Journal of Infectious Diseases*, 182(3):978–82.
- LeCluyse, E. and Sutton, S. C. (1997). In vitro models for selection of development candidates. permeability studies to define mechanisms of absorption enhancement. *Advanced Drug Delivery Reviews*, 23:163–183.
- Lee, H. B., Xu, L., and Meissner, G. (1994). Reconstitution of the skeletal muscle ryanodine receptor-calcium release channel protein complex into proteoliposomes. *Journal of Biological Chemistry*, 269(18):13305–12.
- Lee, S. H. and Altenberg, G. A. (2003). Expression of functional multidrug-resistance protein 1 in *Saccharomyces cerevisiae*: effects of N- and C-terminal affinity tags. *Biochemical and Biophysical Research Communications*, 306(3):644–9.
- Lehrman, S. R., Tuls, J. L., and Lund, M. (1990). Peptide alpha-helicity in aqueous trifluoroethanol: correlations with predicted alpha-helicity and the secondary structure of the corresponding regions of bovine growth hormone. *Biochemistry*, 29(23):5590–6.
- Levy, D., Gulik, A., Bluzat, A., and Rigaud, J. L. (1992). Reconstitution of the sarcoplasmic reticulum Ca(2+)-ATPase: mechanisms of membrane protein insertion into liposomes during reconstitution procedures involving the use of detergents. *Biochimica et Biophysica Acta*, 1107(2):283–98.
- Licari, P. and Bailey, J. E. (1991). Factors influencing recombinant protein yields in an insect cell-baculovirus expression system: multiplicity of infection and intracellular protein degradation. *Biotechnology and Bioengineering*, 37:238–246.
- Lindhardt, K. and Bechgaard, E. (2003). Sodium glycocholate transport across Caco-2 cell monolayers, and the enhancement of mannitol transport relative to transepithelial electrical resistance. *International Journal of Pharmaceutics*, 252:181–186.
- Liu, D. Z., LeCluyse, E., and Thakker, D. R. (1999). Dodecylphosphocholine-mediated enhancement of paracellular permeability and cytotoxicity in Caco-2 cell monolayers. *Journal of Pharmaceutical Sciences*, 88(11):1169–74.

- Lowry, O. H., Rosebrough, N. J., Farr, A. L., and Randall, R. J. (1951). Protein measurement with the Folin phenol reagent. *Journal of Biological Chemistry*, 193(1):265–75.
- Madara, J. L. (1998). Regulation of the movement of solutes across tight junctions. *Annual Review of Physiology*, 60:143–59.
- Makowski, L., Caspar, D. L., Phillips, W. C., and Goodenough, D. A. (1977). Gap junction structures. II. analysis of the x-ray diffraction data. *Journal of Cell Biology*, 74(2):629–45.
- Mankertz, J., Waller, J. S., Hillenbrand, B., Tavalali, S., Florian, P., Schoneberg, T., Fromm, M., and Schulzke, J. D. (2002). Gene expression of the tight junction protein occludin includes differential splicing and alternative promoter usage. *Biochemical and Biophysical Research Communications*, 298(5):657–66.
- Martin-Padura, I., Lostaglio, S., Schneemann, M., Williams, L., Romano, M., Fruscella, P., Panzeri, C., Stoppacciaro, A., Ruco, L., Villa, A., Simmons, D., and Dejana, E. (1998). Junctional adhesion molecule, a novel member of the immunoglobulin superfamily that distributes at intercellular junctions and modulates monocyte transmigration. *Journal of Cell Biology*, 142(1):117–27.
- Martinez-Palomo, A., Meza, I., Beaty, G., and Cereijido, M. (1980). Experimental modulation of occluding junctions in a cultured transporting epithelium. *Journal of Cell Biology*, 87(3 Pt 1):736–45.
- Matsuda, M., Kubo, A., Furuse, M., and Tsukita, S. (2004). A peculiar internalization of claudins, tight junction-specific adhesion molecules, during the intercellular movement of epithelial cells. *Journal of Cell Science*, 117(Pt 7):1247–57.
- Matter, K., Aijaz, S., Tsapara, A., and Balda, M. S. (2005). Mammalian tight junctions in the regulation of epithelial differentiation and proliferation. *Current Opinion in Cell Biology*, 17(5):453–8.
- McCarthy, K. M., Skare, I. B., Stankewich, M. C., Furuse, M., Tsukita, S., Rogers, R. A., Lynch, R. D., and Schneeberger, E. E. (1996). Occludin is a functional component of the tight junction. *Journal of Cell Science*, 109(Pt 9):2287–98.
- McClane, B. A., Hanna, P. C., and Wnek, A. P. (1988). Clostridium perfringens enterotoxin. *Microbial Pathogenesis*, 4(5):317–23.
- McClay, D. R., Wessel, G. M., and Marchase, R. B. (1981). Intercellular recognition: quantitation of initial binding events. *Proceedings of the National Academy of Sciences of the United States of America*, 78(8):4975–9.
- McNeil, E., Capaldo, C. T., and Macara, I. G. (2006). Zonula occludens-1 function in the assembly of tight junctions in Madin-Darby canine kidney epithelial cells. *Molecular Biology of the Cell*, 17(4):1922–32.

- Medina, R., Rahner, C., Mitic, L. L., Anderson, J. M., and Van Itallie, C. M. (2000). Occludin localization at the tight junction requires the second extracellular loop. *Journal of Membrane Biology*, 178(3):235–47.
- Meyer, T., Begitt, A., and Vinkemeier, U. (2007). Green fluorescent protein-tagging reduces the nucleocytoplasmic shuttling specifically of unphosphorylated STAT1. *The FEBS Journal*, 274(3):815–26.
- Michl, P., Barth, C., Buchholz, M., Lerch, M. M., Rolke, M., Holzmann, K. H., Menke, A., Fensterer, H., Giehl, K., Lohr, M., Leder, G., Iwamura, T., Adler, G., and Gress, T. M. (2003). Claudin-4 expression decreases invasiveness and metastatic potential of pancreatic cancer. *Cancer Research*, 63(19):6265–71.
- Milks, L. C., Kumar, N. M., Houghten, R., Unwin, N., and Gilula, N. B. (1988). Topology of the 32-kD liver gap junction protein determined by site-directed antibody localizations. *The EMBO Journal*, 7(10):2967–75.
- Mitic, L. L., Anderson, J. M., and Unger, V. M. (2003). Expression, solubilisation, and biochemical characterisation of the tight junction transmembrane protein claudin-4. *Protein Science*, 12:218–227.
- Miwa, N., Furuse, M., Tsukita, S., Niikawa, N., Nakamura, Y., and Furukawa, Y. (2000). Involvement of claudin-1 in the beta-catenin/Tcf signaling pathway and its frequent upregulation in human colorectal cancers. *Oncology Research*, 12(11/12):469–476.
- Miyamoto, T., Morita, K., Takemoto, D., Takeuchi, K., Kitano, Y., Miyakawa, T., Nakayama, K., Okamura, Y., Sasaki, H., Miyachi, Y., Furuse, M., and Tsukita, S. (2005). Tight junctions in Schwann cells of peripheral myelinated axons: a lesson from claudin-19-deficient mice. *Journal of Cell Biology*, 169(3):527–38.
- Morin, P. J. (2005). Claudin proteins in human cancer: promising new targets for diagnosis and therapy. *Cancer Res*, 65(21):9603–6.
- Morita, K., Furuse, M., Fujimoto, K., and Tsukita, S. (1999). Claudin multigene family encoding four-transmembrane domain protein components of tight junction strands. *Proceedings of the National Academy of Sciences of the United States of America*, 96:511–516.
- Moroi, S., Saitou, M., Fujimoto, K., Sakakibara, A., Furuse, M., Yoshida, O., and Tsukita, S. (1998). Occludin is concentrated at tight junctions of mouse/rat but not human/guinea pig Sertoli cells in testes. *American Journal of Physiology*, 274(6 Pt 1):C1708–17.
- Mrsny, R. J. (2005). Modification of epithelial tight junction integrity to enhance transmucosal absorption. *Critical Reviews in Therapeutic Drug Carrier System*, 22(4):331–418.
- Mrsny, R. J. (2007). Welsh School of Pharmacy, University of Wales, Cardiff, UK. *Personal communication*.

- Mullin, J. M., Laughlin, K. V., Ginanni, N., Marano, C. W., Clarke, H. M., and Peralta Soler, A. (2000). Increased tight junction permeability can result from protein kinase C activation/translocation and act as a tumor promotional event in epithelial cancers. *Annals of the New York Academy of Sciences*, 915:231–6.
- Muresan, Z., Paul, D. L., and Goodenough, D. A. (2000). Occludin 1B, a variant of the tight junction protein occludin. *Molecular Biology of the Cell*, 11(2):627–34.
- Murhammer, D. W. and Goochee, C. F. (1988). Scaleup of insect cell cultures: protective effects of Pluronic F-68. *Biotechnology*, 6:1411–18.
- Nakao, S., Ebata, H., Hamamoto, T., Kagawa, Y., and Hirata, H. (1988). Solubilization and reconstitution of voltage-dependent calcium channel from bovine cardiac muscle. Calcium influx assay using the fluorescent dye Quin2. *Biochimica et Biophysica Acta*, 944(3):337–43.
- Nitta, T., Hata, M., Gotoh, S., Seo, Y., Sasaki, H., Hashimoto, N., Furuse, M., and Tsukita, S. (2003). Size-selective loosening of the blood-brain barrier in claudin-5-deficient mice. *Journal of Cell Biology*, 161(3):653–60.
- Novick, P. and Zerial, M. (1997). The diversity of Rab proteins in vesicle transport. *Current Opinion in Cell Biology*, 9(4):496–504.
- Nusrat, A., Brown, G. T., Tom, J., Drake, A., Bui, T. T., Quan, C., and Mrsny, R. J. (2005). Multiple protein interactions involving proposed extracellular loop domains of the tight junction protein occludin. *Molecular Biology of the Cell*, 16(4):1725–34.
- Nusrat, A., Chen, J. A., Foley, C. S., Liang, T. W., Tom, J., Cromwell, M., Quan, C., and Mrsny, R. J. (2000a). The coiled-coil domain of occludin can act to organize structural and functional elements of the epithelial tight junction. *Journal of Biological Chemistry*, 275(38):29816–22.
- Nusrat, A., Parkos, C. A., Verkade, P., Foley, C. S., Liang, T. W., Innis-Whitehouse, W., Eastburn, K. K., and Madara, J. L. (2000b). Tight junctions are membrane microdomains. *Journal of Cell Science*, 113(Pt 10):1771–81.
- Offner, S., Hekele, A., Teichmann, U., Weinberger, S., Gross, S., Kufer, P., Itin, C., Baeuerle, P. A., and Kohleisen, B. (2005). Epithelial tight junction proteins as potential antibody targets for pancreatic carcinoma therapy. *Cancer Immunology, Immunotherapy*, 54(5):431–45.
- Overall, C. M. (1987). A microtechnique for dialysis of small volume solutions with quantitative recoveries. *Analytical Biochemistry*, 165:208–214.
- Patterson, G. H., Knobel, S. M., Sharif, W. D., Kain, S. R., and Piston, D. W. (1997). Use of the green fluorescent protein and its mutants in quantitative fluorescence microscopy. *Biophysical Journal*, 73(5):2782–90.

- Pauletti, G. M., Gangwar, S., Siahaan, T. J., Aubé, J., and Borchardt, R. T. (1997). Improvement of oral peptide bioavailability: peptidomimetics and prodrug strategies. *Advanced Drug Delivery Reviews*, 27(2-3):235–256.
- Phillippot, J., Mutaftschiev, S., and Liautard, J. P. (1983). A very mild method allowing the encapsulation of very high amounts of macromolecules into very large (1000 nm) unilamellar liposomes. *Biochimica et Biophysica Acta*, 734:137–143.
- Pinto da Silva, P. and Kachar, B. (1982). On tight-junction structure. *Cell*, 28(3):441–50.
- Powell, D. W. (1981). Barrier function of epithelia. *American Journal of Physiology*, 241(4):G275–88.
- Quaroni, A. and Hochman, J. (1996). Development of intestinal cell culture models for drug transport and metabolism studies. *Advanced Drug Delivery Reviews*, 22:3–52.
- Radford, K. M., Cavegn, C., Bertrand, M., Bernard, A. R., Reid, S., and Greenfield, P. F. (1997). The indirect effects of multiplicity of infection on baculovirus expressed proteins in insect cells: secreted and non-secreted products. *Cytotechnology*, 24:73–81.
- Ramundo-Orlando, A., Serafino, A., Schiavo, R., Liberti, M., and d’Inzeo, G. (2005). Permeability changes of connexin32 hemi channels reconstituted in liposomes induced by extremely low frequency, low amplitude magnetic fields. *Biochimica et Biophysica Acta*, 1668(1):33–40.
- Rapoport, S. I. (2001). Advances in osmotic opening of the blood-brain barrier to enhance CNS chemotherapy. *Expert Opinion on Investigational Drugs*, 10(10):1809–18.
- Rhee, S. K., Bevans, C. G., and Harris, A. L. (1996). Channel-forming activity of immunoaffinity-purified connexin32 in single phospholipid membranes. *Biochemistry*, 35(28):9212–23.
- Rhiel, M., Mitchell-Logean, C. M., and Murhammer, D. W. (1997). Comparison of *Trichoplusia ni* BTI-Tn-5B1-4 (Hive Five) and *Spodoptera frugiperda* (Sf9) insect cell line metabolism in suspension cultures. *Biotechnology and Bioengineering*, 55(6):909–920.
- Riazuddin, S., Ahmed, Z. M., Fanning, A. S., Lagziel, A., Kitajiri, S., Ramzan, K., Khan, S. N., Chattaraj, P., Friedman, P. L., Anderson, J. M., Belyantseva, I. A., Forge, A., Riazuddin, S., and Friedman, T. B. (2006). Tricellulin is a tight-junction protein necessary for hearing. *American Journal of Genetics*, 79(6):1040–51.
- Riesen, F. K. (2002). *Dynamics and modulation of tight junctions (Diss. ETH No. 14460)*. PhD thesis, Swiss Federal Institute of Technology (ETH), Zürich, Switzerland.
- Riesen, F. K., Rothen-Rutishauer, B., and Wunderli-Allenspach, H. (2002). A ZO-1 GFP fusion protein to study dynamics of tight junctions in living cells. *Histochemistry and Cell Biology*, 117:307–315.

- Rigaud, J. L. (2002). Membrane proteins: functional and structural studies using reconstituted proteoliposomes and 2-D crystals. *Brazilian Journal of Medical and Biological Research*, 35(7):753–66.
- Rigaud, J. L. and Levy, D. (2003). Reconstitution of membrane proteins into liposomes. *Methods in Enzymology*, 372:65–86.
- Rigaud, J. L., Paternostre, M. T., and Bluzat, A. (1988). Mechanisms of membrane protein insertion into liposomes during reconstitution procedures involving the use of detergents. 2. Incorporation of the light-driven proton pump bacteriorhodopsin. *Biochemistry*, 27(8):2677–88.
- Roh, M. H., Liu, C. J., Laurinec, S., and Margolis, B. (2002). The carboxyl terminus of zona occludens-3 binds and recruits a mammalian homologue of discs lost to tight junctions. *Journal of Biological Chemistry*, 277(30):27501–9.
- Rosevear, P., VanAken, T., Baxter, J., and Ferguson-Miller, S. (1980). Alkyl glycoside detergents: a simpler synthesis and their effects on kinetic and physical properties of cytochrome c oxidase. *Biochemistry*, 19(17):4108–15.
- Rothen-Rutishauer, B., Riesen, F. K., Braun, A., Günthert, M., and Wunderli-Allenspach, H. (2002). Dynamics of tight and adherens junctions under EGTA treatment. *Journal of Membrane Biology*, 188:151–162.
- Rothen-Rutishauser, B., Braun, A., Günthert, M., and Wunderli-Allenspach, H. (2000). Formation of multilayers in the Caco-2 cell culture model: a confocal laser scanning microscopy study. *Pharmaceutical Research*, 17(4):460–5.
- Rothen-Rutishauser, B., Krämer, S. D., Braun, A., Günthert, M., and Wunderli-Allenspach, H. (1998a). MDCK cell cultures as an epithelial in vitro model: cytoskeleton and tight junctions as indicators for the definition of age-related stages by confocal microscopy. *Pharmaceutical Research*, 15(7):964–71.
- Rothen-Rutishauser, B., Messerli, J. M., Voort van der, H., Günthert, M., and Wunderli-Allenspach, H. (1998b). Deconvolution combined with digital colocalisation analysis to study the spatial distribution of tight and adherens junctions. *Journal of Computer-Assisted Microscopy*, 10(3):103–111.
- Rothnie, A., Theron, D., Soceneantu, L., Martin, C., Traikia, M., Berridge, G., Higgins, C. F., Devaux, P. F., and Callaghan, R. (2001). The importance of cholesterol in maintenance of P-glycoprotein activity and its membrane perturbing influence. *European Biophysics Journal*, 30(6):430–42.
- Rueffer, C. and Gerke, V. (2004). The C-terminal cytoplasmic tail of claudins 1 and 5 but not its PDZ-binding motif is required for apical localization at epithelial and endothelial tight junctions. *European Journal of Cell Biology*, 83(4):135–44.

- Saitou, M., Ando-Akatsuka, Y., Itoh, M., Furuse, M., Inazawa, J., Fujimoto, K., and Tsukita, S. (1997). Mammalian occludin in epithelial cells: its expression and subcellular distribution. *European Journal of Cell Biology*, 73(3):222–31.
- Saitou, M., Fujimoto, K., Doi, Y., Itoh, M., Fujimoto, T., Furuse, M., Takano, H., Noda, T., and Tsukita, S. (1998). Occludin-deficient embryonic stem cells can differentiate into polarized epithelial cells bearing tight junctions. *Journal of Cell Biology*, 141(2):397–408.
- Sakakibara, A., Furuse, M., Saitou, M., Ando-Akatsuka, Y., and Tsukita, S. (1997). Possible involvement of phosphorylation of occludin in tight junction formation. *Journal of Cell Biology*, 137(6):1393–401.
- Salama, N. N., Eddington, N. D., and Fasano, A. (2006). Tight junction modulation and its relationship to drug delivery. *Advanced Drug Delivery Reviews*, 58(1):15–28.
- Sambrook, J. and Russell, D. W. (2001). *Molecular cloning: A laboratory manual*. Cold Spring Harbor Laboratory Press, New York.
- Sano, K., Maeda, K., Oki, M., and Maeda, Y. (2002). Enhancement of protein expression in insect cells by a lobster tropomyosin cDNA leader sequence. *FEBS Letters*, 532(1-2):143–6.
- Sasaki, H., Matsui, C., Furuse, K., Mimori-Kiyosue, Y., Furuse, M., and Tsukita, S. (2003). Dynamic behavior of paired claudin strands within apposing plasma membranes. *Proceeding of the National Academy of Sciences of the United States of America*, 100(7):3971–6.
- Sauer, T., Pedersen, M. K., Ebeltoft, K., and Naess, O. (2005). Reduced expression of claudin-7 in fine needle aspirates from breast carcinomas correlate with grading and metastatic disease. *Cytopathology*, 16(4):193–8.
- Sawada, N., Murata, M., Kikuchi, K., Osanai, M., Tobioka, H., Kojima, T., and Chiba, H. (2003). Tight junctions and human diseases. *The Clinical Electron Microscopy Society of Japan*, 36(3):147–156.
- Schopf, B., Howaldt, M. W., and Bailey, J. E. (1990). DNA distribution and respiratory activity of *Spodoptera frugiperda* populations infected with wild-type and recombinant *Autographa californica* nuclear polyhedrosis virus. *Journal of Biotechnology*, 15(1-2):169–85.
- Schubert, R. (2003). Liposome preparation by detergent removal. *Methods in Enzymology*, 367:46–70.
- Seddon, A. M., Curnow, P., and Booth, P. J. (2004). Membrane proteins, lipids and detergents: not just a soap opera. *Biochimica et Biophysica Acta*, 1666(1-2):105–17.
- Sekar, R. B. and Periasamy, A. (2003). Fluorescence resonance energy transfer (FRET) microscopy imaging of live cell protein localizations. *Journal of Cell Biology*, 160(5):629–33.
- Sharma, S., Kulkarni, J., and Pawar, A. P. (2006). Permeation enhancers in the transmucosal delivery of macromolecules. *Pharmazie*, 61(6):495–504.

- Sharom, F. J. (1995). Characterization and functional reconstitution of the multidrug transporter. *Journal of Bioenergetics and Biomembranes*, 27(1):15–22.
- Sharom, F. J., Yu, X., and Doige, C. A. (1993). Functional reconstitution of drug transport and ATPase activity in proteoliposomes containing partially purified P-glycoprotein. *Journal of Biological Chemistry*, 268(32):24197–202.
- Shen, L. and Turner, J. R. (2005). Actin depolymerization disrupts tight junctions via caveolae-mediated endocytosis. *Molecular Biology of the Cell*, 16(9):3919–36.
- Shiraki, K., Nishikawa, K., and Goto, Y. (1995). Trifluoroethanol-induced stabilization of the alpha-helical structure of beta-lactoglobulin: implication for non-hierarchical protein folding. *Journal of Molecular Biology*, 245(2):180–94.
- Simon, A. M. and Goodenough, D. A. (1998). Diverse functions of vertebrate gap junctions. *Trends in Cell Biology*, 8(12):477–83.
- Singh, A. B. and Harris, R. C. (2004). Epidermal growth factor receptor activation differentially regulates claudin expression and enhances transepithelial resistance in Madin-Darby canine kidney cells. *Journal of Biological Chemistry*, 279(5):3543–52.
- Sonoda, N., Furuse, M., Sasaki, H., Yonemura, S., Katahira, J., Horiguchi, Y., and Tsukita, S. (1999). Clostridium perfringens enterotoxin fragment removes specific claudins from tight junction strands: evidence for direct involvement of claudins in tight junction barrier. *Journal of Cell Biology*, 147(1):195–204.
- Sosinsky, G. E. and Nicholson, B. J. (2005). Structural organization of gap junction channels. *Biochimica et Biophysica Acta*, 1711(2):99–125.
- Sreerama, N., Venyaminov, S. Y., and Woody, R. W. (2000). Estimation of protein secondary structure from circular dichroism spectra: inclusion of denatured proteins with native proteins in the analysis. *Analytical Biochemistry*, 287(2):243–51.
- Sreerama, N. and Woody, R. W. (2000). Estimation of protein secondary structure from circular dichroism spectra: comparison of CONTIN, SELCON, and CDSSTR methods with an expanded reference set. *Analytical Biochemistry*, 287(2):252–60.
- Staehelin, L. A. (1973). Further observations on the fine structure of freeze-cleaved tight junctions. *Journal of Cell Sciences*, 13(3):763–86.
- Staehelin, L. A., Mukherjee, T. M., and Williams, A. W. (1969). Freeze-etch appearance of the tight junctions in the epithelium of small and large intestine of mice. *Protoplasma*, 67(2):165–84.
- Stevenson, B. R., Heintzelman, M. B., Anderson, J. M., Citi, S., and Mooseker, M. S. (1989). ZO-1 and cingulin: tight junction proteins with distinct identities and localizations. *American Journal of Physiology*, 257(4 Pt 1):C621–8.

- Stevenson, B. R., Siliciano, J. D., Mooseker, M. S., and Goodenough, D. A. (1986). Identification of ZO-1: a high molecular weight polypeptide associated with the tight junction (zonula occludens) in a variety of epithelia. *Journal of Cell Biology*, 103(3):755–66.
- Sunshine, C., Francis, S., and Kirk, K. L. (2000). Rab3B regulates ZO-1 targeting and actin organization in PC12 neuroendocrine cells. *Experimental Cell Research*, 257(1):1–10.
- Takahashi, A., Kondoh, M., Masuyama, A., Fujii, M., Mizuguchi, H., Horiguchi, Y., and Watanabe, Y. (2005). Role of C-terminal regions of the C-terminal fragment of Clostridium perfringens enterotoxin in its interaction with claudin-4. *Journal of Controlled Release*, 108(1):56–62.
- Tanaka, J., Sadanari, H., Sato, H., and Fukuda, S. (1991). Sodium butyrate-inducible replication of human cytomegalovirus in a human epithelial cell line. *Virology*, 185(1):271–80.
- Tanaka, M., Kamata, R., and Sakai, R. (2005). EphA2 phosphorylates the cytoplasmic tail of claudin-4 and mediates paracellular permeability. *Journal of Biological Chemistry*, 280(51):42375–82.
- Tavelin, S. (2004). Department of Pharmacy, Uppsala University, Uppsala, Sweden. *Personal communication*.
- Tavelin, S., Hashimoto, K., Malkinson, J., Lazorova, L., Toth, I., and Artursson, P. (2003). A new principle for tight junction modulation based on occludin peptides. *Molecular Pharmacology*, 64(6):1530–1540.
- Taylor, A. M., Storm, J., Soceneantu, L., Linton, K. J., Gabriel, M., Martin, C., Woodhouse, J., Blott, E., Higgins, C. F., and Callaghan, R. (2001). Detailed characterization of cysteine-less P-glycoprotein reveals subtle pharmacological differences in function from wild-type protein. *British Journal of Pharmacology*, 134(8):1609–18.
- Thompson, J. D., Higgins, D. G., and Gibson, T. J. (1994). CLUSTAL W: improving the sensitivity of progressive multiple sequence alignment through sequence weighting, position-specific gap penalties and weight matrix choice. *Nucleic Acids Research*, 22(22):4673–80.
- Tirumalasetty, P. P. and Eley, J. G. (2006). Permeability enhancing effects of the alkylglycoside, octylglucoside, on insulin permeation across epithelial membrane in vitro. *Journal of Pharmaceutical Sciences*, 9(1):32–9.
- Tokes, A. M., Kulka, J., Paku, S., Szik, A., Paska, C., Novak, P. K., Szilak, L., Kiss, A., Bogi, K., and Schaff, Z. (2005). Claudin-1, -3 and -4 proteins and mRNA expression in benign and malignant breast lesions: a research study. *Breast Cancer Research*, 7(2):R296–305.
- Tomita, M., Hayashi, M., and Awazu, S. (1996). Absorption-enhancing mechanism of EDTA, caprate, and decanoylcarnitine in Caco-2 cells. *Journal of Pharmaceutical Sciences*, 85(6):608–11.

- Tsukamoto, T. and Nigam, S. K. (1999). Role of tyrosine phosphorylation in the reassembly of occludin and other tight junction proteins. *American Journal of Physiology*, 276(5 Pt 2):F737–50.
- Tsukita, S. and Furuse, M. (2000). Pores in the wall: claudins constitute tight junction strands containing aqueous pores. *Journal of Cell Biology*, 149(1):13–6.
- Tsukita, S., Furuse, M., and Itoh, M. (1999). Structural and signaling molecules come together at tight junctions. *Current Opinion in Cell Biology*, 11:628–633.
- Tsukita, S., Furuse, M., and Itoh, M. (2001). Multifunctional strands in tight junctions. *Molecular Cell Biology, Nature Reviews*, 2:285–93.
- Turksen, K. and Troy, T. C. (2004). Barriers built on claudins. *Journal of Cell Science*, 117(Pt 12):2435–2447.
- Ueno, M., Tanford, C., and Reynolds, J. A. (1984). Phospholipid vesicle formation using non-ionic detergents with low monomer solubility. Kinetic factors determine vesicle size and permeability. *Biochemistry*, 23(13):3070–6.
- Umeda, K., Ikenouchi, J., Katahira-Tayama, S., Furuse, K., Sasaki, H., Nakayama, M., Matsui, T., Tsukita, S., Furuse, M., and Tsukita, S. (2006). ZO-1 and ZO-2 independently determine where claudins are polymerized in tight-junction strand formation. *Cell*, 126(4):741–54.
- Umeda, K., Matsui, T., Nakayama, M., Furuse, K., Sasaki, H., Furuse, M., and Tsukita, S. (2004). Establishment and characterization of cultured epithelial cells lacking expression of ZO-1. *Journal of Biological Chemistry*, 279(43):44785–94.
- van de Waterbeemd, H., Lennernäss, H., and Artursson, P. (2003). Estimation of solubility, permeability, absorption and bioavailability. In *Drug bioavailability*. Wiley-VCH, Weinheim.
- van der Merwe, S. M., Verhoef, J. C., Verheijden, J. H., Kotze, A. F., and Junginger, H. E. (2004). Trimethylated chitosan as polymeric absorption enhancer for improved peroral delivery of peptide drugs. *European Journal of Pharmaceutics and Biopharmaceutics*, 58(2):225–35.
- Van Itallie, C. M. and Anderson, J. M. (1997). Occludin confers adhesiveness when expressed in fibroblasts. *Journal of Cell Science*, 110(Pt 9):1113–21.
- Van Itallie, C. M. and Anderson, J. M. (2006). Claudins and epithelial paracellular transport. *Annual Review of Physiology*, 68:403–429.
- Van Itallie, C. M., Fanning, A. S., and Anderson, J. M. (2003). Reversal of charge selectivity in cation or anion selective epithelial lines by expression of different claudins. *American Journal of Physiology. Renal Physiology*, 285(6):F1078–84.
- Van Itallie, C. M., Gambling, T. M., Carson, J. L., and Anderson, J. M. (2005). Palmitoylation of claudins is required for efficient tight-junction localization. *Journal of Cell Science*, 118(Pt 7):1427–36.

- Van Itallie, C. M., Rahner, C., and Anderson, J. M. (2001). Regulated expression of claudin-4 decreases paracellular conductance through a selective decrease in sodium permeability. *The Journal of Clinical Investigation*, 107(10):1319–27.
- van Meer, G., Gumbiner, B., and Simons, K. (1986). The tight junction does not allow lipid molecules to diffuse from one epithelial cell to the next. *Nature*, 322(6080):639–41.
- van Meer, G. and Simons, K. (1986). The function of tight junctions in maintaining differences in lipid composition between the apical and the basolateral cell surface domains of MDCK cells. *The EMBO Journal*, 5(7):1455–64.
- Vedula, S. R., Lim, T. S., Kausalya, P. J., Hunziker, W., Rajagopal, G., and Lim, C. T. (2005). Biophysical approaches for studying the integrity and function of tight junctions. *Molecular and Cellular Biomechanics*, 2(3):105–23.
- Vietor, I., Bader, T., Paiha, K., and Huber, L. A. (2001). Perturbation of the tight junction permeability barrier by occludin loop peptides activates beta-catenin/TCF/LEF-mediated transcription. *EMBO Reports*, 2(4):306–12.
- Voet, D. and Voet, J. G. (1995). *Biochemistry*. John Wiley & Sons, New York.
- Wang, Z., Mandell, K. J., Parkos, C. A., Mrsny, R. J., and Nusrat, A. (2005). The second loop of occludin is required for suppression of Raf1-induced tumor growth. *Oncology*, pages 1–9.
- Ward, P. D., Tippin, T. K., and Thakker, D. (2000). Enhancing paracellular permeability by modulating epithelial tight junctions. *Pharmaceutical Science and Technology Today*, 3:346–358.
- Warren, K. E., Patel, M. C., Aikin, A. A., Widemann, B., Libucha, M., Adamson, P. C., Neuwirth, R., Benziger, D., O'Toole, T., Ford, K., Patronas, N., Packer, R. J., and Balis, F. M. (2001). Phase I trial of lobradimil (RMP-7) and carboplatin in children with brain tumors. *Cancer Chemotherapy and Pharmacology*, 48(4):275–82.
- Watson, C. J., Rowland, M., and Warhurst, G. (2001). Functional modeling of tight junctions in intestinal cell monolayers using polyethylene glycol oligomers. *American Journal of Physiology. Cell Physiology*, 281(2):C388–97.
- Waugh, D. S. (2005). Making the most of affinity tags. *Trends in Biotechnology*, 23(6):316–20.
- Wen, H., Watry, D. D., Marcondes, M. C., and Fox, H. S. (2004). Selective decrease in paracellular conductance of tight junctions: role of the first extracellular domain of claudin-5. *Molecular and Cellular Biology*, 24(19):8408–17.
- Willott, E., Balda, M. S., Heintzelman, M., Jameson, B., and Anderson, J. M. (1992). Localization and differential expression of two isoforms of the tight junction protein ZO-1. *American Journal of Physiology*, 262(5 Pt 1):C1119–24.

- Wittchen, E. S., Haskins, J., and Stevenson, B. R. (1999). Protein interactions at the tight junctions. *Journal of Biological Chemistry*, 274(3):35179–35185.
- Wong, V. (1997). Phosphorylation of occludin correlates with occludin localization and function at the tight junction. *American Journal of Physiology. Cell Physiology*, 273(6):C1859–1867.
- Wong, V. and Gumbiner, B. M. (1997). A synthetic peptide corresponding to the extracellular domain of occludin perturbs the tight junction permeability barrier. *Journal of Cell Biology*, 136(2):399–409.
- Wu, C. H., Apweiler, R., Bairoch, A., Natale, D. A., Barker, W. C., Boeckmann, B., Ferro, S., Gasteiger, E., Huang, H., Lopez, R., Magrane, M., Martin, M. J., Mazumder, R., O'Donovan, C., Redaschi, N., and Suzek, B. (2006). The Universal Protein Resource (UniProt): an expanding universe of protein information. *Nucleic Acids Research*, 34:D187–91.
- Wunderli-Allenspach, H. (2001). Methodologies in cell cultures. In *Pharmacokinetic optimization in drug research: biological, physicochemical and computational strategies*. Wiley-VCH, Weinheim.
- Yamamoto, T., Harada, N., Kano, K., Taya, S., Canaani, E., Matsuura, Y., Mizoguchi, A., Ide, C., and Kaibuchi, K. (1997). The Ras target AF-6 interacts with ZO-1 and serves as a peripheral component of tight junctions in epithelial cells. *Journal of Cell Biology*, 139(3):785–95.
- Yang, Q. and Lundahl, P. (1995). Immobilized proteoliposome affinity chromatography for quantitative analysis of specific interactions between solutes and membrane proteins. Interaction of cytochalasin B and D-glucose with the glucose transporter Glut1. *Biochemistry*, 34(22):7289–94.
- Yang, T. T., Cheng, L., and Kain, S. R. (1996). Optimized codon usage and chromophore mutations provide enhanced sensitivity with the green fluorescent protein. *Nucleic Acids Research*, 24(22):4592–3.
- Yap, A. S., Briehner, W. M., and Gumbiner, B. M. (1997). Molecular and functional analysis of cadherin-based adherens junctions. *Annual Review of Cell and Developmental Biology*, 13:119–46.
- Zahraoui, A., Joberty, G., Arpin, M., Fontaine, J. J., Hellio, R., Tavitian, A., and Louvard, D. (1994). A small rab GTPase is distributed in cytoplasmic vesicles in non polarized cells but colocalizes with the tight junction marker ZO-1 in polarized epithelial cells. *Journal of Cell Biology*, 124(1-2):101–15.
- Zeidel, M. L., Ambudkar, S. V., Smith, B. L., and Agre, P. (1992). Reconstitution of functional water channels in liposomes containing purified red cell CHIP28 protein. *Biochemistry*, 31(33):7436–40.

- Zhang, L., Wu, G., Tate, C. G., Lookene, A., and Olivecrona, G. (2003). Calreticulin promotes folding/dimerization of human lipoprotein lipase expressed in insect cells (Sf21). *Journal of Biological Chemistry*, 278(31):29344–51.
- Zhong, Y., Saitoh, T., Minase, T., Sawada, N., Enomoto, K., and Mori, M. (1993). Monoclonal antibody 7H6 reacts with a novel tight junction-associated protein distinct from ZO-1, cingulin and ZO-2. *Journal of Cell Biology*, 120(2):477–83.

Acknowledgements

On the first place, I would like to express my thanks to Prof. Dr. Heidi Wunderli-Allespach for offering me a PhD-position in the Biopharmacy group. From the beginning on, she trusted in me and even in the deepest moments of desperation, she did not stop to support me and give me hope to continue. I am grateful to PD Dr. Stefanie D. Krämer for being always ready to discuss the projects and daily problems in the lab, if necessary, for many hours. She will stay in my mind not only as a researcher with deep knowledge and enthusiasm for science, but also as a person with big smile making all the troubles half so terrible as they were. Many thanks to Prof. Dr. Dario Neri for taking the role of co-referee for the thesis and showing me the world of phage display technology in his course. I very much appreciated the possibility to use the equipment of his laboratory for my own experiments. Many thanks belong to Maja Günthert. She showed me many tips'n'tricks for the routine work in the lab including how to be 'nice and ugly' to the cell cultures. She also acquired many CLSM pictures for me and, no doubts, those are the best ones around the globe. Thanks to Prof. Dr. Karl-Heinz Altmann, Dr. Bernhard Pfeiffer and Kurt Hauenstein, who helped me with the synthesis of 2-aminotetradecanoic acid. Many thanks to Prof. Dr. Annette Beck-Sickinger for the supply of several claudin peptide homologues. Many thanks to Dr. Sandra Citi for the supply of the anti-cingulin antibody and the kind visit in Zurich. I am grateful to Belinda Schegg and Christoph Rutschmann from the University of Zurich, who gave me advice to the baculovirus expression system.

Anita Thomae, Sara Belli, Denise Ilgen, Karsten Bucher, Marco Marenchino, Dario Lombardi and Samuel Murri, you all have been good friends and colleagues. Anita, thanks for introducing me to \LaTeX . I really enjoy to explore its features! Thanks for the two great days in Woerlitz. It is a wonderful place. And I still envy your mother her antique pharmacy bottles. Sara, thanks for the delicious Panforte you brought to me. I wish I could visit you in Massa sometime. Denise, I wish you no more surprises from the Swiss habitude. It's just the question of getting used to it. Karsten, thanks to you I know, that one chocolate bar per day does not make somebody fat. If one runs and bike as you did. Thanks for organizing the trip to Chruetzegg. It woke up my hidden passion for mountains and made my foot full of blisters, because of the new hiking shoes. Marco, I have never met somebody so skilled in creating nick names! Thanks for the Easter in Rome, you have shown us many beautiful places and I tasted the tail of a cow! Dario, thanks for joining me for the concert of Bad Religion, we lost some hundreds of hair cells in our ears, but it was worth to. Samuel, thanks to you I understand a bit more of Swiitzerdütsch. We discussed the 'Claudin' guy more than once, and it was always very helpful. Wanda Surber, thank you for the contribution to the Peptide project. It was a pleasure to have such a good student! I enjoyed very much the sunflower festival in Frauenfeld. My colleagues from the lab of Prof. Dr. André Brändli, thanks for your friendship and great help with the molecular biology techniques.

Sebastian C. Commichau, thanks for the several thousands of kilometers you have shared with me on the bike tours. I will never forget the sound of our machines on the road and the burning pain in the lungs and legs. I enjoyed to be your navigator in many rallies we made with your Vespa and Opel GT or other vehicles you were currently driving. Thank you, Brigittka Guldemann, for teaching me the French pronunciation of 'toilette water' and for the common jogging in the forrest. René Guldemann, thanks for listening any time I complained. I enjoyed many fondues you made! I will also remember your strong Maserati and the 'Tomaten & Mozzarella' you were passionate for. I would also like to thank to Lucie Mališová for her support during my first year in Zurich.

Many thanks to my family, you supported and encouraged me for all those years. It was great to come back home and see you any time. I apologize for the rare phone calls and emails!

Gábinko, you are my light in the darkness and without you I would have been lost.

Curriculum vitæ

Biographical data

Name Jiri Hofmann
Date of birth September 22, 1978
Place of birth Ústí nad Labem, Czech Republic

Education & Professional Experience

2002-2007 Postgraduate studies in the group of Prof. Dr. Heidi Wunderli-Allenspach at the Institute of Pharmaceutical Sciences, Department of Chemistry and Applied Biosciences, Swiss Federal Institute of Technology in Zurich, Switzerland

2002 Diploma in Pharmacy. Diploma thesis on 'Studies on Interactions of Quinlukast in the Central Compartment', performed under the supervision of Prof. PharmDr. Ing. Milan Lázníček, CSc., Faculty of Pharmacy, Department of Pharmacology, Section of Radiopharmacy, Charles University in Prague

1997-2002 Undergraduate studies in Pharmacy at Charles University in Prague, Faculty of Pharmacy in Hradec Kralové, Czech Republic

1993-1997 Secondary school 'Gymnázium Jateční', Ústí nad Labem, Czech Republic

1985-1993 Primary school, Ústí nad Labem, Czech Republic